Generation and Relaxation Processes of Multiexciton in Colloidal CdTe and CdS Quantum Dots

Thesis for the Degree of

Doctor of Science

Submitted to

School of Science and Technology

Kwansei Gakuin University

Yoichi KOBAYASHI

January, 2011

Abbreviations

QDs	Quantum dots
IPCE	Incident photon-to-current conversion efficiency
APCE	Actual absorbed photon-to-current conversion efficiency
Δ^r_S	resonant Stokes shift
Δ^g_S	global Stokes shift
MEG	Multiple exciton generation
hh	heavy hole
lh	light hole
so	split-off hole
E_g	Bandgap
D	diameter
ΔOD	the differential optical density
$\langle N_0 \rangle$	initial average numbers of excitons per QD
TDPA	*n*-Tetradecylphosphonic acid
ODE	1-Octadecene
Φ	Quantum yields
TGA	Thioglycolic acid
TOP	Trioctylphosphine
OA	Oleic acid
GSH	*L*-glutathione
MA	Myristic acid
CM	Carrier multiplication
QE	Quantum efficiency of CM
HRTEM	High resolution transmission electron microscopy
EMA	effective mass approximation

Chapter 1
Introduction

1.1 Preface

Semiconductor quantum dots (QDs) are nanometer-sized particles, which show size-dependent optical properties because electron and hole wavefunctions are confined in the smaller size than the exciton Bohr radius. Although semiconductor nanocrystals have been known as the color matrices of stained glass for centuries, the systematic study of their physical properties had not been examined until the 20th centuries.[1] The first investigation of II-VI semiconductor nanocrystals was published by A. Henglein in 1982.[2] This paper revealed the first absorption spectrum of a colloidal solution of size-quantized CdS nanocrystals. Brus, Ekimov and Efros groups also independently gave correct interpretations of the observed blue shift of the absorption as a quantum mechanical effect.[3-5] Since then, various kinds of work have been reported in the preparation and characterization of semiconductor nanocrystals.[6-16] In the late of 1980, heterostructural-QDs named "core/shell" QDs, whose surface are overcoated by other inorganic materials, have been developed such as Ag_2S on CdS,[17] ZnS on CdS,[18] CdSe on ZnS,[19] CdSe on ZnSe,[20] PbS on CdS.[21] A milestone in the preparation of II-VI semiconductor nanocrystals is the work by Murray, Norris and Bawendi in 1993.[22] Their synthesis is based on the pyrolysis of organometallic reagents like dimethylcadmium and torioctylphosphine selenide after injection of Se precursors into a hot coordinating Cd solvent. This approach provides temporally discrete nucleation and permits a controlled growth of the nanocrystals.[23,24] By applying this technique, high quality core/shell QDs were also developed such as CdS on CdSe[25] and vice versa.[26] A fine example of the most careful characterization of the overgrowth of CdSe QDs with ZnS is reported in the paper of Dabbousi et al. in 1997.[27] In addition to spherical nanocrystals, non-spherical nanocrystals such as rod, wire and tetrapod shapes have been developed in the late of 1990.[28-33] The crystal shape are carefully controlled by the monomer concentration, the crystal structure and the choice of capping reagents bacause it strongly depends on the difference in the growth rates at

each facets.[34,35] Until the mid-1990s, semiconductor nanomaterials were synthesized with highly toxic and dangerous reagents such as organometallic compounds. Peng group has developed safer procedures for the synthesis of high quality II-VI semiconductor QDs by replacing dimethylcadmium to cadmium oxide.[36,37] Weller group has developed the synthesis of high quality II-VI semiconductor QDs in aqueous solutions. This procedure is much safer than that with organic solvents and has a potential for the biological applications.[38-40] In the late 2000s, more complex heterostructure QDs have been reported such as seeded core/shell nanorods,[41-43] where a QD is overcoated with nanorod, and alloyed QDs, whose composition gradually changes from the core to the shell.[44,45] These complex structures are used to control wave functions in QDs.

QDs consist of smaller atoms as compared with bulk crystals, while the number of atoms in a QD is much larger than that of molecules. So to speak, QDs are the intermediate system between bulk and molecule. QDs have discrete electronic structures like atoms despite semiconductors. Unveiling how optical properties change from small clusters to bulk crystals is important from the standpoint of an academic interest.

In addition to an academic interest, QDs have various potential applications such as solar cells,[46-49] laser amplifications,[50-52] biological labels[53-55] and quantum information.[56,57] One striking example is an application to solar cells. QDs have large absorption cross sections and size-tunable absorption features. Besides, carrier multiplication (or multiple exciton generation: MEG) is typically observed in QDs, in which multiple excitons are obtained by one photon absorption.[49,58] While the maximum incident photon-to-current conversion efficiency (IPCE) in 2010 is 42.4% in three-junction cells of bulk semiconductors, the actual absorbed photon-to-current conversion efficiency (APCE) of solar cells based on PbS QDs films exceeds 200%.[59] However, several problems remain on the way to the applications. Nonradiative Auger recombination, in which multiple carriers recombine nonradiatively in

several ps to tens of ps time scale, is greatly enhanced in nanomaterials and hinder the effective use of carriers.[60] Auger recombination has been shown to depend on QD size in several QDs, while the mechanism has not been closely investigated. Auger recombination is a fundamental optical process in QDs and is one of bottleneck for various potential applications of QDs; therefore the detailed understanding of Auger recombination is immediately required.

In the present thesis, the generation and relaxation processes of multiexcitons in semiconductor QDs are discussed. Multiexcitons can be easily generated in a QD and therefore they are important for not only a scientific interest but also the application to the photon-to-current conversion devices. I expect that this work will help unveiling great phenomena or developing a photon-to-current conversion system such as solar cells in the near future.

1.2 Semiconductor quantum dots (QDs)

1.2.1 General features 3D-confined nanomaterials

Semiconductor quantum dots (QDs) are nm-sized particles whose radius is less than the exciton Bohr radius.[18,61] Bulk semiconductors contain many atoms (~10^{23} atoms per mol), and thus the electronic structure forms band structures such as valence band and conduction band. As compared with bulk semiconductors, QDs contain at most 100-10,000 atoms, and thus, the electronic structure becomes partially discrete (Figure 1.1). In addition, optical properties of QDs depend on the QD size because the smaller size than the exciton Bohr radius directly affects the spatial carrier distribution. In the absence of band-mixing effect, the discrete electronic structure can be described with two quantum numbers. One, L, determines the angular momentum (symmetry) of an envelope wave function and the other, n, denotes the

number of the state in the series of states of a given symmetry.[62] In the typical notation of QDs quantized states, the momentum indicated by a letter (S for $L = 0$, P for $L = 1$ etc.) is preceded by the value of n. The three lowest energy states in the order of increasing energy are $1S$, $1P$, and $1D$.

An important consequence of strong spatial confinement is a significant enhancement of Coulomb interaction between charge carriers. In the case of bulk semiconductors at room temperature, photo-excited carriers are thermally diffused and nonradiatively recombined because they are spatially separated. On the other hand, in the case of QDs, the strong Coulomb interaction dramatically enhances the probability of the radiative recombination as compared with the bulk materials. As similar to the electron-hole interaction, the exciton-exciton interaction (exciton is an electron-hole pair) is also enhanced in QDs. The strong exciton-exciton interaction results in sizable spectral shift of multiexciton emission bands from the single-exciton transition energy. Multiexcitons relax to the single exciton state in ps to tens of ps mainly through multiexciton Auger recombination.

In addition to characteristics, the optical properties of QDs strongly depend on the QD interface and surface defects because of the large surface to volume ratio as compared with the bulk semiconductors.[63-66] In the case of colloidal QDs, capping reagents cover QDs and effectively passivate dangling bonds at the QD surface. How to immobilize dangling bonds strongly depends on the synthetic method, capping reagents and pH etc. When the QD surface is well passivated, the band-edge emission is only observed. On the other hand, when the surface coverage are not sufficient, surface dangling bonds serve as a carrier trap and a broad emission associated with the trap states is observed at longer wavelength (Figure 1.2).[67,68]

Synthetic methods of QDs fall into two approaches, one is top-down approach and the other is bottom-up approach. A bottom-up approach is suitable to synthesize high quality and uniformly-sized QDs. Bottom-up approach falls into two synthetic methods, one is an

epitaxial growth on the substrate and the other is colloidal synthesis in an aqueous solution. Epitaxial QDs on a substrate are suitable for extracting an electric energy, while the equipment is quite large-scale and it is not so easy to fabricate uniform QDs. On the other hand, colloidal QDs are easy to synthesize and much cheaper as compared with the epitaxial growth methods. In addition, the size dispersion of colloidal QDs is around 5%, that is much smaller than the epitaxial growth QDs. Problems in colloidal QDs are the extraction of carriers from QDs and the immobilization on the substrate.

1.2.2 Electronic structures of semiconductor QDs

The simplified model of QD electronic states shown in Figure 1.1 provides a reasonable description of the QD energy levels (conduction band states) corresponding to the conduction band of the bulk.[62] However, because of the complex multi-subband character of the QD energy levels (valence band states) corresponding to the valence band of the bulk, the confinement-induced mixing between different subbands has to be taken into account. The valence band state Hamiltonian of QDs consists of both the crystal lattice and QD confinement potentials. For this situation, the true quantum number is the total angular momentum, $\vec{F} = \vec{J} + \overrightarrow{L_h}$, in which $\vec{J}$ and $\overrightarrow{L_h}$ represent the Bloch-function angular momentum and the orbital momentum of the hole envelope function, respectively. The hole wavefunction can be expanded using the eigenstates of the orbital momentum $\overrightarrow{L_h}$, which leads to mixing between different valence subbands. Size-dependent hole energies of CdTe QDs are calculated in references 69 and 70 by taking into account the mixing between heavy, light and split-off valence subbbands. According to these calculation, the three lowest energy hole states are $1S_{3/2}$, $1P_{3/2}$ and $2S_{3/2}$. (Figure 1.1b)

Although the band-mixing explains the overall structure of QDs absorption spectra, the emission properties of QDs can only be understood by taking into account the fine structure

splitting of the band-edge exciton produced by combined effect of strong e-h exchange interactions and anisotropies associated with the crystal symmetry and QD shape asymmentry.[71,72] The energy of the e-h exchange interaction is proportional to the overlap between the electron and hole wavefunctions, and therefore it is greatly enhanced in QDs as compared with bulk materials. In the presence of strong e-h exchange, the lowest $1S$(e) and $1S_{3/2}$(h), which are characterized by angular momenta 1/2 and 3/2, cannot be considered independently but should be treated as a combined exchange-correlated exciton with a total angular momentum, N, of either 1 or 2. These two states are split by the exchange interaction forming a high-energy optically active $N = 1$ "Bright" exciton and lower-energy optically passive $N = 2$ "Dark" exciton. These states are further split into five sublevels because of the anisotropy of the crystal structure and the nonspherical QD shape forming two manifolds of upper (U) and lower (L) five-structure states, which are labeled according to the magnitude of the projection of the exciton total angular momentum, N_m, along the unique axis (Figure 1.3).[71-73] The energy between the lowest energy state $N_m = 2$ (dark) and the higher energy state $N_m = 1^L$ (bright) is called "resonant" Stokes shift (Δ^r_S) and can be experimentally measured via size-selective fluorescence-line-narrowing spectroscopy or single-QD emission excitation spectroscopy. The steady-state band-edge absorption is dominated by the superposition of upper-manifold strong optical transitions that correspond to the 1^U and 0^U exciton states. On the other hand, the steady-state emission band is dominated by lower-manifold optical transitions which correspond to the 1^L and 2 exciton states. The energy difference between the lowest absorption maximum and the emission peak is called "global" Stokes shift (Δ^g_S).

1.2.3 Carrier dynamics of semiconductor QDs

When a bulk semiconductor absorbs a photon whose energy is higher than the bandgap, a hot electron and hole are generated in the semiconductor. Hot carriers in a bulk semiconductor relax to the band-edge via phonon emissions within 1 ps.[74] On the other hand, phonon mediated relaxation of hot carriers are highly suppressed in semiconductor QDs because their electronic structures are discrete (the energy separation between the $1S$(e) and $1P$(e) of CdSe QDs is over tenfold of a LO phonon energy). For this reason, the relaxation of hot carriers in semiconductor QDs was expected to be slow down, which is called "phonon bottleneck".[75,76]. However, the rate of the hot carrier relaxation was still sub ps time scale, which was inconsistent with phonon bottleneck. In II-VI semiconductor QDs, there are two possible relaxation passways from the $1P$(e) to the $1S$(e), Auger cooling and the energy transfer to the vibration states of capping reagents.

Auger cooling was proposed as a new relaxation passway of hot electrons in II-VI semiconductor QDs by Efros et al. in 1995.[77] Auger cooling is a nonradiative decay process whereby a hot electron relaxes to the band-edge $1S$(e) state by transferring its energy to a hole (Figure 1.4a). The re-excited hole can undergoes a fast relaxation within 1 ps via phonon emissions because hole level spacings are an order of magnitude smaller than those of electrons. This is due to the higher effective mass and the degeneracy of the valence band states. The electron-hole Coulomb interaction becomes stronger in smaller nanomaterials so that the rate of Auger cooling becomes faster in smaller QDs. To examine the Auger cooling in CdSe QDs experimentally, Klimov et al. examined femtosecond transient absorption experiments with CdSe QDs capped with bipyridine, which is a hole scavenger and thus photoexcited holes in CdSe QDs can be effectively trapped. This experiments showed that the relaxation time from $1P$(e) to $1S$(e) increased from ~300 fs to 3 ps due to the hole trapping.[78] However, if Auger cooling is a dominant relaxation process the relaxation time should be

much longer (over ns scale). This result indicates that other effective relaxation process exists in addition to Auger cooling.

Another possible effective passway of the $1P$(e)-$1S$(e) relaxation is the energy transfer to the vibrational states of capping reagents (Figure 1.4b). Guyot-Sionnest examined capping-reagent dependence of $1P$(e)-$1S$(e) relaxation in CdSe QDs by pump-probe IR experiments.[79,80] They showed that capping reagents also affect the $1P$(e)-$1S$(e) relaxation, in which 27 ps of the relaxation time was observed in 1-dodecanethiol capped CdSe QDs. In addition, they found that $1P$(e)-$1S$(e) relaxation time of multishell CdSe QDs coated with ZnS, ZnSe and CdSe and capped with alkanethiolate was over 1 ns.[81] This slower relaxation time is due to a thick ZnSe shell to separate electrons and holes and to increase the distance of the electronic states from capping reagents.

Above reports show that the relaxation passway of hot carriers occurs via initial multi-phonon emissions to the $1P$(e) or $1D$(e) state and subsequent competing process of Auger cooling and the energy transfer to capping reagents to the band-edge. Recently, another relaxation mechanism was observed in several QDs at high energy excitation, which is called carrier multiplication or multiple exciton generation (MEG).[49,58] Carrier multiplication is a process in which multiple excitons are generated at the band-edge by one photon absorption whose energy is over twice times of bandgap energy. The carrier multiplication process is much faster than other relaxation passway (less than 50 fs).[58] Details are expressed in the next section.

After hot carriers relax to the band-edge and form a band-edge exciton, single exciton relaxes to the ground state via radiative recombination, nonradiative recombination or trapping by defect states at the QD surface. Radiative recombination of the $1S$ state at room temperature occurs from the bright state. With the decrease of temperature, carriers cannot be thermally excited from the dark state to the bright state and radiative recombination from the

dark state is also observed, whose lifetime is optically forbidden and hundreds of ns to sub ms time scale.[82-84]

With the increase of pump intensity, one QD absorbs two or more photons. In this case, a new relaxation passway related to the carrier-carrier interaction is observed in addition to the single exciton relaxation. A typical relaxation process of the carrier-carrier interaction is Auger recombination. Auger recombination in semiconductors is the process that one excited electron interacts with another excited electron in the conduction band states. One interacted electron recombines with a hole in valence band states and the other electron is excited at higher states including ionized states. Auger recombination in semiconductor QDs strongly depends on the QD size and the lifetime of Auger recombination increases from ps to hundreds of ps with the increase of the size.[60] In addition, strong carrier-carrier interaction also induces multiexciton emissions such as biexciton and $1P$ emission.[85] Understanding of fundamental properties of Auger recombination and the multiexciton states in semiconductor QDs is important for the application to optical pumping and solar cells. Details are expressed in section **1.4** and **1.5**.

1.3 Carrier multiplication (Multiple exciton generation: MEG)

In principle, one photon whose energy is higher than the bandgap (E_g) can excite only one electron in semiconductors irrespective of the photon energy. The excited hot electron relaxes nonradiatively to the band edge via phonon emission and forms a single exciton. However, carrier multiplication can produce two or more band-edge excitons by one photon absorption (Figure 1.5). In bulk semiconductors, carrier multiplication has been observed repeatedly over the past five decades, both in elemental semiconductors such as germanium,[86] silicon[87] and also in lead chalcogenides.[88] However, the photon-to-carrier efficiency is quite low (at most

several %) and the energy threshold is high (higher than 4 E_g), and thus carrier multiplication in bulk semiconductors was difficult in practical use. In 2004, Klimov et al. discovered the efficient carrier multiplication over 200% in colloidal PbSe QDs.[49] After that, efficient carrier multiplication has been observed in various semiconductor QDs such as CdSe,[89] PbS,[58] PbTe,[90] Si,[91] InAs,[92] InP[93] and carbon nanotubes.[94] In addition to carrier multiplication in solution phase, carrier multiplication in a conductive film of colloidal PbS QDs has been also reported.[95,96] Recently, enhanced photoconductivity by carrier multiplication was observed in conductive films of colloidal PbS QDs.[97,59] Carrier multiplication in nanomaterials has great potentials for the photon-to-energy conversion systems such as third generation solar cells and the low threshold laser amplification.

1.4 Auger recombination

1.4.1 Auger recombination in bulk semiconductors

Auger recombination in semiconductors is firstly reported in 1940's.[98] After the theoretical reports by Beattie and Landsberg in 1959,[99] various experimental and theoretical studies on Auger recombination in semiconductors have been done.[100-110] In bulk materials, carriers have to conserve their energies and translational momenta simultaneously during Auger recombination because bulk semiconductors have band structures due to their periodicities of crystals structures. They form one electron band and three hole bands named heavy hole (hh), light hole (lh) and split-off hole (so). Because of these conservations, Auger recombination in bulk semiconductors strongly depends on temperature and the energy gap. Several kinds of Auger recombination have been proposed because of the splitting of hole bands. CHCC and CHHS processes are well-known examples of Auger recombination, where "C", "H" and "S" represent the conduction band, the heavy hole and the split-off band,

respectively. In indirect semiconductors, Auger recombination probability is suppressed because of the existence of few energy states conserved for energy and momentum. In the case of the strict conservation, Auger recombination occurs with a participation of phonons (phonon-assisted Auger recombination, Figure 1.6). Although theoretical calculations predict that phonon-assisted Auger recombination also occurs in direct-gap semiconductors, it is difficult to demonstrate experimentally because Auger recombination without phonons in direct-gap semiconductor also strongly depends on temperature.[111,112]

The kinetics model of Auger recombination in bulk semiconductors can be expressed as three-body process, two electrons and one hole, or one electron and two holes. Thus, the rate of Auger recombination is written by[107,110]

$$\frac{dN}{dt} = -k_{AR}\, n_e^2\, n_h \qquad \text{or} \qquad \frac{dN}{dt} = -k_{AR}\, n_e\, n_h^2 \tag{1.1}$$

where N, n_e, n_h and k_{AR} are the total carrier density, the electron density, the hole density and the Auger constant, respectively. In the case of molecules, the carrier-carrier interaction can be expressed as two-body process because carriers form excitons, so this process is called the exciton annihilation. In the case of bulk semiconductors, Coulomb interaction is so small that Auger recombination cannot be expressed as two-body process.

1.4.2 Auger recombination in semiconductor QDs

In the case of semiconductor QDs, Auger recombination is quite different from that in bulk semiconductors. The number of atoms per QD decreases and the periodical effect disappears, which induces the discrete electronic states and the relaxation of the translational momentum conservations. In addition, Coulomb interaction is greatly enhanced in QDs. For these reasons, Auger recombination occurs efficiently without the momentum conservations Figure 1.7).[60] The theoretical calculation of Auger recombination in semiconductor QDs is firstly established by Chepic et al. in 1990,[113] in which the lifetime of Auger ionization

obtained by theory is compared with the experimental result of glass-doped CdS QDs. The rate constant of Auger recombination in QDs is given by using Fermi's Golden Rule as below,[114]

$$\frac{1}{\tau_{AR}} = \frac{2\pi}{\hbar} \int |M_{if}|^2 \delta(E_i - E_f) d\Re_f \qquad (1.2)$$

where M_{if} is the electronic transition matrix element of the interparticle Coulomb interaction, $E_{i(f)}$ is the initial (final) energy of the system, and R_f is the complete set of variables quantifying the final state of the system. The theoretical calculation predicts that the lifetime of Auger recombination has the power-law dependence of the QD diameter (D), D^m, where m is the scaling index and varies $5 < m < 7$ depending on the band offset. The theoretical calculation also predicts that Auger recombination depend on the QD interface. In 2000, Klimov et al. have experimentally demonstrated that the Auger recombination lifetime of biexciton, triexciton and tetraexciton depends on D^3 in CdSe QDs.[60] They also demonstrated the same size dependence in PbSe, InAs and Ge QDs, so called "*V scaling*".[115] Efros considered that the difference of the scaling index between Auger recombination and Auger ionization comes from the final state of Auger process.[116] In Auger recombination, an Auger electron transits to a QD state that has finite density of states depending on the QD volume, while in Auger ionization it transits to outside of QD which has infinite density of states. They suggested that different size dependence of Auger recombination in CdSe QDs is due to the size dependence of the density of states, which is proportional to D^3. However, they do not examine detailed analysis and not mention the effect of the QD interface; therefore the detailed the size dependence of Auger recombination is still unclear.

The rate equation of Auger recombination based on three-body process is only appropriate in bulk semiconductors, where huge number of carriers exists and the experimental result can be assumed as average events. In the case of QDs, where the number of carriers is a few, the rate analysis should be done stochastically. Barzykin and Tachiya analyzed multiexciton

Auger processes in semiconductor QDs and nanowires by stochastic approach.[117] By using the stochastic model, the average number of excitons per QD ($\bar{n}(t)$) can be written by

$$\bar{n}(t) = \sum_{i=1}^{\infty} A_i \exp\left[-i\left(\frac{1}{\tau_1} + \frac{1}{2}(i-1)k_{ex}^{A}\right)t\right] \quad (1.3)$$

where τ_1 and k_{ex}^{A} are the lifetime of single exciton and the rate constant of Auger recombination, respectively. Coefficients, A_i, can be calculated by following equation,

$$A_i = \langle N_0 \rangle^i e^{-\langle N_0 \rangle}(r + 2i - 1)\sum_{j=0}^{\infty} \frac{\langle N_0 \rangle^j}{j!} \frac{\Gamma(r+i+j)}{\Gamma(r+2i+j)} \quad (1.4)$$

where $r = 2\gamma/\gamma_A$, γ and γ_A is the rate constant of lifetime of single exciton and of Auger recombination. $\langle N_0 \rangle$ and $\Gamma(x)$ are initial average numbers of excitons per QD and the gamma function, respectively. This calculation of A_i indicates that the ratio of multiexciton can be determined only by $\langle N_0 \rangle$, γ and γ_A. They calculated the ratio of the rate constant of single exciton, biexciton and triexciton and compared these calculations with the experimental result obtained by Klimov et al.[60] Barzykin and Tachiya concluded that Auger recombination in semiconductor QDs can be expressed with the stochastic two-body process rather than the stochastic three-body process.

1.5 Multiexciton states

When multiple excitons are generated in a QD additional electronic states are formed, which are called multiexciton states. Multiexcitons efficiently relax via Auger recombination in ps to hundreds of ps, and therefore multiexciton states can be observed by time-resolved spectroscopy.[85,118] In time-resolved emission spectroscopy, with filling the electronic states with carriers, Auger cooling between $1P$(e)- $1S$(e) is suppressed and the emission from 1P state can be observed in sub ps to tens of ps time scale (Figure 1.8). The spectral shift of the

biexciton emission as compared with the single exciton emission gives useful information about the biexciton binding energy of QDs. Experimental reports of the biexciton binding energy are mainly for epitaxial QDs such as GaAs and only a few report exist in colloidal QDs, however these reports of colloidal QDs are almost all for CdSe QDs.[119-122] The biexciton binding energy of bare CdSe QDs ranges from 10 to 35 meV, which is the "attractive" interaction. In the case of CdSe/CdS core/shell QDs, the biexciton binding energy is almost the same or relatively stronger than bare CdSe QDs for Type I configurations, and it suddenly decreases and becomes "repulsive" interactions for Type II configurations.[122]

1.6 Outline of this thesis

In this thesis, a general introduction of three dimensional confined semiconductor QDs and their fundamental optical properties induced by strong Coulomb interactions are given in Chapter 1. In Chapter 2, after the brief expression of the general growth mechanism and the synthetic method of colloidal semiconductor QDs, the synthetic procedures of CdTe QDs and CdS QDs capped with different materials and their basic information are respectively introduced. In Chapter 3, carrier multiplication in CdTe QDs was examined by single photon timing spectroscopy. From the fast decay component associated with Auger recombination, we firstly observed carrier multiplication in CdTe QDs. In Chapter 4, the size-dependent biexciton Auger recombination of CdTe QDs capped with different organic materials was examined. We observed different size dependence and concluded that Auger recombination in CdTe QDs depends on capping reagents or the thin gradient structure of thioglycolic acid capped CdTe QDs. In order to examine the effect of surface states on Auger recombination more precisely, the size-dependent biexciton Auger recombination was also examined in CdS QDs capped with different organic materials in Chapter 5. The size dependence of CdS QDs

is very similar irrespective of capping reagents and we concluded that Auger recombination only depends on the interfacial electronic structure rather than the surface defects and capping reagents of one monolayer level. In Chapter 6, the size dependence of multiexciton states in CdTe QDs was examined by time-resolved emission spectroscopy. The biexciton and triexciton binding energy was estimated from the energy shift of the biexciton emission. The triexciton binding energy of CdTe QDs was larger than the biexciton binding energy, which may come from the polarization nature of the $1S$ and $1P$ state. In Chapter 7, the effect of temperature on Auger recombination was examined in CdTe QDs, and the origin of the temperature dependence was discussed. Among several factors of temperature dependence, the participation of phonons in Auger recombination of semiconductor QDs was considered to the most likely possibility of the temperature dependence.

References

(1) Gaponenko, S. V. *Optical Properties of Semiconductor Nanocrystals*; Cambridge University Press: United Kingdom, 1998.

(2) Henglein, A. *Ber. Bunsenges. Phys. Chem.* **1982**, *86*, 301.

(3) Brus, L. E. *J. Chem. Phys.* **1983**, *79*, 5566.

(4) Ekimov, Al.; Onushuchenko, A. A. *Sov. Phys. -Semiconductors* **1982**, *16*, 775.

(5) Efros, Al.; Efros, Al. *Sov. Phys. -Semiconductors* **1982**, *16*, 772.

(6) Rossetti, R.; Nakahara, S.; Brus, L. E. *J. Chem. Phys.* **1983**, *79*, 1086.

(7) Henglein, A.; Gutierrez, M.; Fischer, C. *Ber. Bunsenges. Phys. Chem.* **1984**, *88*, 170.

(8) Weller, H.; Koch, H.; Gutierrez, M.; Henglein, A.; *Ber. Bunsenges. Phys. Chem.* **1984**, *88*, 649.

(9) Ramsden, J. J.; Gratzel, M. *J. Chem. Soc. Farad. Trans. 1* **1984**, *80*, 919.

(10) Nozik, A. J.; Williams, F.; Nenadavic, M. T.; Raja, T.; Micic, O. I. *J. Phys. Chem.* **1985**, *89*, 397.

(11) Brus, L. E. *J. Chem. Phys.* **1984**, *80*, 4403.

(12) Brus, L. E. *J. Phys. Chem.* **1986**, *90*, 2555.

(13) Nemeljokvic, J. M.; Nenadavic, M. T.; Micic, O. I.; Nozik, A. J. *J. Phys. Chem.* **1986**, *90*, 12.

(14) Steigerwald, M. L.; Alivisatos, A.P.; Gibson, J. M.; Harris, T.D.; Kortan, R.; Muller, A. J.; Thayer, A. M.; Duncan, T. M.; Douglass, D. C.; Brus, L. E. *J. Am. Chem. Soc.* **1988**, *110*, 3046.

(15) O'Neil, M.; Marohn, J.; McLendon, G. *J. Phys. Chem.* **1990**, *94*, 4356.

(16) Hoffman, A. J.; Mills, G.; Yee, H.; Hoffmann, M. R. *J. Phys. Chem.* **1992**, *96*, 5546.

(17) Spanhel, L.; Weller, H.; Fojtik, A.; Henglein, A. *Ber. Bunsenges. Phys. Chem.* **1987**, *91*, 88.

(18) Youn, H. -C.; Baral, S.; Fendler, J. H. *J. Phys. Chem.* **1988**, *92*, 6320.

(19) Kortan, A. R.; Hull, R.; Opila, R. L.; Bawendi, M. G.; Steigerwald, M. L.; Carrol, P. J.; Brus, L. E. *J. Am. Chem. Soc.* **1990**, *112*, 1327.

(20) Hoener, C. F.; Allan, K. A.; Bard, A. J.; Campion, M. A.; Fox, M. A.; Mallouk, T. E.; Webber, S. E.; White, J. M. *J. Phys. Chem.* **1992**, *96*, 3812.

(21) Zhou, H. S.; Honma, I.; Komiyama, H.; Haus, J. W. *J. Phys. Chem.* **1993**, *97*, 895.

(22) Murray, C. B.; Norris, D. J.; Bawendi, M. G. *J. Am. Chem. Soc.* **1993**, *115*, 8706.

(23) Alivisatos, A. P. *Science*, **1996**, *271*, 933.

(24) Peng, X.; Wickham, J.; Alivisatos, A. P. *J. Am. Chem. Soc.* **1998**, *120*, 5343.

(25) Kuno, M.; Lee, J. K.; Dabbousi, B. O.; Mikulec, F. V.; Bawendi, M. G. *J. Chem. Phys.* **1997**, *106*, 9869.

(26) Peng, X.; Schlamp, M. C.; Kadavanich, A. V.; Alivisatos, A. P. *J. Am. Chem. Soc.* **1997**, *100*, 8927.

(27) Dabbousi, B. O.; Rodriguez-Viejo, J.; Mikulec, F. V.; Heine, J. R.; Mattoussi, H.; Ober, R.; Jensen, K. F.; Bawendi, M. G. *J. Phys. Chem. B* **1997**, *101*, 9463.

(28) Yu, S. H.; Wu Y. S.; Yang, J.; Han, Z. H.; Xie, Y.; Qian, Y. T.; Liu, X. M. *Chem. Mater.* **1998**, *10*, 2309.

(29) Morales, A. M.; Lieber, C. M. *Science* **1998**, *279*, 208.

(30) Li, Y. D.; Liao, H. W.; Ding, Y.; Fan, Y.; ZhangY.; Qian, Y. T. *Inorg. Chem.* **1999**, *38*, 1382.

(31) Duan, X. F.; Liber, C. M.; *Adv. Mater.* **2000**, *12*, 198.

(32) Peng, X.; Manna, L.; Yang, W.; Wickham, J.; Scher, E.; Kadavanich, A.; Alivisatos, A. P. *Nature*, **2000**, *404*, 59.

(33) Chen, C. C.; Chao, C. Y. ; Lang, Z. H. *Chem. Mater.* **2000**, *12*, 1516.

(34) Peng, Z. A.; Peng, X. *J. Am. Chem. Soc.* **2001**, *123*. 1389.

(35) Rogach, A. L. *Semiconductor Nanocrystal Quantum Dots: Synthesis, Assmbly, Spectroscopy and Applicatioins*; Springer Wien New York, Austria, 2008.

(36) Peng, Z. A.; Peng, X. G. *J. Am. Chem. Soc.* **2001**, *123*, 183.

(37) Peng, Z. A.; Peng, X. G. *J. Am. Chem. Soc.* **2002**, *124*, 3343.

(38) Rogach, A. L.; Kastsikas, Kornowski, A.; Su, D. S.; Eychmullaer, A.; Weller, H. *Ber. Bunsenges. Phys. Chem.* **1996**, *100*, 1772.

(39) Gao, M.; Kirstein, S.; Mohwald, H.; Rogach, A. L.; Kornowski, A.; Eychmuller, A.; Weller, H. *J. Phys. Chem. B* **1998**, *102*, 8360.

(40) Gaponik, N.; Talapin, D. V.; Rogach, A. L.; Shevchenko, E. V.; Kornowski, A.; Eychmuller, A.; Weller, H. *J. Phys. Chem. B* **2002**, *106*, 7177.

(41) Talapin, D. V.; Koeppe, R.; Gotzinger, S.; Kornowski, A.; Lupton, J. M.; Rogach, A. L.; Benson, O.; Freedmann, J.; Weller, H. *Nano Lett.* **2003**, *3*, 1677.

(42) Carbone, L.; Nobile, C.; De Giorgi, M.; Sala, F. D.; Morello, G.; Pompa, P.; Hytch, M.; Snoeck, E.; Fiore, A.; Franchini, I. R.; Nadasan, M.; Sivestre, A. F.; Chiodo, L.; Kudera, S.; Cingolani, R.; Krahne, R.; Manna, L. *Nano Lett.* **2007**, *7*, 2942.

(43) Sitt, A.; Sala, F. D.; Menagen, G. ; Banin, U. *Nano Lett.* **2009**, *9*, 3470.

(44) Wang, X. Y.; Ren, X. F.; Kahen, K.; Hahn, M. A.; Rajeswaran, M.; Maccagnano-Zacher, S.; Silcox, J.; Cragg, G. E.; Efros, A. L.; Krauss, T. D. *Nature*, **2009**, *459*, 686.

(45) Maikov, G. I.; Vaxenburg, R.; Sashchiuk, A.; Lifshitz, E. *ACS Nano*, **2010**, *11*, 6547.

(46) Nozik, A. J. *Physica E* **2002**, *14*, 115.

(47) HuynhW. U.; Dittmer, J. J.; Alivisatos, A. P. *Science* **2002**, *295*, 2425.

(48) Robel, I.; Subramanian, V.; Kuno, M.; Kamat, P. V. *J. Am. Chem. Soc.* **2006**, *128*, 2385.

(49) Schaller, R. D.; Klimov, V. I. *Phys. Rev. Lett.* **2004**, *92*, 186601.

(50) Klimov, V. I.; MIkhailovsky, A. A.; Xu, S.; Malko, A.; Hollingworth, J. A.; Leatherdale, C. A.; Eisler, H. J.; Bawendi M. G. Science, 2000. 295, 314.

(51) Schaller, R. D.; Petruska, M. A.; Klimov, V. I. *J. Phys. Chem. B* **2003**, *107*, 13765.

(52) Klimov, V. I.; Ivanov, S. A.; Nanda, J.; Achermann, M.; Bezel, I.; McGuire, J. A.; Piryatinski, A. *Nature*, **2007**, *447*, 441.

(53) Chan, W. C. W.; Nie, S. M. *Science*, **1998**, *281*, 2016.

(54) Bruchez, M.; Moronne, M.; Gin, P.; Weiss, S.; Alivisatos, A. P. *Science* **1998**, *281*, 2013.

(55) Medintz, I. L.; Uyeda, H. Y.; Goldman, E. R.; Mattoussi, H. *Nature Mater.* **2005**, *4*, 435.

(56) Chen, G.; Bonadeo, N. H.; Steel, D. G.; Gammon, D.; Katzer, D. S.; Park, D.; Sham, L. J. *Science* **2000**, *289*, 1906.

(57) Beveratos, A.; Brouri, R.; Gacoin, T.; Villing, A.; Poizat, J. P.; Grangier, P. *Phys. Rev. Lett.* **2002**, *87*, 187901.

(58) Ellingson, R. J.; Beard, M. C.; Johnson, J. C.; Yu, P. R.; Micic, O. I.; Nozik, A. J.; Shavaev, A.; Efros, A. L. *Nano Lett.* **2005**, *5*, 865.

(59) Sambur, J. B.; Novet, T.; Parkinson, B. A. *Science* **2010**, *330*, 63.

(60) Klimov, V. I.; Mikhailovski, A. A.; McBranch, D. W.; Leatherdale, C. A.; Bawendi, M. G. *Science* **2000**, *287*, 1011.

(61) Klimov, V. I. *Ann. Rev. Phys. Chem.* **2007**, *58*, 635.

(62) Klimov, V. I. *Semiconductor and Metal Nanoparticles*;

(63) Allan, G.; Delerue, C.; Lannoo, M. *Phys. Rev. Lett.* **1996**, *76*, 2961.

(64) Chen, W.; Wang, Z. G.; Lin, Z. J.; Lin, L. Y. *J. Appl. Phys.* **1997**, *82*, 3111.

(65) Frantsuzov, P. A.; Marcus, R. A. *Phys. Rev. B* **2005**, *72*, 155321.

(66) Jones, M.; Lo, S. S.; Scholes, G. D. *J. Phys. Chem. C* **2009**, *113*, 18632.

(67) Hasselbarth, A.; Eychmuller, A.; Weller, H. *Chem. Phys. Lett.* **1993**, *203*. 271.

(68) Spanhel, L.; Hasse, M.; Weller, H.; Henglein, A. *J. Am. Chem. Soc.* **1987**, *109*, 5649.

(69) Efros, Al. L.; Rosen, M. *Phys. Rev. B* **1998**, *58*, 7120.

(70) Prado, S. J.; Trallero-Giner, C.; Alcalde, A. M.; Lopez-Richard, V.; Marques, G. E. *Phys.*

Rev. B **2003,** *68*, 235327.

(71) Nirmal, M.; Norris, D. J.; Kuno, M.; Bawendi, M. G.; A. L. Efros,; Rosen, M. *Phys. Rev. Lett.* **1995**, *75*, 3728.

(72) Efros, A. L.; Rosen, M.; Kuno, M.; Nirmal, M.; Norris, D. J.; Bawendi, M. G. *Phys. Rev. B* **1996**, *54*, 4843.

(73) Norris, D. J.; Sacra, A.; Murray, C. B.; Bawendi, M. G. *Phys. Rev. Lett.* **1994**, *72*, 2612.

(74) Conwell, E. *High Field Transport in Semiconductors*; Academic, New York, 1967.

(75) Bockelmann, U.; Bastard, G. *Phys. Rev. B* **1990**, *42*, 8947.

(76) Benisty, H.; Sotomayor-Torres, C. M.; Weisbuch, C. *Phys. Rev. B* **1991**, *44*, 10945.

(77) Efros, A. L.; Kharchenko, V. A.; Rosen, M. *Solid State Commun.* **1995**, *93*, 281.

(78) Klimov, V. I.; Mikhailovski, A. A.; McBranch, D. W.; Leatherdale, C. A.; Bawendi, M. G. *Phys. Rev. B* **2000**, *61*, 13349.

(79) Guyot-Sionnest, P.; Shim, H.; Matranga, C.; Hines, M. *Phys. Rev. B* **1999**, *60*, R2181.

(80) Guyot-Sionnest, P.; Wehrenberg, B.; Yu, D. *J. Chem. Phys.* **2005**, *123*, 074709.

(81) Pandey, A.; Guyot-Sionnest, P.; *Science* **2008**, *322*, 929.

(82) Klimov, V. I. *J. Phys. Chem. B* **2006**, *110*, 16827.

(83) Oron, D.; Aharoni, A.; Donega, C. M.; Rijssel, J.; Meijerink, A.; Banin, U. *Phys. Rev. Lett.* **2009**, *102*, 177402.

(84) Califano, M.; Franceschetti, A.; Zunger, A. *Nano Lett.* **2005**, *5*, 2360.

(85) Achermann, M.; Hollingsworth, J. A.; Klimov V. I. *Phys. Rev. B* **2003**, *68*, 245302.

(86) Tauc, J. *J. Phys. Chem. Solids* **1959**, *8*, 219.

(87) Kolodinski, S.; Werner, H.; Wittchen, T.; Queisser, H. J. *Appl. Phys. Lett.* **1993**, *63*, 2405.

(88) Baryshev, N. S.; Shchetinin, M. P.; Chashchin, S. P.; Kharionovski, Y. S.; Averyanov, IS. *Sov. Phys. Semicond.* **1974**, *8*, 194.

(89) Schaller, R. D.; Petruska, M. A.; Klimov, V. I. *Appl. Phys. Lett.* **2005**, *87*, 253102.

(90) Murphys, J. E.; Beard, M. C.; Norman, A. G.; Ahrenkiel, S.P.; Johnson, J C.; Yu, P. R.; Micic, O. I.; Ellingson, R. J.; Nozik, A. J. *J. Am. Chem. Soc.* **2006**, *128*, 3241.

(91) Beard, M. C.; Knutsen, K. P.; Yu, P. R.; Luther J. M.; Song, Q.; Metzger, W. K.; Ellingson, R. J.; Nozik, A. J. *Nano Lett.* **2007**, *7*, 2506.

(92) Schallaer, R. D.; Pietryga, J. M.; Klimov, V. I. *Nano Lett.* **2007**, *7*, 3469.

(93) Stubbs, S. K.; Hardman, S. J. O.; Graham, D. M.; Spencer, B. F.; Flavell, W. R.; Glavery, P.; Masala, O.; Pickett, N. L.; Binks, B. J. *Phys. Rev. B* **2010**, *81*, 081303.

(94) Ueda, A.; Matsuda, K.; Kanemitsu, Y. *Appl. Phys. Lett.* **2008**, *92*, 233105.

(95) Beard, M. C.; Midgett, A.G.; Law, M.; Semonin, O. E.; Ellingson, R. J.; Nozik, A. J. *Nano Lett.* **2009**, *9*, 836.

(96) Luther, J. M.; Beard, M. C.; Song, Q.; Law, M.; Ellingson, R. J.; Nozik, A. J. *Nano Lett.* **2007**, *7*, 1779.

(97) Sukhovatkin, V.; Hinds, S.; Brzozowski, L.; Srgent, E. H. *Science* **2009**, *324*, 542.

(98) Landsberg, P. T. *Recombination in Semiconductors*; Cambridge University Press, Cambridge, 1991.

(99) Beattie, A. R.; Landsberg, P. T. *Proc. R. Soc. Lond. A* **1959**, *249*, 16.

(100) Landsberg, P. T.; Rhys-Roberts, C.; Lal, P. *Proc. Phys. Soc.* **1964**, *84*, 915.

(101) Hill, D. *Proc. R. Soc. Lond. A* **1976**, *347*, 565.

(102) Emtage, P. R. *J. Appl. Phys.* **1976**, *47*, 2565.

(103) Haug, A. *Solid State Commun.* **1977**, *22*, 537.

(104) Haug, A. *Solid State Commun.* **1978**, *28*, 291.

(105) Lochmann, W. *Phys. Stat. Sol. (a)* **1978**, *45*, 423.

(106) Dutta, N. K.; Nelson, R. J. *Appl. Phys. Lett.* **1981**, *38*, 407.

(107) Sermage, B.; Heritage, J. P.; Dutta, N. K. *J. Appl. Phys.* **1985**, *57*, 5443.

(108) Haug, A. *J. Phys. C: Solid State Phys.* **1987**, *20*, 1293.

(109) Jiang, Y.; Teich, M. C.; Wang, W. I.; Meyer, J. R. *J. Appl. Phys.* **1992**, *71*, 3394.

(110) Klann, R.; Hofer, T.; Buhleier, R.; Elsaesser, T.; Tomm, J. W. *J. Appl. Phys.* **1995**, *77*, 277.

(111) Takeshima, M. *Jpn. J. Appl. Phys.* **1983**, *22*, 491.

(112) Nee, T. –E.; Chen, C. –C.; Lin, R. –M. *Jpn. J. Appl. Phys.* **2004**, *43*, 890.

(113) Chepic, D. I.; Efros, A. L.; Ekimov, A. I.; Vanov, M. G.; Kharchenko, V. A.; Kudriavtsev, I. A.; Yazeva, T. V. *J. Lumin.* **1990**, *47*, 113.

(114) Cragg, G. E.; Efros, A. L. *Nano Lett.* **2010**, *10*, 313.

(115) Robel, I.; Gresback, R.; Kortshagen, U.; Scaller, R. D.; Klimov, V. I. *Phys. Rev. Lett.* **2009**, *102*, 177404.

(116) Efros, A. L.; Lockwood, D. J.; Tsybeskov, L. *Semiconductor Nanocrystals: From Basic to Principles to Applications*; Plenum, New York, 2000.

(117) Barzykin, A. V.; Tachiya, M. *J. Phys.: Condens. Matter* **2007**, *19*, 065105.

(118) Caruge, J. M.; Chan Y. T.; Sundar, V.; Eisler, H. J.; Bawendi, M. G. *Phys. Rev. B* **2004**, *70*, 085316.

(119) Bonati, C.; MohamedM. B.; Tonti, D.; Zgrablic, G.; Haacke, S.; van Mourik, F.; Chergui, M. *Phys. Rev. B* **2005**, *71*, 205317.

(120) Oron, O.; Kazes, M.; Shweky, I.; Banin, U. *Phys. Rev. B 2006*, *74*, 115333.

(121) Oron, O.; Kazes, M.; Banin, U. *Phys. Rev. B 2007*, *75*, 035330.

(122) Sitt, A.; Della, S. F.; Menagen, G.; Banin, U. *Nano Lett.* **2009**, *9*, 3470.

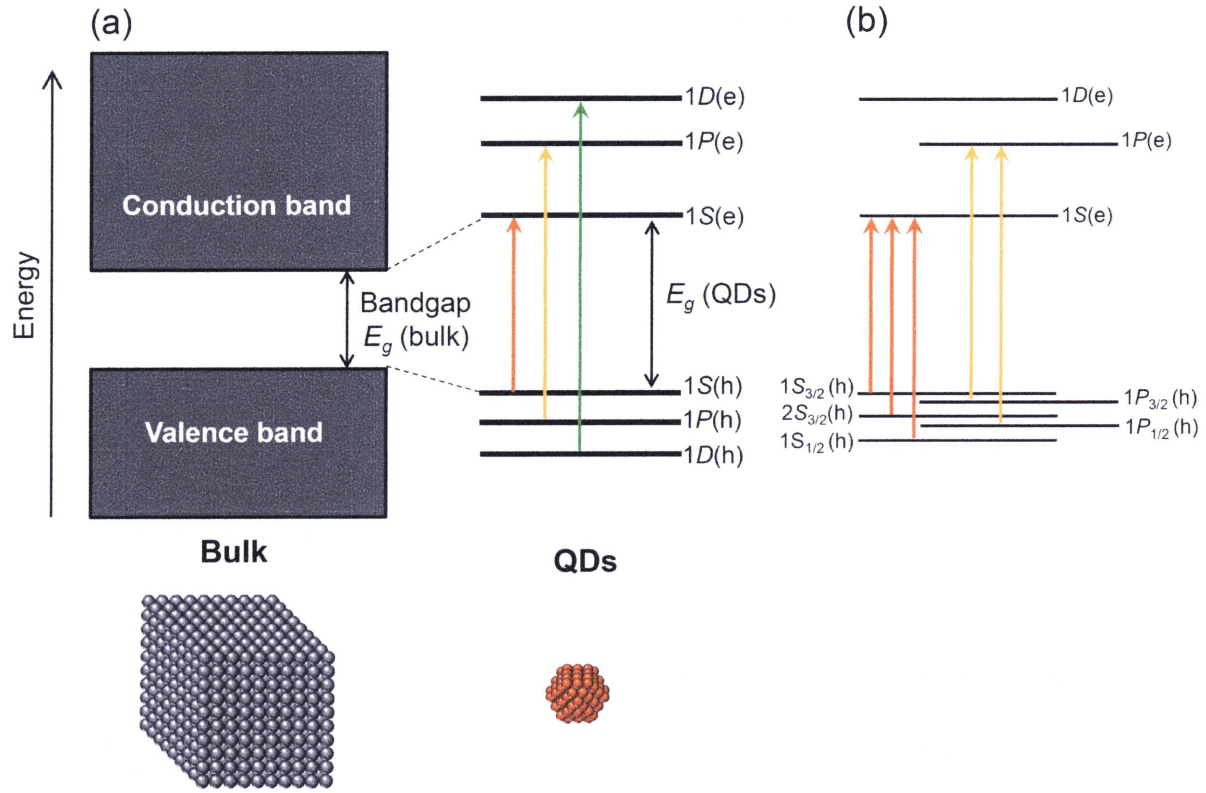

Figure 1.1 (a) Illustration of bulk semiconductors and semiconductor QDs and their energy diagrams. (b) Illustration of energy states by the combination of the total angular momentum.

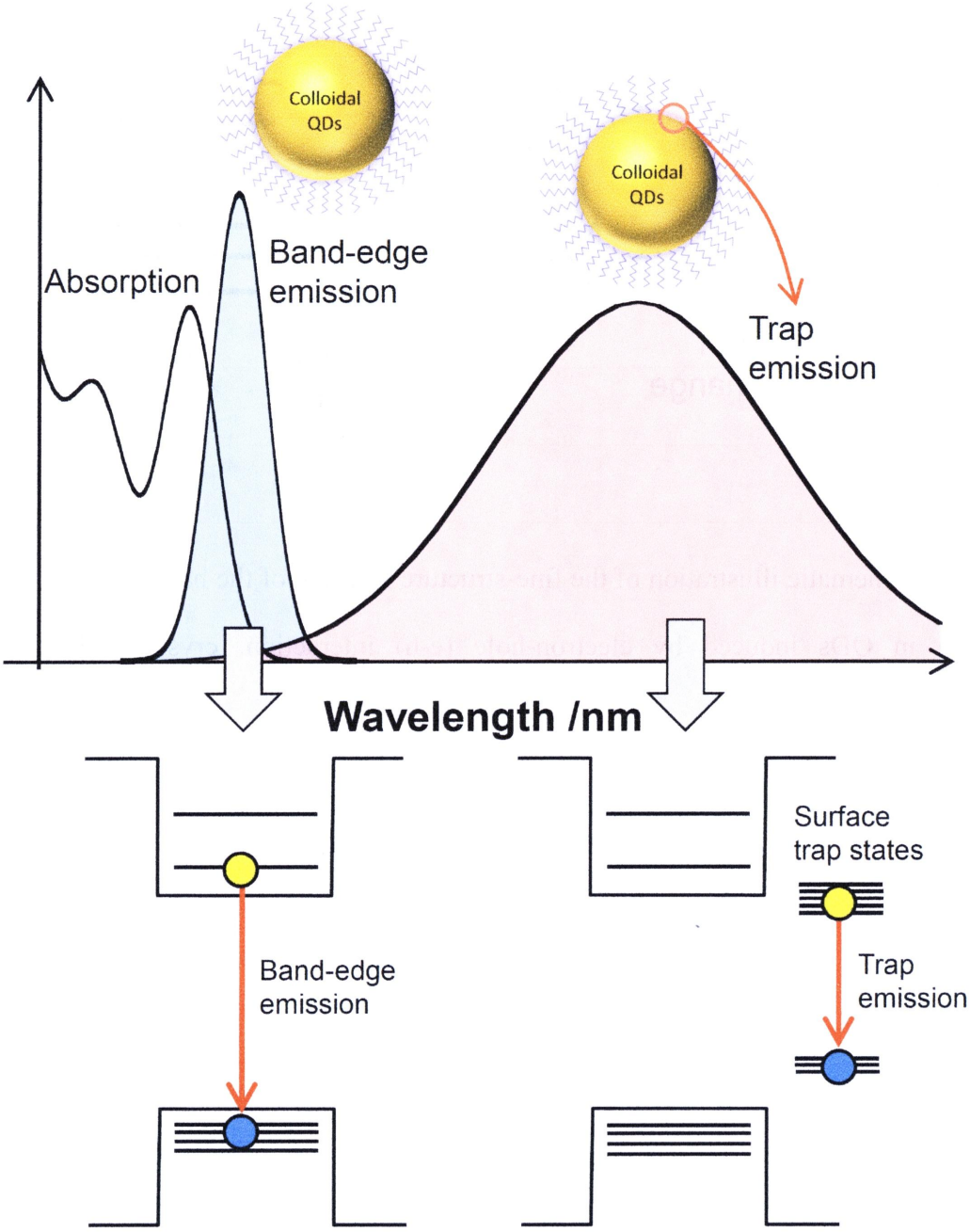

Figure 1.2 Steady-state absorption spectrum of semiconductor QDs and their emission spectra from the band-edge and surface trap states.

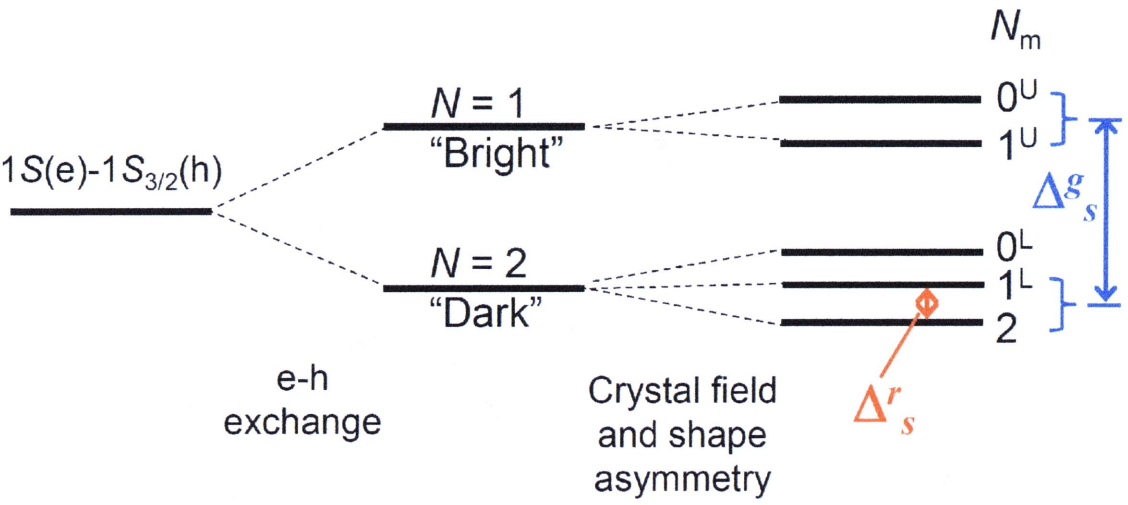

Figure 1.3 Schematic illustration of the fine-structure splitting of the band-edge $1S(e)$-$1S_{3/2}(h)$ transition in QDs induced by electron-hole (e-h) interaction, crystal field and shape asymmetry.

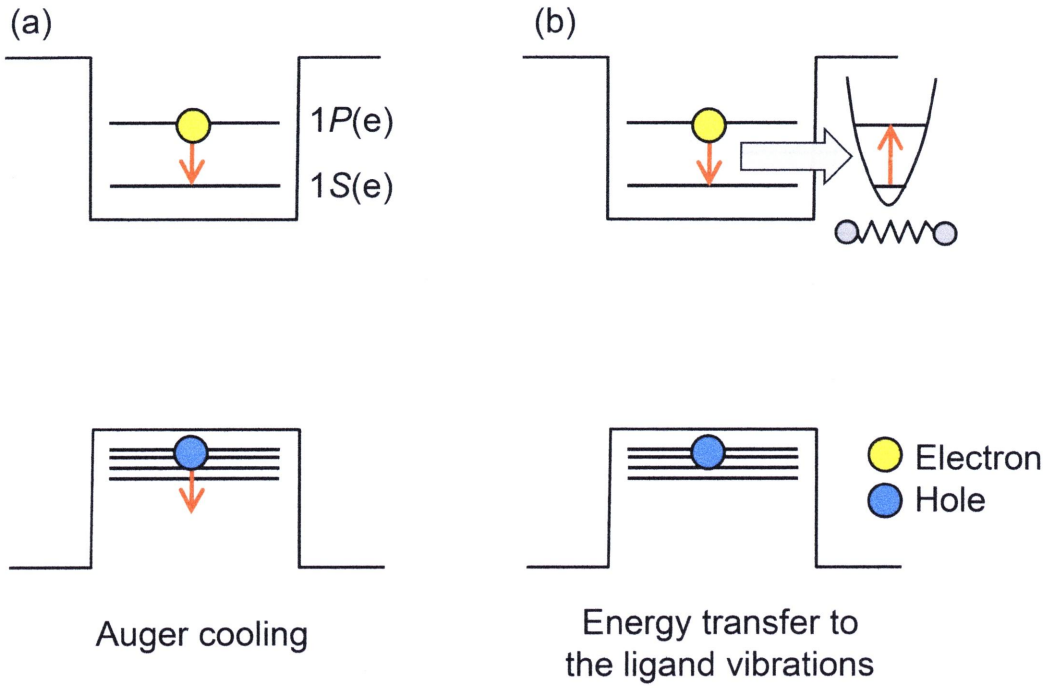

Figure 1.4 Energy relaxation of hot electrons between 1*S*(e)-1*P*(e) via Auger cooling (a) and the energy transfer to the ligand vibrations (b).

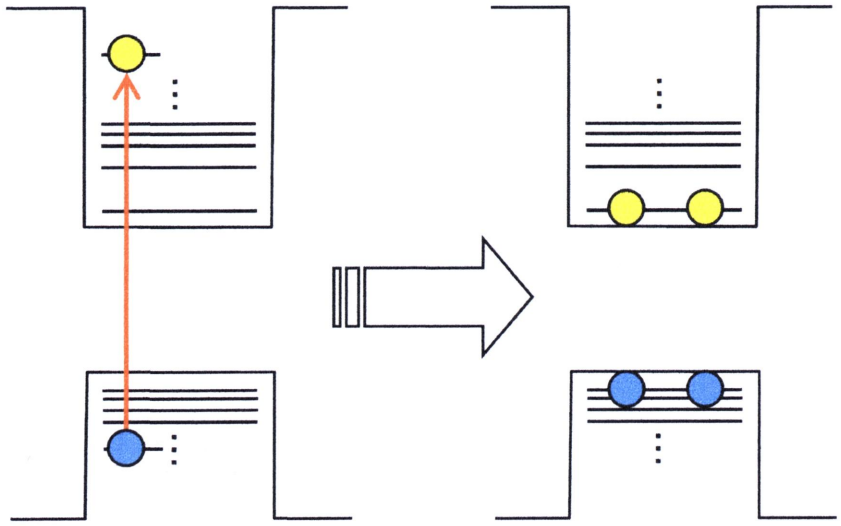

Figure 1.5 Concept of carrier multiplication. In carrier multiplication process, multiple e-h pairs can be generated by one photon absorption whose energy is over twice time of the energy gap.

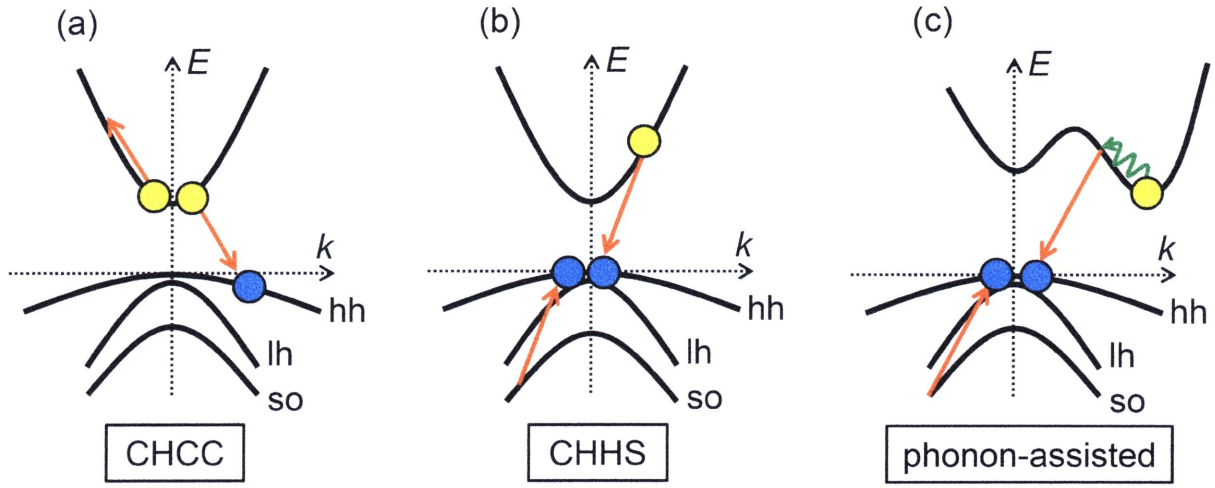

Figure 1.6 Examples of Auger recombination in bulk semiconductors. (a) and (b) are CHCC and CHHS Auger recombination in direct-gap semiconductors. "C", "H" and "S" represent "Conduction band", "Heavy hole band" and "split-off band", respectively. (c) is phonon-assisted Auger recombination in indirect-gap semiconductors. A green winding arrow represents phonon processes.

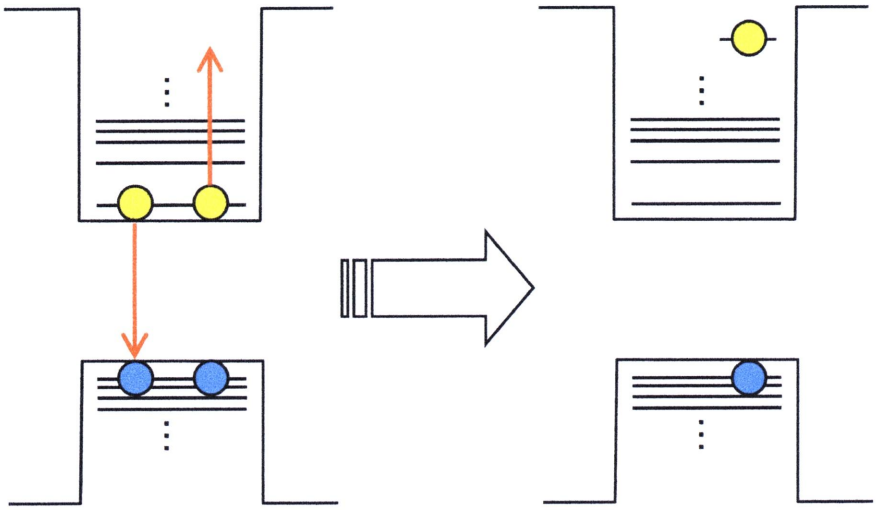

Figure 1.7 Concept of Auger recombination in semiconductor QDs.

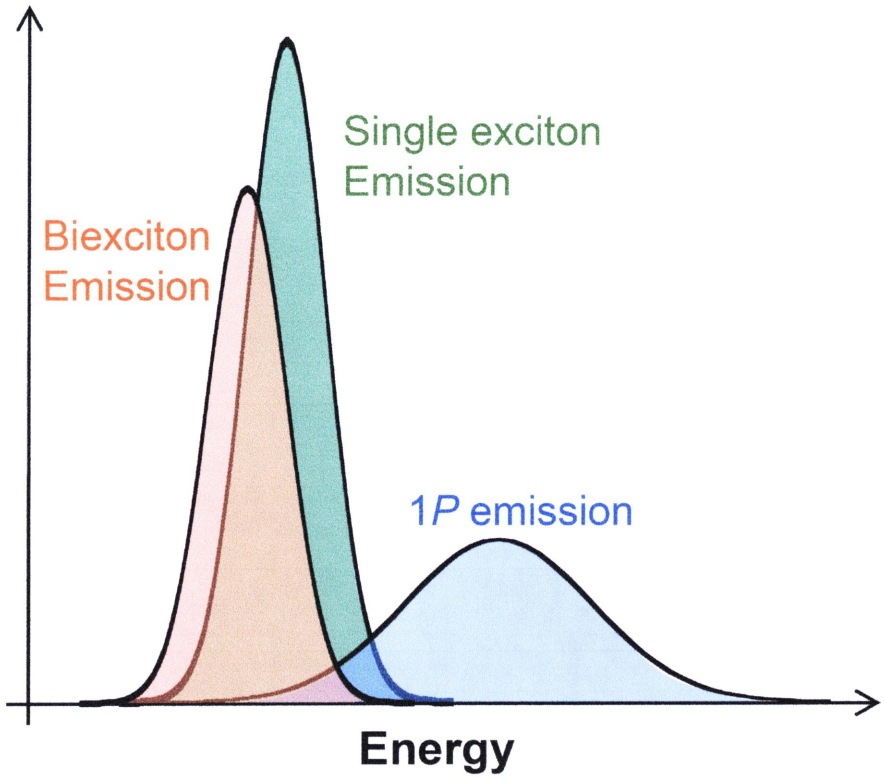

Figure 1.8 Typical multiexciton emission spectra of semiconductor QDs obtained from time-resolved and intensity-dependent emission spectroscopy. The emission from the 1*P* state can be observed in the presence of triexciton.

Chapter 2
Synthesis of colloidal CdTe QDs and CdS QDs and their characteristics

2.1 How to synthesize colloidal QDs: general growth mechanism

2.1.1 Introduction

Tunability of various physical and chemical properties of materials by varying the size in the region of nanometer has opened up many new directions in several fields of current research and modern technologies. In particular, the study of systematic changes in the electronic structure of QDs as a function of size has intensively been investigated in recent times. One of the major aspects necessary for the actual realization of technical applications is the ability to synthesize nanocrystals of the required size with a controlled size distribution. Although there is a popular belief that the growth of nanocrystals in solution occurs via diffusion limited Ostwald ripening process, the optimal condition is the main difficulty of these methods and, therefore, they are arrived at essentially in an empirical and intuitive manner.

The general growth mechanism of colloidal particles has been reported in 1950's by La Mer and coworkers.[1,2] They studied extensively nucleation and growth in sulfur sols, from which they developed an understanding of the mechanism for the formation of colloids or nanocrystals from a homogeneous and super saturated medium. Their mechanism suggest that a synthesis of the colloid should be designed in such a way that 1) the concentration increases rapidly, 2) the concentration rises above the saturation for a brief period and 3) a short burst of nucleation occurs with the formation of a large number of nuclei in a short space of time. These particles grow rapidly and lower the concentration below the nuclei level, and then particles further grow at a rate determined by the slowest step in the growth process. La Mer's mechanism is schematically depicted by means of the simple diagram shown in Figure 2.1. In this way, the growth mechanism of colloidal particles is divided into two parts: the nucleation event in which particles spontaneously form through an assembly of freely dispersed atoms and the actual growth process. We regard spherical QDs as model system.[3]

In this chapter, the introduction and the general growth mechanism are given in 2.1. Synthetic methods of colloidal CdTe and CdS QDs are introduced in 2.2 and 2.3, respectively.

2.1.2 General growth mechanism of colloidal particles: "Nucleation"[4]

The first step in the growth of colloidal QDs is the nucleation. Through a density fluctuation of the medium several atoms assemble to a small crystal that is thermodynamically stable and thus does not decay to free atoms or ions. In that sense, the nucleation can be understood as the overcoming the activation barrier between the crystalline phase and the solution phase, in which the atoms are dispersed freely. At the simplest, the driving forces in the nucleation event can be reduced two factors, the chemical potential in the system and the total surface energy. Upon the formation of a spherical nucleus consisting of n atoms the total free energy of the system changes by

$$\Delta G = n(\mu_c - \mu_s) + 4\pi r^2 \sigma \qquad (2.1)$$

where μ_c and μ_s are the chemical potentials of crystal and the solution phase respectively, r is the radius of the nucleus and σ the surface tension. In the equation, the surface term constitutes the main difference between QDs and bulk crystals, which is important in QDs whereas it can be neglected in bulk crystals. In the equation, σ is assumed to be constant for any size and morphology of the crystal. Although it is very rough approximation, it is good for the qualitatively understanding. In order to understand more precisely, we have to take into account an effect related to the small size of QDs and an effect of the faceting of QDs.

2.1.3 General growth mechanism of colloidal particles: "Growth"

The actual process of the deposition of monomers onto the growing QDs can be split into two steps. First the monomers have to be transported toward the surface of the QDs and in the second process they have to react with the QDs. When the concentration of monomers is high,

the growth rate depends only on the reaction rate of the monomer with the nuclei because monomers are available whenever there is a free site for QD incorporation into a growing crystal. The growth rate (dr/dt, r represent a crystal radius) is described by

$$\frac{dr}{dt} = \frac{1}{4\pi r^2 d_m}\left(\frac{dn}{dt}\right) \tag{2.2}$$

where d_m denotes the density of monomers in the crystal and dn/dt is the derivative of number of monomers in the crystal solved for the growth.

After a while reservoir of monomers is partially depleted and growth rate is dictated by the rate at which monomers reach the surface of the crystal. The following process can be understood by diffusion-controlled process, which is expressed by Fick's law of diffusion:

$$J(x > r) = 4\pi x^2 D \frac{dC}{dx} \tag{2.3}$$

where J is the flux of monomers towards a growing crystal and C is the concentration of monomers. By introducing the monomer concentration C_i on the surface of the crystal and the monomer concentration C_b in the bulk of the solution, the rate of the growth can be calculated as follows,

$$\frac{dr}{dt} = \frac{D}{r d_m}(C_b - C_i) \tag{2.4}$$

To this point an infinite stability of the nanocrystals is assumed. However, this assumption cannot be maintained. In order to express a competing effect to the growth, the Gibbs-Thompson effect should be introduced.[5] According to this effect, the smaller the crystal is the higher the vapor pressure of the crystals is, and thus monomers evaporate into solution more easily from smaller crystals than from larger ones. By using this effect, the diffusion-controlled growth rate can be calculated as follows,[6,7]

$$\frac{dr}{dt} = \frac{2\sigma D C_\infty}{d_m^2 k_B T}\frac{1}{r}\left(\frac{1}{r^*} - \frac{1}{r}\right) \tag{2.5}$$

where C_∞ is the vapor pressure of a flat surface, r^* is the critical size of the growth process and k_B is the Boltzmann constant. In the regime around $r = r^*$, the smallest QDs melt to free monomers that are incorporated into the larger QDs, which is called Ostwald ripening regime.

2.2 Synthesis of colloidal CdTe QDs

2.2.1 *n*-tetradecylphosphonic acid (TDPA) capped QDs

a) Synthesis

n-Tetradecylphosphonic acid (TDPA; 98%) was purchased from Alfa Aesar. 1-Octadecene (ODE; 90.0%) was obtained from Wako Pure Chemical Industries, Ltd. Tellurium (Te; 99.999%) and cadmium oxide (CdO, 99%) were purchased from Kojundo Chemical Laboratory and Kanto Chemical Co. respectively. *n*-Hexane, chloroform and methanol were special grade from Kishida Chemical. Co. Inc.

TDPA-capped CdTe QDs were prepared by high temperature colloidal methods in organic solvents reported in the literature.[8] Briefly, a mixture of CdO (0.0256 g, 0.20 mmol), TDPA (0.0114 g, 0.41 mmol), and technological-grade ODE (8.0 g) was heated to 300 °C to get a clear solution. A 4-g solution of Te (0.050 g, 0.4 mmol, dissolved in 0.95 g of TBP and diluted by 3.0 g of ODE) was quickly injected into this hot solution, and then the reaction mixture was allowed to cool to 250 °C for the growth of CdTe nanocrystals. Aliquots of growing CdTe QDs at high temperature were taken out at different reaction times, mixed with *n*-hexane and stored under nitrogen. The synthesis was carried out under nitrogen with a glove box. Unreacted cadmium precursors were separated by the extraction method.[11] After the extraction, hexane/ODE phase containing QDs was precipitated with acetone. The precipitate was isolated by centrifugation and decantation. The final product was redissolved in hexane for carrier multiplication experiments.

b) Basic information

Figure 2.3 shows steady-state absorption and emission spectra of TDPA capped CdTe QDs. A sharp peak at the band-edge and two shoulders are observed in absorption spectra, which are attributed to $1S_{3/2}$(h)-$1S$(e), $2S_{3/2}$(h)-$1S$(e) and $1P_{3/2}$(h)-$1P$(e), respectively.[9] In emission spectra, almost all spectral shapes are expressed as a single Gaussian function attributed to the band-edge emission, although a few spectra have a small shoulder at the shorter wavelength of the band-edge emission. It disappears after the extraction. Average QD diameters (D, nm) are calculated from the $1S$(e)-$1S_{3/2}$ (h) absorption peak obtained from the experimental fitting function,[8]

$$D = (9.827 \times 10^{-7})\lambda^3 - (1.7147 \times 10^{-3})\lambda^2 - (1.0064)\lambda - 194.84 \quad (2.6)$$

where λ is the band-edge absorption peak (nm). The energy gap (E_g) was calculated from the exploration of the band offset. D and E_g of TDPA capped CdTe QDs were 3.6-5.4 nm and 1.93-1.73 eV, respectively. The luminescence quantum yields (Φ) of TDPA capped CdTe QDs were determined at room temperature by comparing the integrated emission spectrum of the CdTe QDs in solution to the emission spectrum of rhodamine B in ehanol and were less than 10% in all samples. These samples were used for carrier multiplication experiments in Chapter 3.

2.2.2 Thioglycolic acid (TGA) capped CdTe QDs

a) Synthesis

Cadmium perchlorate hexahydrate [$Cd(ClO_4)_2 \cdot 6H_2O$] and aluminum telluride (Al_2Te_3) lumps were purchased from Strem Chemicals and MP Biomedicals Inc., respectively. Thioglycolic acid (TGA) were purchased from Aldrich Chemical Co. The water used throughout this research was obtained from Milli-Q water purification system (Yamato, Millipore WQ 500). All chemicals were used without further purification.

Water-soluble CdTe QDs capped with TGA were prepared according to the procedure reported in the literature.[10-12] In a typical synthesis 2.6 mmol $Cd(ClO_4)_2 \cdot 6H_2O$ was dissolved in 200 mL water and 3.4 mmol TGA was added followed by adjusting pH = 10.0 with 1 M NaOH solution under vigorous stirring. The solution was continuously stirred until the solution became optically clear. Separately 1.2 mmol Al_2Te_3 chunks was placed in a 50 mL three-neck flask. 20 mL of 1 M H_2SO_4 solution was added dropwise into the Al_2Te_3 chunks to produce H_2Te gas, and the gas passed through the previous resulting mixture with a slow N_2 flow for 20 min. The CdTe precursors are formed at this stage, which is accompanied by yellow color. The molar ratio of Cd^{2+}: TGA: Te^{2-} was fixed at 1:1.3:0.47. The size of the QDs was controlled by the reflux time and was monitored by absorption and luminescence spectra.

b) Basic information

We observed steady-state absorption and emission spectra of TGA-capped CdTe QDs. Figure 2.4 shows that both absorption and emission spectra are broader in TGA-capped CdTe QDs as compared with TDPA-capped CdTe QDs, and thus $2S_{3/2}$(h)-$1S$(e) and $1P_{3/2}$(h)-$1P$(e) peak were difficult to resolve in absorption spectra. Average QD diameters of TGA-capped CdTe QDs were determined from the $1S_{3/2}$(h)-$1S$(e) peak, which is calculated by the tight binding model.[13] The previous method for the determination of D in the last section cannot be applied because the empirical equation can only apply to relatively lager QDs (over 550 nm of absorption peak). Calculated D was 2.3 to 3.5 nm. Besides, other researcher conducted X-ray diffraction measurements of TGA-capped CdTe QDs and concluded that some cubic CdS components are included in cubic CdTe QDs due to the prolonged reflux in the presence of TGA (Figure 2.5).[14] These results suggest that thin CdS gradients are also formed at the surface of CdTe QDs capped with TGA in our experiments. Φ of TDPA-capped CdTe QDs were determined at room temperature by comparing the integrated emission spectra of the CdTe QDs in solution to the emission spectra of rhodamine B or coumarin343 in ehanol. Φ

increased gradually with the increase of the reflux time, and then decreased. Φ ranged from ~10 to 40% depending on the reflux time, the ratio of Cd and TGA, and pH of the solution.[15,16] These samples were used for size- and capping reagent-dependent Auger recombination experiments in Chapter 4.

2.2.3 Oleic acid and trioctylphosphine (OA/TOP) capped CdTe QDs

a) Synthesis

Trioctylphosphine (TOP) and oleic acid (OA) were purchased from Alfa Aesar and Kishida Chemical Co., respectively. Tellurium powder and CdO powder were purchased from Kojundo Chemical Laboratory Co. and Aldrich Chemical Co., respectively. All chemicals were used without further purification.

CdTe QDs capped with OA/TOP was prepared according to the procedure reported in the literature.[17] The synthesis of CdTe QDs was initiated by the preparation of the precursor solutions under inert conditions in a standard glovebox. In a typical synthesis the Te precursor solution was prepared by dissolving 0.1 mmol of Te in 0.25 mL of TOP. The solution was further diluted with 1-octadecene to a total of 2.5 mL. The Cd precursor solution was prepared by mixing 0.2 mmol of CdO with 200 μL of OA in 10 mL of 1-octadecene solution. The Cd solution was heated to 100 °C for 40 min in a vacuum in a three-neck flask, removing the water contents and resulting in the appearance of a homogeneous red mixture. The system was flushed by dry Ar gas and the temperature was raised to 300 °C, followed by the formation of a homogeneous transparent solution and the generation of ($Cd(OA)_2$). When the solution was further heated to 310 °C for ~10 min, an additional gray precipitate appeared, which was characterized as crystalline Cd_0 nanoparticles. When the TOP/Te precursor solution was injected into the three-neck flask ~1 min after the first appearance of the gray precipitate, the nucleation of the CdTe QDs took place. The solution color was changed

immediately and a temperature was dropped to 250 °C, where further growth of the CdTe QDs took place. The growth of the QDs occurred during the 1-5 min, with the solution gradually changing its color from yellow to red. Aliquots of the prepared CdTe QDs were drawn periodically from the reaction. Cooling the aliquots to room temperature quenched the QDs growth. These aliquots were then centrifuged to precipitate the crystalline Cd_0 nanoparticles and separate them from the CdTe QDs' colloidal solution. The CdTe QDs was isolated from the remaining organic solution by the addition of an ethanol/acetone mixture (1:1) and by additional centrifugation. Purified CdTe QDs had been redissolved in hexane.

b) Basic information

We observed steady-state absorption and emission spectra of OA/TOP-capped CdTe QDs. Figure 2.6 shows that a sharp peak at the band-edge and two shoulders attributed to $1S_{3/2}$(h)-$1S$(e), $2S_{3/2}$(h)-$1S$(e) and $1P_{3/2}$(h)-$1P$(e) were observed in absorption spectra while single Gaussian-like spectra attributed to the band-edge emission were clearly observed in emission spectra. They are similar to those of TDPA capped CdTe QDs. Average QD diameters of OA/TOP-capped CdTe QDs were estimated to 2.6-4.5 nm by using previous two methods.[8,13] Figure 2.7 shows transmission electron microscopy (TEM; Tecnai G2 F20 200keV, FEI) images of a typical OA/TOP capped CdTe QDs. Homogeneous and spherical QDs were clearly observed and the average QD diameter is ~3.9 nm, which is fairly consistent with the size obtained from the absorption peak D = 3.9 nm. Φ of OA/TOP capped CdTe QDs were determined as similar to that of TDPA capped CdTe QDs and ranged from 50 to 90% for D = 3.3-4.5 nm. However, Φ decreased steeply below D = 3.3 nm due to the synthesis limit and Φ were 15-30% for D = 2.6-3.2 nm. These high Φ are probably due to the presence of Cd_0 nanoparticles during the synthesis, which controls the concentration of Cd in solution and thus the optimal reaction rate to minimize defects could be achieved.[17]

2.3 Synthesis of colloidal CdS QDs

2.3.1 *L*-glutathione (GSH) capped CdS QDs

a) Synthesis

L-glutathione (GSH, >99%) and thiourea (98.0%) were purchased from Wako Pure Chemical Industries, Ltd. Cadmium chloride hemi(pentahydrate) ($CdCl_2$, 99.9%) was obtained from Sigma-Ardrich. All chemicals were used as received.

CdS QDs capped with GSH was prepared according to the procedure reported in the literature.[18] Typically, 0.2 mmol of $CdCl_2$ solution and 0.26 mmol of GSH solution were mixed in 40 mL of distilled water, and the pH of the resulting solution was adjusted to 10.0 by dropwise addition of 1.0 M NaOH solution with stirring. Then 0.36 mmol of thiourea was added to the solution under continuous vigorous stirring. The mixture was loaded in a 50 mL three-necked flask and the system was degassed by bubbling dry N_2 gas for an hour. Subsequently, the reaction mixture was heated to 90 °C under N_2 atmosphere. Timing started when the temperature reached 90 °C. With the proceeding of the reaction and the formation of CdS QDs, the initial colorless solution turned bright yellow with the passing time. Aliquots of the sample were taken at different time intervals.

b) Basic information

Steady-state absorption and emission spectra of GSH capped CdS QDs are shown in Figure 2.8. In absorption spectra, only a shoulder was observed at the absorption edge due to the relatively larger size dispersion. In emission spectra, much broader spectra were observed at longer wavelength, which is attributed to an emission from trap states. Average QD diameters are calculated from the $1S(e)$-$1S_{3/2}(h)$ absorption peak obtained from the experimental fitting function,[8]

$$D = -(6.6521 \times 10^{-8})\lambda^3 + (1.9557 \times 10^{4})\lambda^2 - (9.2352 \times 10^{-2})\lambda + 13.29 \quad (2.7)$$

Calculated D were D = 2.5-5.2 nm. Figure 2.9 displays a TEM image of GSH capped CdS

QDs. The image shows spherical shape of CdS QDs with well established lattice structures. Φ of GSH capped CdS QDs were determined at room temperature by comparing the integrated emission to that of coumarin 343 in ethanol and ranged from 5 to 23%.

2.3.2 Synthesis of myristic acid (MA) capped CdS QDs

a) Synthesis

All of the following materials were commercially available and used as received. Cadmium acetate dihydrate ($Cd(OAc)_2 \cdot 2H_2O$, 98.0%) and myristic acid (MA, 98%) were purchased from Wako Pure Chemical Industries, Ltd.). Pure sulfur (99.99%) and 2,2′-dithiobisbenzothiazole (99%) was obtained from Kojundo Chemical Laboratory Co. and Acros organics, respectively.

MA capped CdS QDs were prepared in organic solvents reported in the literature.[19] Briefly, 0.10 mmol of pure S, 6.5 mmol of 2,2-dithio(bis)benzothiazol and 6.0 g of ODE were sonicated together for 1 h. The solution was then added into a 50 mL three-necked flask containing 0.10 mmol of $Cd(OAc)_2 \cdot 2H_2O$, 0.20 mmol of MA and 4.0 g of ODE. Subsequently, the reaction mixture was heated up to 120 °C with stirring under vacuum. A clear solution was obtained after ~2 h. The resulting solution was heated up to 240 °C in N_2 atmosphere. When the temperature reached 200 °C, the growth of the CdS QDs was monitored via the temporal evolution of the optical properties of the growing CdS QDs.

b) Basic information

Figure 2.10 shows steady-state absorption and emission spectra of MA capped CdS QDs. Because the heating time does not give large influences on the spectral shifts of absorption and emission spectra in this procedure, different sized CdS QDs were obtained by changing the synthesis temperature. In absorption spectra, two peaks and two shoulders were clearly observed due to the quite narrow size dispersion, which are attributed to $1S(e)$-$1S_{3/2}(h)$,

$2S_{3/2}$(h)-1S(e), $1P_{3/2}$(h)-1P(e) and $3S_{3/2}$(h)-1S(e), respectively. In emission spectra, a sharp bend-edge emission was mainly observed while little amount of defect emission was observed. Φ of MA capped CdS QDs were determined as similar to those of GSH capped CdS QDs and ranged from 2 to 11%, which are relatively lower values.

2.3.3 OA capped CdS QDs

OA capped CdS QDs were purchased from Sigma-Aldrich. Figure 2.11 shows steady-state absorption and emission spectra of OA capped CdS QDs. Sharp absorption spectra were observed as similar to that of MA capped CdS QDs. Both emissions from the band-edge and surface states are clearly observed in CdS 420 (this is a name of commodity). This result suggests that surface states of OA capped CdS QDs are partially immobilized, which is the intermediate state between GSH capped CdS and MA capped CdS QDs. Φ of OA capped CdS QDs ranged from 9 to 55%, which were determined as similar to the procedure for Φ of GSH capped CdS QDs.

References

(1) La Mer, V. K.; Dinegar, R. H. *J. Am. Chem. Soc.* **1950**, *72*, 4847.

(2) La Mer, V. K. *Ind. Eng.* **1952**, *44*, 1270.

(3) Rao, C. N. R.; Muller, A.; Cheetham, A. K. Nanomaterials Chemistry: Recent Developments and New Directions; Wiley-VCH,

(4) Rogach, A. L.; Semiconductor Nanocrystal Quantum Dots: Synthesis, Assembly, Spectroscopy and Applications; Springer Wien New York, New York, 2008.

(5) Malkov, V. I. Crystal Growth for Beginners; World Scientific, Singapore, 2003.

(6) Peng, X.; Wickham, J.; Alivisatos P. *J. Am. Chem. Soc.* **1998**, *120*, 5343.

(7) Talapin, D. V.; Rogach, A. L.; Shevchenko, E. V.; Kornowski, A.; Hasse, M.; Weller, H. *J. Am. Chem. Soc.* **2002**, *124*, 5782.

(8) Yu, W. W.; Qu, L.; Guo, W.; Peng, X. *Chem. Mater.* **2003**, *15*, 2854.

(9) Klimov, V. I. *J. Phys. Chem. B* **2000**, *104*, 6112.

(10) Gaponik, N.; Talapin, D. V.; Rogach, A. L.; Hoppe, K.; Shevchenko, E. V.; Kornowski, A.; Eychmuller, A.; Weller, H. *J. Phys. Chem. B* **2002**, 106, 7177.

(11) Wolcott, A.; Gerion, D.; Visconate M.; Sun, J.; Schwartzberg, A.; Chen, S.; Zhang, Z. *J. Phys. Chem. B* **2006**, 110, 5759.

(12) Tomasulo, M.;Yildiz, I.; Raymo, F.M. *J. Phys. Chem. B* **2006,** 110, 3853.

(13) Perez-Conde, J.; Bhattacharjee, A. K.; Chamarro, M.; Lavallard, P.; Petrikov, V. D.; Lipovskii, A. A. *Phys. Rev. B* **2001**, 64, 113303.

(14) Talapin, D. V. *PhD thesis*; The University of Hamburg, 2002.

(15) Li, C.; Murase, N. *Chem. Lett.* **2005**, 34, 92.

(16) Mandal, A.; Tamai, N. *J. Phys. Chem. B* **2008**, *112*, 8244.

(17) Osovsky, R.; Klooper, V.; Kolny-Olesiak, J.; Sashchiuk, A.; Lifshitz, E. *J. Phys. Chem. C* **2007**, 111, 10841.

(18) Zou, L.; Fang, Z.; Gu, Z.; Zhong, X. *J. Lumin.* **2009**, *129*, 536.

(19) Ouyang, J.; Kuijiper, J.; Brot, S.; Kingston, D.; Wu, X.; Leek, D. M.; Hu, M. Z.; Ripmeester, J. A.; Yu, K. *J Phys. Chem. C*, **2009**, *113*, 7579.

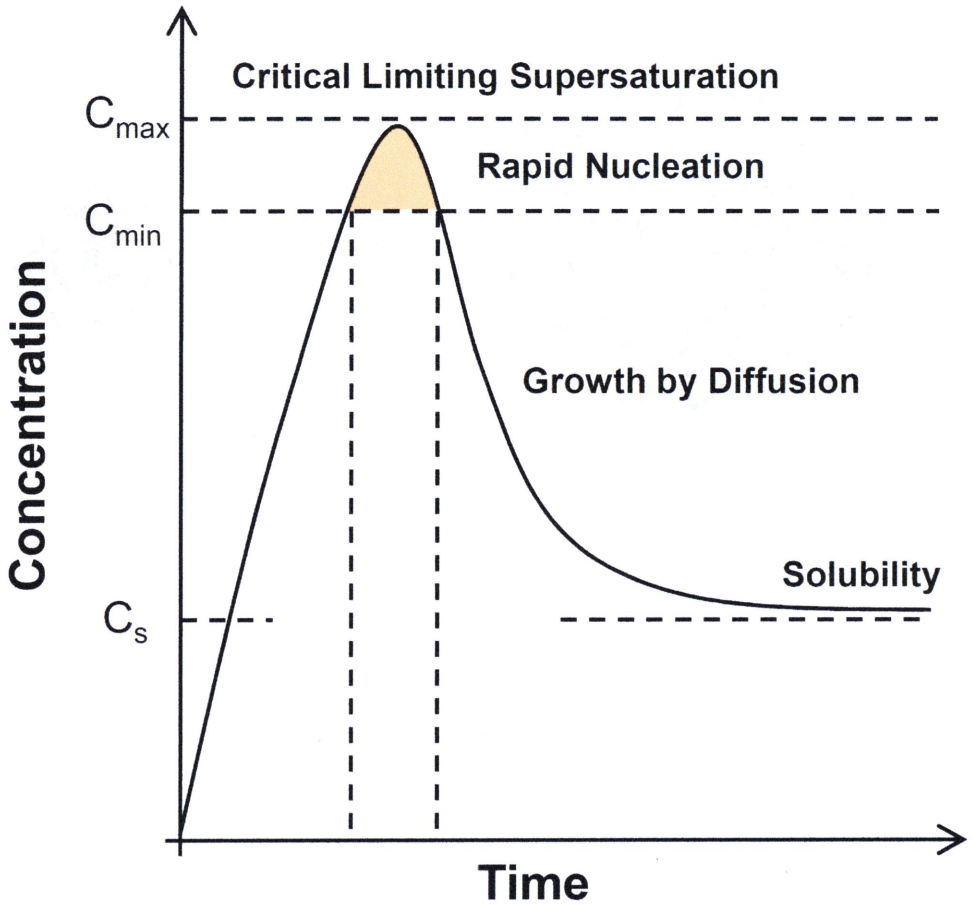

Figure 2.1 Schematic diagram illustrating La Mer's condition for nucleation.

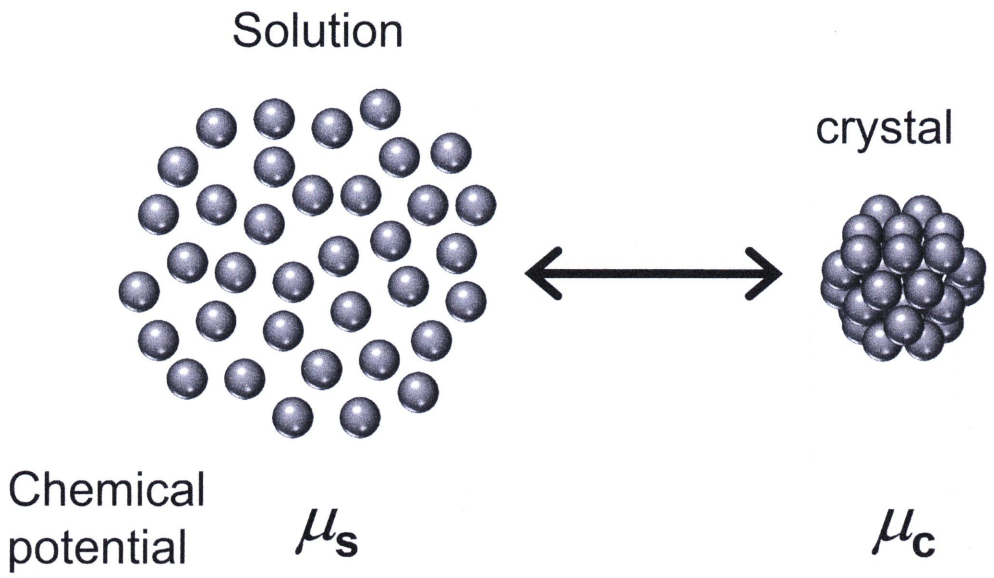

Figure 2.2 A schematic illustration of the conformation and the chemical potential in solution and crystal phase. In the case of $m_c > m_s$, the nucleation does not occur.

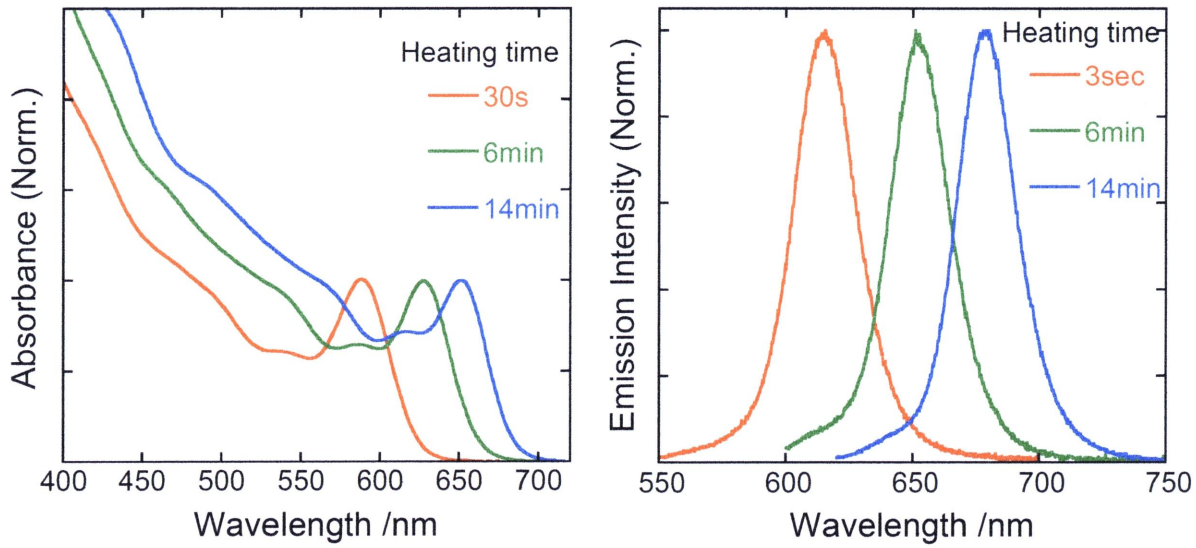

Figure 2.3 Steady-state absorption and emission spectra of TDPA capped CdTe QDs. With the increase of the heating time, both absorption and emission spectra shifts to the red, which indicates that the size of CdTe QDs gradually increases.

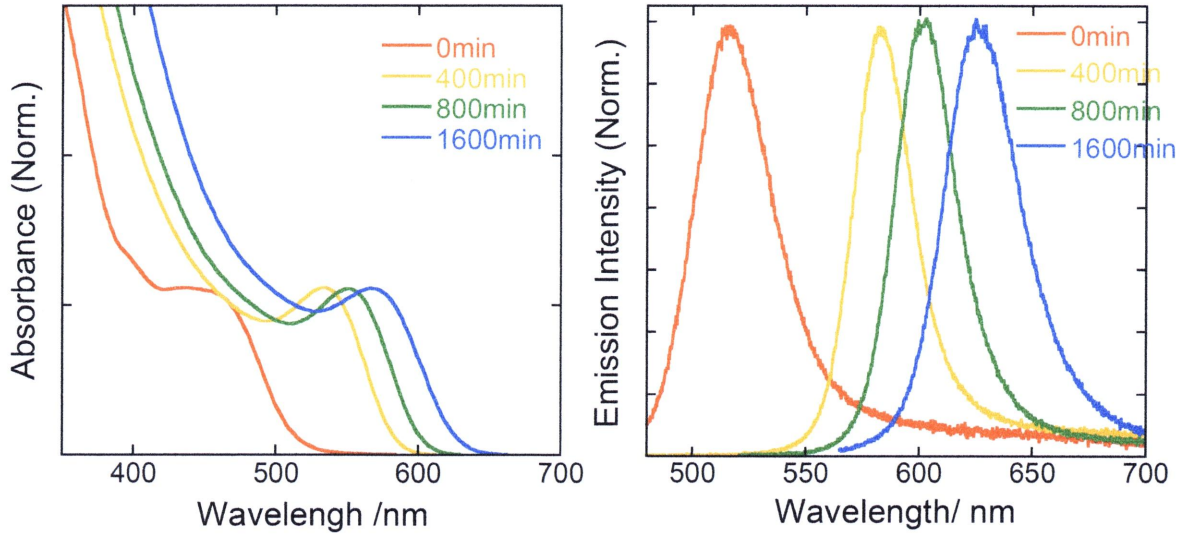

Figure 2.4 Steady-state absorption and emission spectra of TGA capped CdTe QDs.

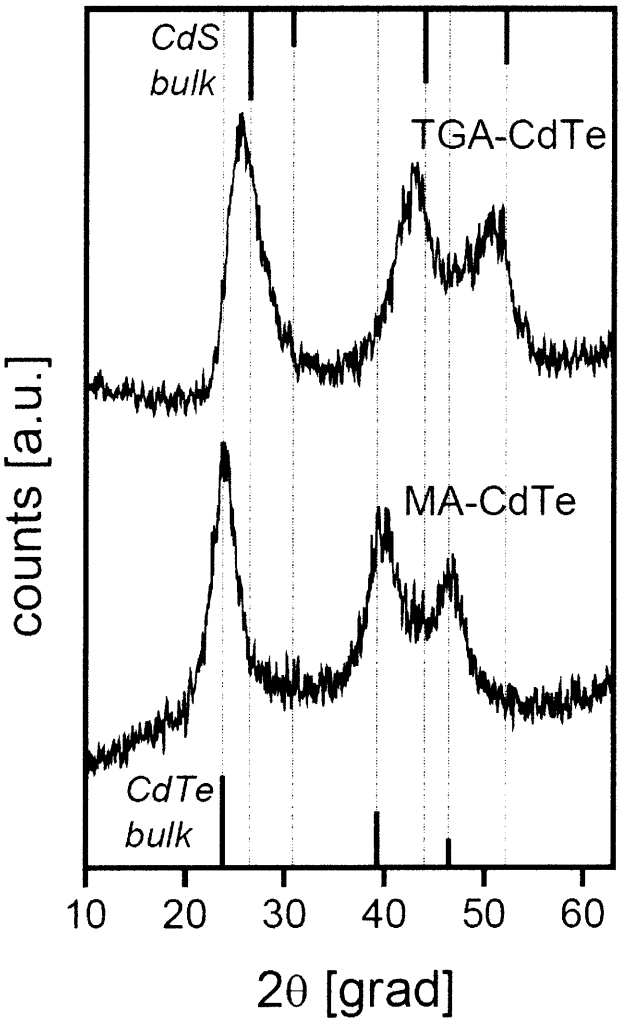

Figure 2.5 X-ray diffractograms of CdTe nanocrystals obtained in aqueous solutions in the presence of thioglycolic acid (TGA) and 2-mercaptoethylamine (MA). This graph is taken from ref 14.

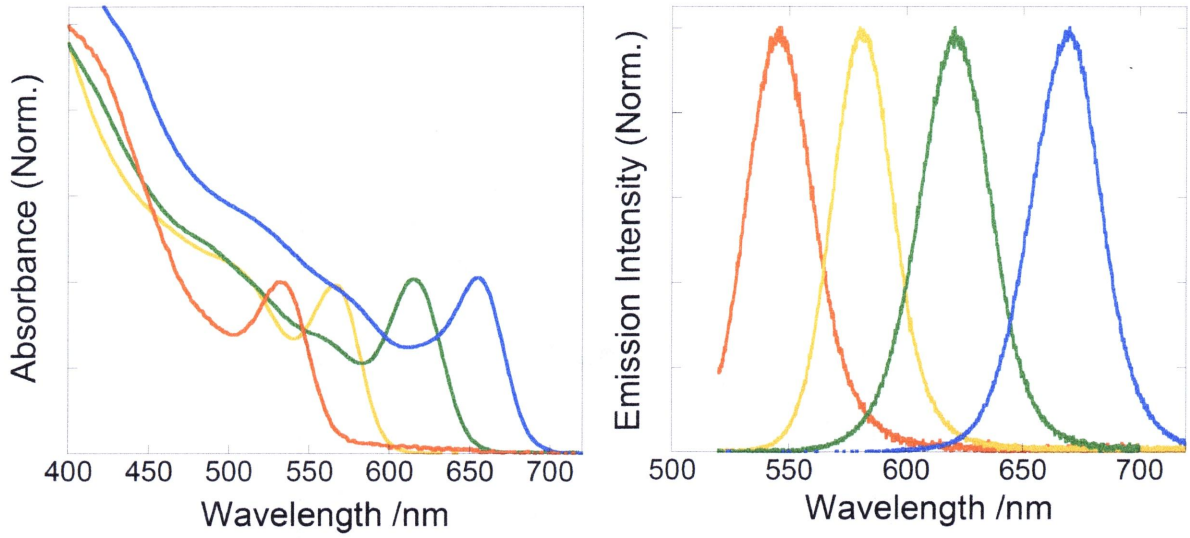

Figure 2.6 Steady-state absorption and emission spectra of OA capped CdTe QDs.

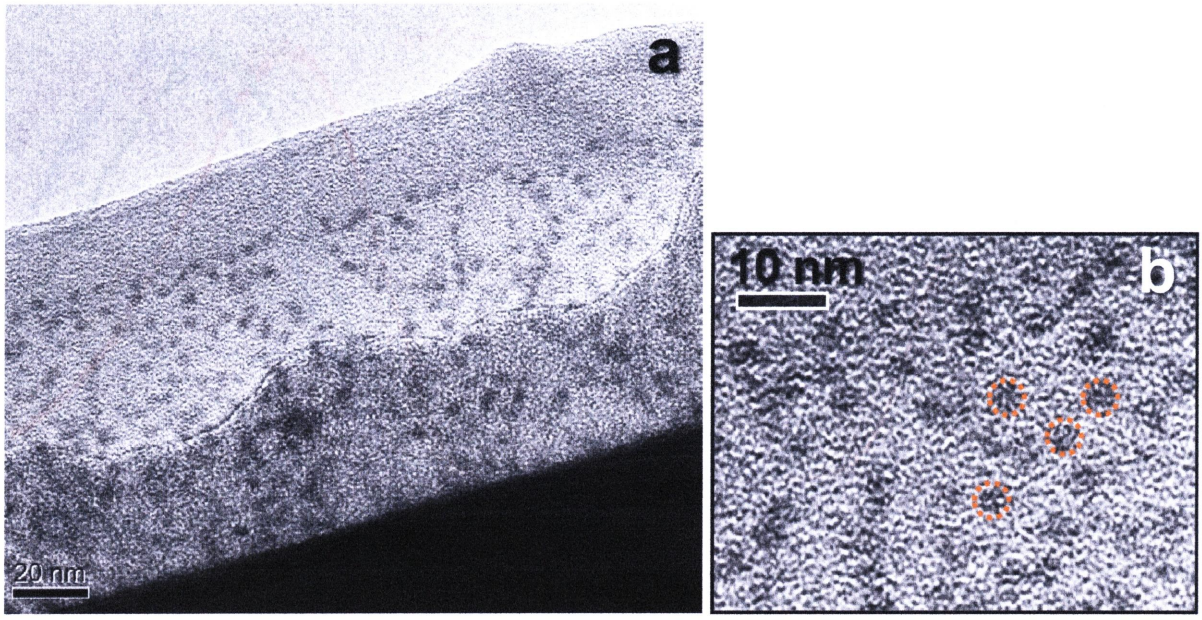

Figure 2.7 TEM images of CdTe QDs capped with OA/TOP at lager scale (a) and smaller scale (b).

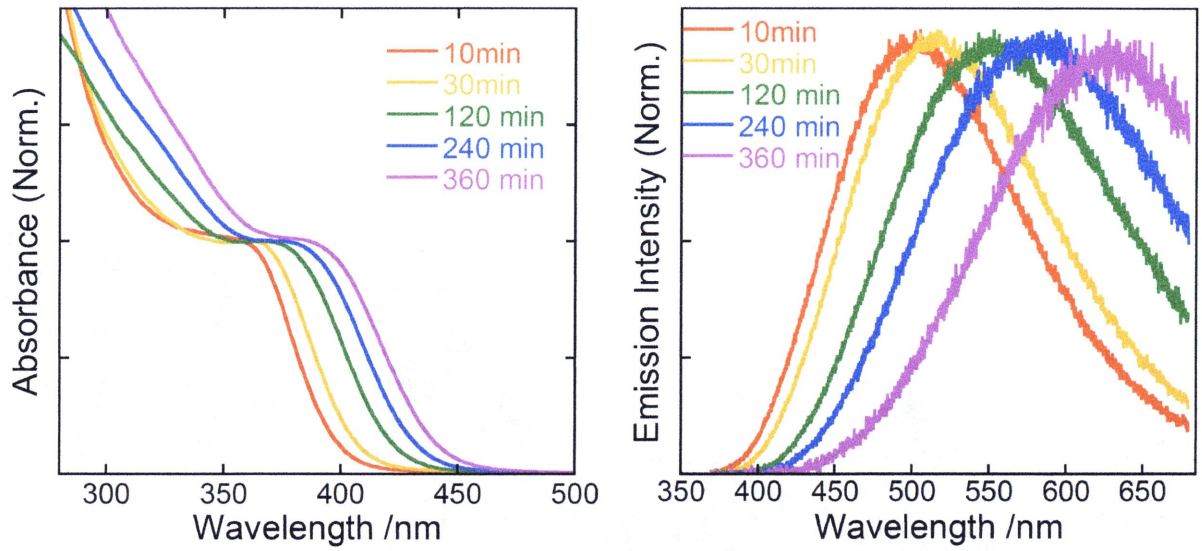

Figure 2.8 Steady-state absorption and emission spectra of GSH capped CdS QDs.

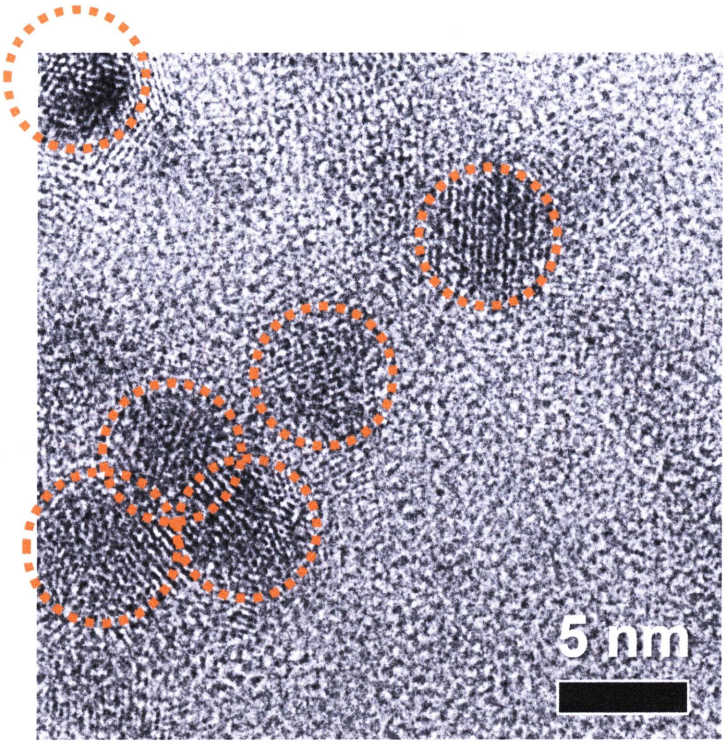

Figure 2.9 TEM images of GSH capped CdS QDs.

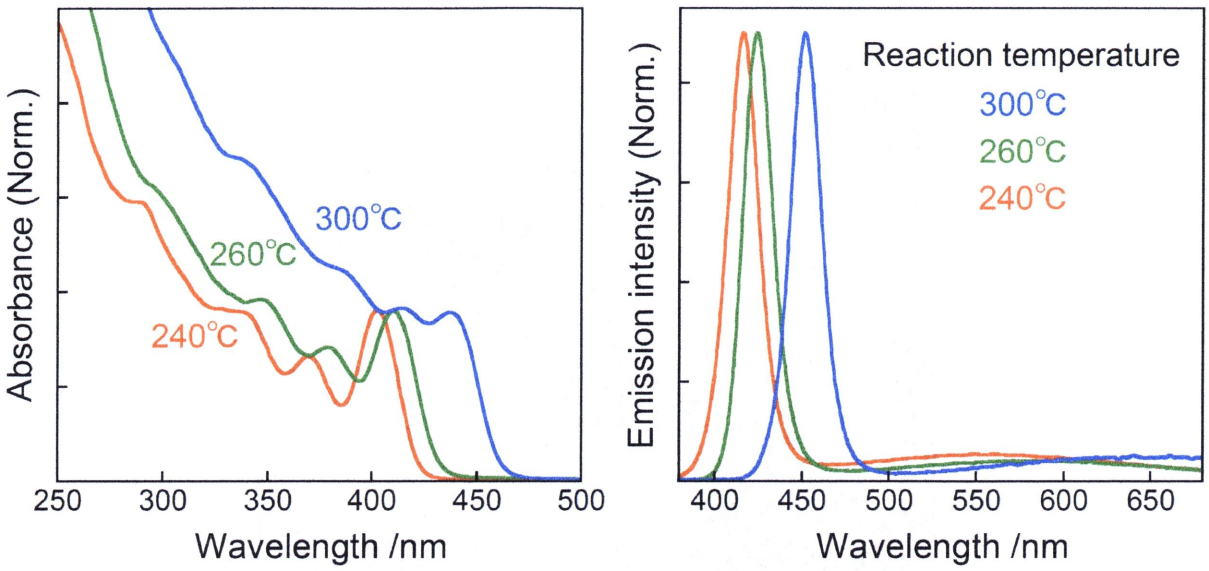

Figure 2.10 Steady-state absorption and emission spectra of MA capped CdS QDs. Temperature in the figure represents a reaction temperature for the synthesis.

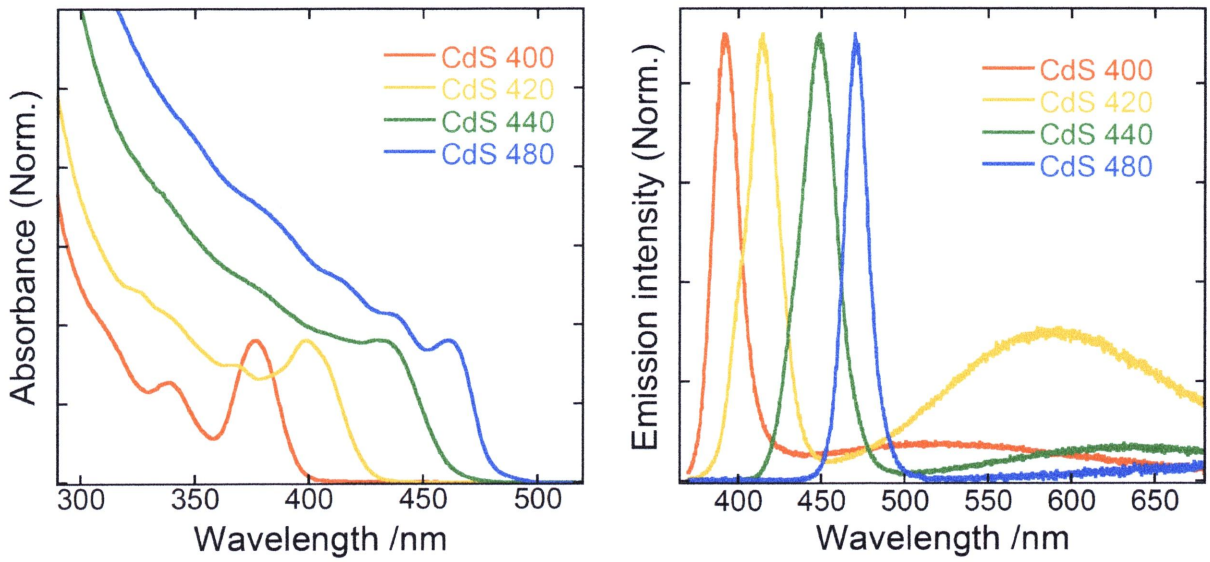

Figure 2.11 Steady-state absorption and emission spectra of OA capped CdS QDs. Each names are name of commodity (Sigma-Aldrich).

Chapter 3
Carrier multiplication in CdTe QDs

3.1 Abstract

Carrier multiplication (CM) was observed in CdTe quantum dots (QDs) capped with tetradecylphosphonic acid (TDPA) at $h\nu/E_g > 2.5$ by picosecond single-photon timing spectroscopy, where $h\nu$ and E_g are the excitation and the bandgap energies, and the CM efficiency increased rapidly with increasing $h\nu/ E_g$. No CM was observed below threshold value of $h\nu/E_g \sim 2.5$, which is close to that of CdSe QDs. As compared to the previous report by Nair and Bawendi, our result suggests that CM is sensitive to the QD surface conditions.

3.2 Introduction

Carrier multiplication (CM) in semiconductors is a process that multiple excitons are generated by one photon absorption with energy higher than the bandgap energy of E_g. CM can potentially improve the performance of many semiconductor-based devices such as solar cells, photocatalists and optical amplifiers. CM in bulk semiconductors is first observed in 1950's; however, significantly higher energy is required for CM. For example, CM in bulk PbS has a threshold energy of $\sim 5E_g$ and an efficiency of 170% is obtained at high energy of $\sim 9E_g$.[1] In 2004, Klimov et al. reported the highly efficient CM up to 700% in PbSe QDs by transient absorption spectroscopy.[2,3] Efficient CM has been reported for several semiconductor QDs such as CdSe,[4] PbS[5,6] and PbTe.[7] However, some reports have claimed that CM does not occur in CdSe, CdTe QDs[8] and InAs/CdSe/ZnSe core/shell/shell QDs,[9] and that CM efficieny of PbSe QDs is not so high as compared with the firstly reported result.[10] These descrepancies may come from surface and environmental conditions of QDs. In this chapter, we examined CM of CdTe QDs capped with tetradecylphosphonic acid (TDPA) by picosecond single-photon timing spectroscopy, and found that CM was observed with the threshold energy of $\sim 2.5E_g$.

3.3 Experimental

TDPA capped CdTe QDs were prepared by high temperature colloidal methods in organic solvents reported in the literature and described in Chapter 2.[11] The final product was redissolved in hexane and used for absorption spectroscopy (U3210; Hitachi), luminescence spectroscopy (FluoroMax-2; Jobinyvon-Spex), and luminescence decay measurements. Luminescence decays were measured by using picosecond single-photon timing spectroscopy.[12] QDs were excited at 400 nm (3.10 eV) and 266 nm (4.67 eV) of Ti: Sapphire laser with a repetition rate of 8 MHz. All measurements were performed at room temperature.

3.4 Results and discussion

We measured absorption and luminescence spectra of TDPA capped CdTe QDs. Figure 1a shows that the first excitonic absorption peak was clearly observed at 649 nm. The diameter (D) and the bandgap (E_g) were estimated from the first excitonic absorption peak and absorption edge, respectively. D and E_g of a series of CdTe QDs ranged from 3.6 to 5.4 nm and from 1.93 to 1.73 eV, respectively.[10] Luminescence spectra of CdTe QDs excited at 400 and 266 nm are illustrated in Figure 3.1(b). As clearly shown in the Figure, both luminescence spectra are very similar irrespective of the excitation energy, suggesting that the effect of impurities on luminescence spectra is negligible at both excitation wavelengths. The excitation energy dependence on luminescence spectra was not detected for all the CdTe QDs examined here.

Figure 3.2 shows luminescence decays of different size CdTe QDs (D = 3.7 and 5.4 nm) excited at 400 and 266 nm and probed at the wavelength of maximum intensity. The decay curve excited at 400 nm was normalized to unity at the peak height of the curve and the curve at 266 nm was normalized to the decay of 400 nm at the long time scale of 8 ns. In the sample whose E_g = 1.93 eV and D = 3.7 nm (Figure 3.2a), luminescence decays excited at 400 and

266 nm are similar to each other. This result indicates that no CM occurs in this sample (E_g = 1.93 eV) even at 266 nm (4.67 eV). On the other hand, an additional fast decay component was detected for CdTe QDs (E_g = 1.73 eV, D = 5.4 nm) in the decay dynamics excited at 266 nm as compared with the decay at 400 nm (Figure 3.2b). When the multiple carriers are formed in a single CdTe QD, Auger recombination easily occurs with a time constant of a few tens of ps ~ a few hundreds of ps depending on the QD size and the QD surface conditions.[13] In our experimental results (Figure 3.2b), a faster decay of ~ 140 ps was observed as a difference decay dynamics, in which the time constant is comparable to that of Auger recombination of ~ 5 nm CdTe QDs.[13] Thus the faster decay component detected at 266 nm excitation is most likely due to the carrier-carrier interaction of Auger recombination originated from CM.

Quantum efficiency of CM (QE), which determines how many excitons are generated by one photon absorption, is calculated from the ratio of the maximum amplitudes of luminescence decays excited at 400 and 266 nm like the procedure by Klimov et al.[4] As shown in Figure 3.3, No CM was observed below $h\nu/E_g$ ~ 2.5 and then the CM efficiency increased at $h\nu/E_g$ > 2.5. For large sized CdTe QDs (E_g = 1.73 eV) shown in Figure 2b, CM efficiency was calculated to be 190% at 266 nm excitation ($h\nu$ = 4.67 eV). This result indicates that CM efficiency has a threshold of $h\nu/E_g$ ~ 2.5 for TDPA capped CdTe QDs. This threshold is very similar to that of CdSe QDs ($h\nu/E_g$ ~ 2.5) and smaller than that of PbSe QDs ($h\nu/E_g$ ~ 3.0).[3]

The threshold of CM efficiency has been interpreted in terms of simple bulk-semiconductor effective-mass arguments without invoking a precise structure of quantized states.[3] From the energy conservation, the minimum photon energy required to produce CM ($h\nu_{CM}$) is determined by the following equation, $h\nu_{CM} = (2 + m_e / m_h) E_g$, where m_e and m_h are the effective mass of electron and hole, respectively. In CdTe, $m_e : m_h = 1 : 4$,[14]

and hence $h\nu_{CM}/E_g \sim 2.3$. This simple estimation explains the experimental result ($h\nu_{CM}/E_g \sim 2.5$) although the value is a little larger than the expectation.

In the previous report by Nair and Bawendi, CM has not been detected for CdSe/ZnS core/shell QDs and CdSe and CdTe QDs capped with triocthylphosphine.[8] In addition, recent transient absorption experiments on PbSe QDs suggest that CM is sensitive to the chemical and surface treatments of QDs.[15] The difference in surface conditions may be the reason why CM was not observed in triocthylphoshine capped CdTe QDs and observed in TDPA capped CdTe QDs.

3.5 Conclusion

We observed efficient CM in TDPA capped CdTe QDs at $h\nu/E_g > 2.5$ by picosecond single-photon timing spectroscopy, in which the threshold of CM efficiency is close to that of CdSe QDs. As compared with the previous report, our result suggests that CM is sensitive to the QD surface conditions.

References

(1) Smith, A.; Dutton, D. *J. Opt. Soc. Am.* **1958**, *48*, 1007.

(2) Schaller, R. D.; Klimov, V. I.*Phys. Rev. Lett.* **2004**, *92*, 186601.

(3) Schaller, R. D.; Petruska, M. A.; Klimov, V. I. *Appl. Phys. Lett.* **2005**, *87*, 253102.

(4) Schaller, R. D.; Sykora, M.; Jeong, S.; Klimov, V. I. *J. Phys. Chem. B*, **2006**, *110*, 25332.

(5) Ellingson, R. J.; Beard, M. C.; Hohnson, J. C.; Yu, P.; Micic, O. I.; Nozik, A. J. Shabaev, A.; Efros, A. L. *Nano Lett.***2005**,*5*, 865.

(6) Nair, G.; Geyer, S. M.; Chang, L.; Bawendi, M. G. *Phys. Rev. B*, **2008**, *78*, 125325.

(7) Murphy, J. E.; Beard, M. C.; Norman, A. G.; Ahrenkiel, S. P.; Johnson, J. C.; Yu, P.; Micic, O. I.; Ellingson, R. J.; Nozik, A. J. *J. Am. Chem. Soc.* **2006**, *128*, 3241.

(8) Nair, G. ; Bawendi, M. G. *Phys. Rev. B*, **2007**, *76*, 081304.

(9) Ben-Lulu, M.; Mocatta, D.; Bonn, M.; Banin, U.; Ruhman, S. *Nano Lett.* **2008**, *8*, 1207.

(10) Trinh, M. T.; Houtepen, A. J.; Schins, J. M.; Hanrath, T.; Piris, J.; Knulst, W.; Goossens, A. P. L. M.; Siebbeles, L. D. A. *Nano lett.* **2008**, *8*, 1713.

(11) Yu, W. W.; Qu, L.; Guo, W.; Peng, X. *Chem. Mater.* **2003**, *15*, 2854.

(12) Boens N. *et al. Anal. Chem.* **2007**, *79*, 2137.

(13) Kobayashi, Y.; Pan, L.; Tamai, N. *J. Phys. Chem. C*, **2009**, 113, 11783.

(14) Gaponenko, S. V. *Optical Properties of Semiconductor Nanocrystals, Cambridge Universuty press*, New York, **1998**, Chap. 1.3, pp. 19.

(15) Beard, M. C.; Midgett, A. G.; Law, M.; Semonin, O.; E. Ellingson, R. J.; Nozik, A. J. *Nano Lett.* **2009**, *9*, 836.

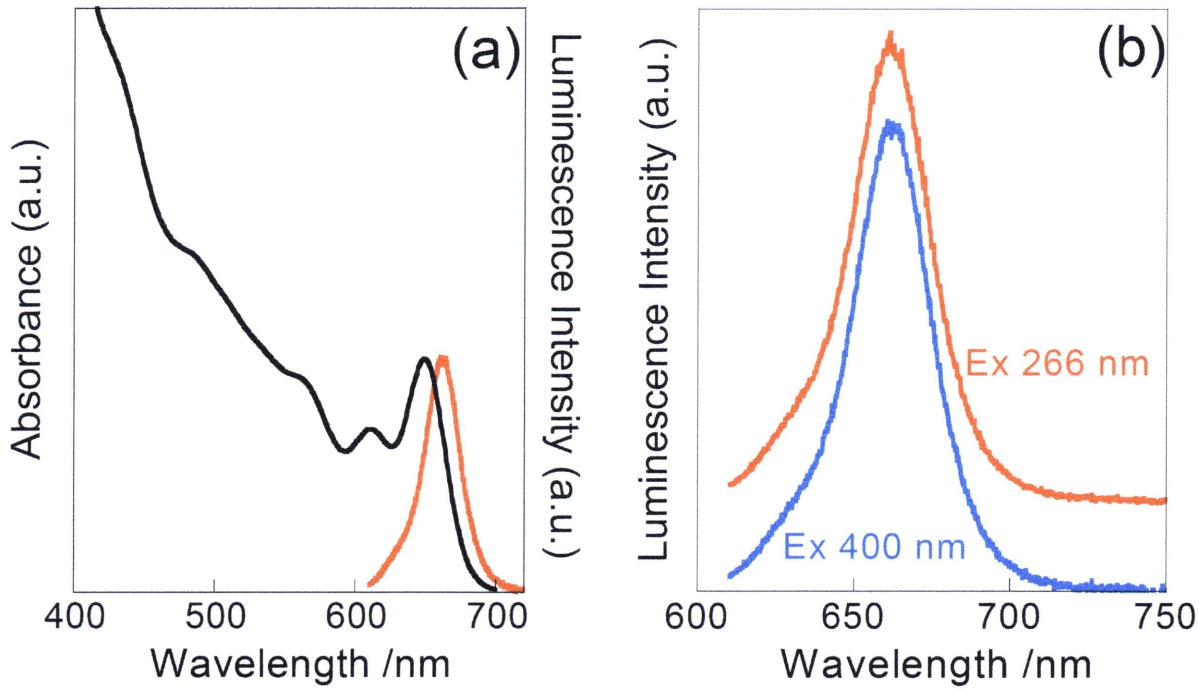

Figure 3.1 Typical absorption (black) and luminescence spectra (red) of TDPA-capped CdTe QDs, D = 4.3 nm and E_g = 1.83 eV(a). Luminescence spectra excited at 266 nm (red) and 400 nm (blue) (b).

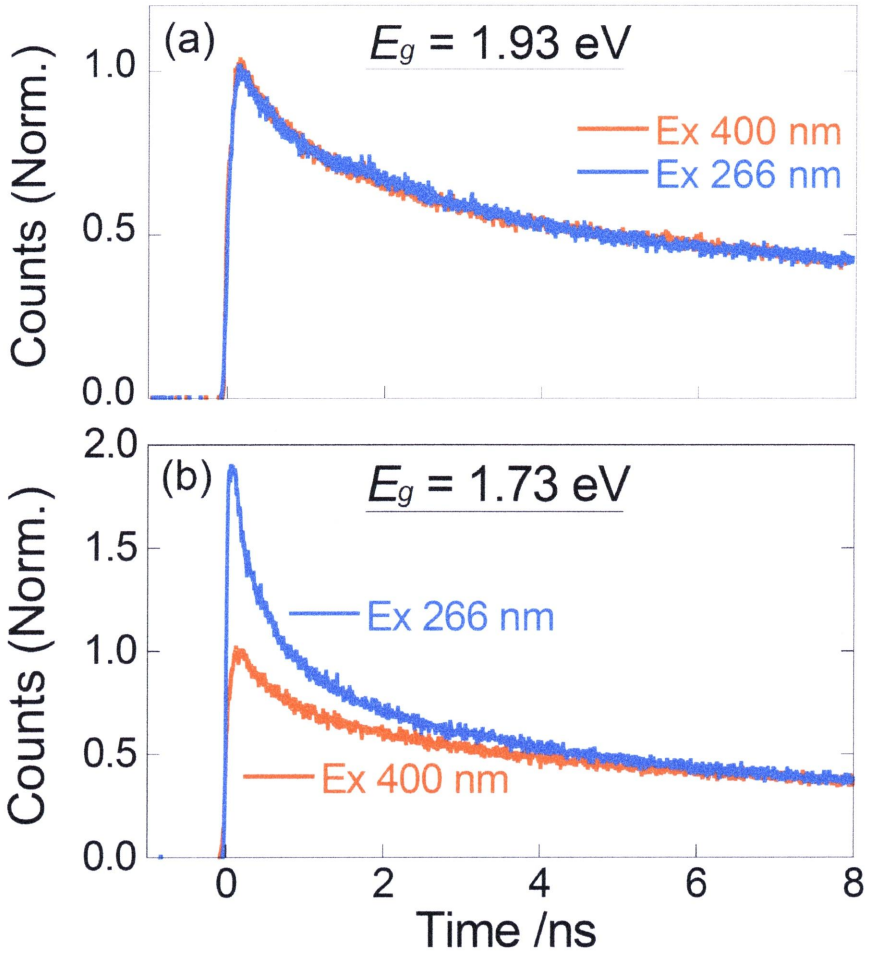

Figure 3.2 Luminescence decay dynamics of TDPA capped CdTe QDs excited at 400 nm (solid line) and 266 nm (dotted line) whose E_g = 1.93 eV (a) and 1.73 eV (b).

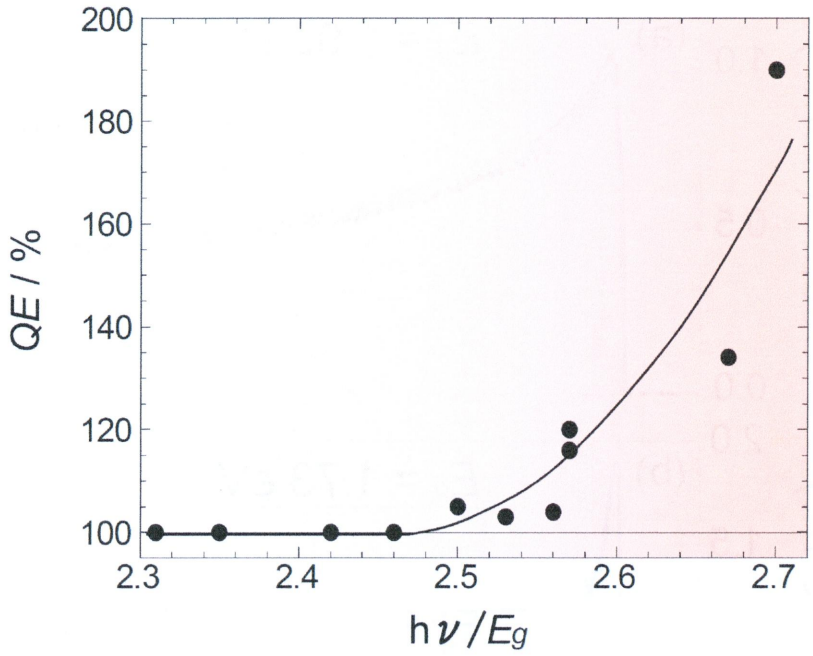

Figure 3.3 Quantum efficiency of CM (*QE*) as a function of $h\nu/E_g$. The CM efficiency threshold of TDPA capped CdTe QDs was around $h\nu/E_g \sim 2.5$. A solid line was written by eyes.

Chapter 4

Effect of capping reagents on Auger recombination in CdTe QDs

4.1 Abstract

CdTe quantum dots (QDs) were synthesized using oleic acid and trioctylphosphine (OA/TOP) and thioglycolic acid (HS-CH_2COOH, TGA) as capping reagents. Biexciton Auger recombination of CdTe QDs was examined by femtosecond transient absorption spectroscopy with changing excitation intensity. The lifetime of biexciton Auger recombination τ_{Auger} was analyzed as a function of QD diameter, D, and capping reagents. τ_{Auger} is proportional to D^{α}, and the scaling index, α, depends on capping reagent or surface conditions. α is 4.6 for TGA capped CdTe QDs, whereas it is 7.0 for OA/TOP capped CdTe QDs with high luminescence quantum yields, Φ, of 60-85%. This relationship did not hold for small size OA/TOP capped CdTe QDs with rather low Φ of 15-30%, in which τ_{Auger} became as short as 2-3 ps irrespective of the diameter. These results suggest that biexciton Auger recombination of CdTe QDs depends on the QD surface conditions and capping reagents.

4.2 Introduction

Auger effect in semiconductors is a process that one excited electron interacts with another excited electron in the conduction band where one interacted electron recombines with a hole in valence band and the other electron is excited at higher states including ionized states. In bulk semiconductors, Auger processes are reduced by kinematic restrictions imposed by energy and translational-momentum conservation.[1] However, because of the relaxation of momentum conservation in zero-dimentional nanocrystals (NCs), its efficiency dramatically increases in quantum dots (QDs) as compared with the bulk semiconductors.[2] QDs have interesting features such as size-controlled optical properties,[3-5] optical nonlinearlity,[6] and high efficiency carrier multiplication[7-9] due to their discrete electronic states and strong Coulomb interactions. QDs also have potential applications such as biolabeling,[10,11] light-emitting diodes,[12-15] lasing,[16-19] and solar cells.[20,21] However, Auger

effect interferes with the effective use of carriers, induces ionization and luminescence intermittency (blinking),[22] and deteriorates these materials; therefore, significant interest have been attracted how to suppress Auger effects in nanomaterials. Auger effect of nanomaterials has been reported theoretically and experimentally. Chepic et al. reported that the lifetime of Auger ionization of glass doped CdS NCs are proportional to D^{α} ($5 < \alpha < 7$), where α is the scaling index and D is the diameter of QD.[23] Wang et al. reported that biexciton Auger recombination mainly occurs the surface of QD.[24] Experimentally, Klimov et al. reported that Auger recombination in CdSe QDs is proportional to D^3 and is dominated by processes involving states inside QDs.[1] The difference in the size dependence between the lifetime of Auger recombination and Auger ionization can be connected with the finite density of states in the NCs where the Auger electron can be transferred,[25] though the effect of surface states on Auger recombination is not mentioned. The Auger recombination dynamics was also examined for inverted core-shell ZnSe/CdSe QDs, in which the lifetime of Auger recombination became 2-6 times longer as compared with that of mono component CdSe QDs.[26] For type II CdTe/CdSe QDs, the lifetime of Auger recombination significantly increased up to ns time scale as expected from the carrier separation,[27] and it increased much faster than the QD volume to deviate from D^3 dependence. In addition, Pandey et al. reported that power law dependence of the lifetime of multiple carrier recombination for CdSe QDs is approximately expressed as D^3 only for large size QDs, though these dependences do not hold for small size QDs.[28] Many reports on Auger recombination dynamics of colloidal QDs are about CdSe QDs; thus few reports has been done on other II-VI semiconductor QDs. In the present study, we have examined biexciton Auger recombination dynamics of CdTe QDs capped with OA/TOP and TGA by femtosecond transient absorption spectroscopy. Size-dependent biexciton Auger recombination was revealed by analyzing intensity dependence on transient absorption dynamics. These results suggest that the lifetime of

biexciton Auger recombination depends on the kind of capping reagents or on the nature of surface conditions.

4.3 Experimental

Synthetic procedures of CdTe QDs capped with OA/TOP or TGA are described in Chapter 2. The luminescence quantum yields (Φ) of various sized CdTe QDs were determined at room temperature by comparing the integrated emission of the CdTe QDs in solution to the emission of rhodamine B or coumarin 343 in ehanol. Φ were 10-40% for TGA capped CdTe QDs and 15-85% for OA capped CdTe QDs.[35,36] UV-vis absorption and luminescence spectra were recorded using Hitachi U-4100 and FluoroMax-2 (Jobinyvon-Spex) spectrophotometers, respectively. Time-resolved transient absorption spectra were measured by femtosecond pump-probe experiments. CdTe QDs were excited at 400 nm by second harmonic of an amplified modelocked Ti:Sapphire laser (Spitfire and Tsunami, Spectra-Physics). Excitation intensity was 2-200 μW with the repetition rate of 0.5 kHz by using a chopper (Model 3501, New Focus, Inc.). Excitation intensity was measured by calibrated power meter (Orion/PD, Ophir). Absorption transients were probed by delayed pulses of a femtosecond white-light continuum generated by focusing fundamental laser pulse (800 nm) into a D_2O cell and detected by a polychromator-CCD combination (Spectra Pro-275 and Spec-10, Acton Research Co. and Princeton Instruments). As a measure of transient absorption we used the differential optical density (ΔOD) defined by $\Delta OD = \log(I_{OFF}/I_{ON})$, where I_{OFF} and I_{ON} are transmitted whitelight intensity in the absence and the presence of the pump pulse, respectively. The spectral range was 420-780 nm and the temporal resolution was 100 fs. A temporal dispersion of the white-light continuum was corrected for the transient absorption spectra. All measurements reported below were performed at room temperature.

4.4 Results and discussion

We measured absorption and luminescence spectra of OA/TOP and TGA capped CdTe QDs with different diameters, respectively. Figure 4.1 shows that size-dependent absorption and luminescence spectra were observed in both samples. In absorption spectra of OA/TOP capped CdTe QDs, the first excitonic peak at the absorption edge and several shoulders were observed, which is consistent with previously reported one.[29,37] On the other hand, the first excitonic peak at the absorption edge was observed and other shoulders were not clearly detected in TGA capped QDs. QD diameters were estimated from the first excitonic absorption peak as described in refs 37 and 38. In OA/TOP capped CdTe QDs, the diameters of 11 samples were estimated to be 2.6-4.5 nm. In TGA capped CdTe QDs the diameters were 2.3-3.5 nm for seven samples. In both samples, size-dependent narrow luminescence spectra were observed. The size dispersion for OA/TOP capped CdTe QDs was reported to be approximately 5% for 30 nm fwhm (full width at half-maximum)[29] and about 10% for 35-55 nm fwhm for TGA capped CdTe QDs.[31] The size distribution may be 5-10% in our synthesized OA/TOP and TGA capped CdTe QDs. Stokes shift of TGA capped CdTe QDs was larger than that of OA/TOP capped QDs. The Stokes shift comes from a combination of fine structure splitting and exciton-LO-phonon coupling.[39] Larger Stokes shift probably come from two factors. One is the strong exciton-LO-phonon coupling of TGA capped CdTe QDs because of more broadened absorption spectra as compared with that of OA/TOP capped QDs. Another possibility of larger Stokes shift may be due to the penetration of wave functions inside the QD into surrounding shell-like structures formed by capping regent, TGA.[40,41] Prolonged refluxing of aqueous solutions of TGA capped CdTe QDs in the presence of an excess of thiols leads to partial hydrolysis of the thiols and to the incorporation of the sulfur from the thiol molecules into the growing QDs. The above process forms thin gradient

structures of sulfur distribution from the inside to the surface of QDs,[40,41] which is similar to the shell-like structures of CdS. In OA/TOP capped CdTe QDs, on the other hand, surroundings of QDs are probably one monolayer of OA/TOP. These differences in surrounding conditions may also lead to a difference in the Stokes shift. Φ depends on the QD size and surrounding capping reagents. Φ of OA/TOP capped CdTe QDs is 15-30% for smaller size QDs, D = 2.6-3.1 nm, and increases to 60% when the QD size becomes 3.3 nm. Φ is 60-85% for QDs of D = 3.3-4.5 nm. Φ of TGA capped CdTe QDs is 14-19% for smaller sized QDs (D = 2.3-2.9 nm) and gradually increases with increasing the size and finally becomes 42% when the QD size becomes 3.5 nm. We measured transient absorption spectra of OA/TOP and TGA capped CdTe QDs as a function of excitation intensity. Figure 4.2 illustrates transient absorption spectra of OA/TOP capped CdTe QDs whose diameters are 3.4 and 4.5 nm. Excitation intensities in Figure 4.2, panels a and b, are 60 μW (3.0×10^{13} photon cm^{-2}) and 40 μW (2.0×10^{13} photon cm^{-2}), respectively, which correspond to the number of photons to generate 1.6 and 1.9 excitons in a CdTe QD on average. The average number of excitons per QD, $\langle N_0 \rangle$, is calculated by the equation $\langle N_0 \rangle = j_p \sigma_0$, where j_p is the pump photon fluence and σ_0 is the QD absorption cross section.[1,37,42] In Figure 4.2a, two negative peaks (563 and 509 nm) and two positive absorption peaks (595 and 478 nm) are observed. The wavelength of negative absorption peaks correspond to those of ground-state absorption spectra. Two possible reasons are conceivable for the positive absorption peaks at 0.1 and 1 ps. One is carrier-induced Stark effects[43] because transient absorption spectra at these time delays are similar to the second derivatives of the ground state absorption spectrum. The other possibility is a transient absorption from the excited state to upper state. In Figure 4.2b, the spectrum shifts to the red as compared to that in Figure 4.2a because of the larger size (D = 4.5 nm). Four negative peaks (650, 570, 510, and 440 nm), one shoulder (620 nm) and two positive peaks (around 679 and 588 nm) are observed, corresponding to the ground-state

absorption spectra. Figure 4.3 illustrates transient absorption spectra of TGA capped QDs whose diameters are 2.3 and 3.5 nm, respectively. Excitation intensities in Figure 4.3, panels a and b, are 120 μW (6.1×10^{13} photon cm^{-2}) and 60 μW (3.0×10^{13} photon cm^{-2}), respectively, which correspond to $\langle N_0 \rangle$ = 1.5 and 1.7. In both spectra, a negative bleaching peak corresponding to ground-state absorption (487 nm in Figure 4.3a and 588 and 530 nm in Figure 4.3b) and a positive absorption peak corresponding to carrier-induced Stark effects (527 and 632 nm, respectively) are observed. Spectral features of transient absorption are almost the same from few ps up to 1 ns in both CdTe QDs capped with OA/TOP and TGA. As shown later, the spectrum at 1 ns is mainly due to one exciton and the spectrum at few ps contains biexciton. In addition, the spectrum of the first excitonic absorption at 3 ps in Figure 4.2b ($\langle N_0 \rangle$ = 1.9) is almost the same as the spectrum at very low excitation intensity, $\langle N_0 \rangle$ = 0.1-0.2 (data not shown) in the same time window. These results suggest that the effect of biexciton on the spectral features of first excitonic absorption was negligible. As a measure of instant QD populations, we used the transient absorption bleaching of the first excitonic optical transition. The bleaching decay is dominated by the intraband relaxation at early times of excitation.[44] After that, bleaching dynamics are entirely due to population changes of the QD quantized states and surface states. Figure 4.4 displays normalized absorption changes at the first excitonic peak ($-\Delta OD_0/\alpha_0$) of OA/TOP capped CdTe QDs with D = 3.4 nm against $\langle N_0 \rangle$, where ΔOD_0 and α_0 are the minimum bleaching absorbance and the ground-state absorbance at the first excitonic peak, respectively. Absorption changes does not directly represent the population change at higher excitation intensity or larger $\langle N_0 \rangle$. The excitation intensity dependence of the bleaching change is written by

$$-\frac{\Delta OD_0}{\alpha_0} = \frac{k_1 \langle N_0 \rangle}{k_2 + \langle N_0 \rangle} \tag{4.1}$$

and the empirical parameters were numerically analyzed to be k_1 = 1.14 ± 0.04, k_2 = 2.29 ±

0.17 (line in Figure 4.4). The average population dynamics $\langle N(t) \rangle$ is obtained from the absorbance change $\Delta OD(t)$ by using the above expression with numerically obtained k_1 and k_2. As shown in Figure 4.5a, population dynamics of OA/TOP capped CdTe QDs for $D = 3.4$ nm at the low excitation intensity ($\langle N_0 \rangle = 0.13$) is nearly fitted with a single exponential decay function with a lifetime longer than 10 ns. The precise fitting gives an additional fast decay lifetime of 70 ps (7.7%), which might be due to the surface trapping process. The surface trapping is a minor contribution to the relaxation because of the small amplitude component. As excitation intensity increased additional ps to tens of ps decay component appeares, which is most probably due to Auger recombination. Auger recombination dynamics has been simply analyzed by a sum of exponential decay function as a first approximation,[1] although the following rate equation has also been used to analyze biexciton Auger recombination:[45]

$$\frac{\mathrm{d}}{\mathrm{d}t} c_{\mathrm{eh}}(t) = -k_{\mathrm{A}} c_{\mathrm{eh}}^3(t) \tag{4.2}$$

where c_{eh} is the effective carrier concentration in a QD and k_{A} is the Auger constant. This free carrier model is based on the recombination between two electrons and one hole (one electron and two holes) in strong confinement systems. Recently, Barzykin and Tachiya have analyzed the multiple carrier dynamics in semiconducting nanosystems by stochastic approach.[46] In their generalized stochastic model, the decay kinetics of e-h pairs is given by

$$\frac{\mathrm{d}}{\mathrm{d}t} \rho_{\mathrm{n}}(t) = -\frac{\rho_{\mathrm{n}}(t)}{\tau_{\mathrm{n}}} + \frac{\rho_{\mathrm{n+1}}(t)}{\tau_{\mathrm{n+1}}} \tag{4.3}$$

where $\rho_n(t)$ is the fraction of QDs which contain n e-h pairs at time t and $1/\tau_n$ is the rate constant for the transition from n e-h pairs to n - 1 pairs. In their theoretical and numerical analyses of Auger recombination dynamics in CdSe QDs examined by Klimov et al.,[1] the exciton model where an electron and a hole are paired is more suitable to explain the experimental results of Auger recombination than the free carrier model.[46] In this condition, the dynamics of multiexciton Auger recombination is expressed by

$$\bar{n}(t) = \sum_{i=1}^{\infty} A_i \exp\left[-i\left(\frac{1}{\tau_1} + \frac{1}{2}(i-1)k_{ex}^{A}\right)t\right] \tag{4.4}$$

$$A_i = \langle N_0 \rangle^i e^{-\langle N_0 \rangle}(r + 2i - 1)\sum_{j=0}^{\infty} \frac{\langle N_0 \rangle^j}{j!} \frac{\Gamma(r+i+j)}{\Gamma(r+2i+j)} \tag{4.5}$$

where $1/\tau_1$ is the rate of linear relaxation, k_{ex}^{A} is the first order rate constant for Auger recombination and corresponds to the biexciton rate constant, and r is the ratio between the rate of linear relaxation and Auger recombination. In the current experimental conditions, r is on the order of 10^{-2}-10^{-3},[1] and is negligible to estimate the amplitude A_i. For relatively low population of excitons ($<N_0> < 2$) in one QD, the dynamics can be approximately expressed by a sum of two exponentials. For example, when $<N_0> = 1$ (one exciton is formed in one CdTe QD in average), A_1 and A_2 are calculated to be 0.63 (63%) and 0.32 (32%), respectively, suggesting that the dynamics can be expressed as a biexponential decay function and the fast component of A_2 corresponds to the lifetime of biexciton Auger recombination, $\tau_2 = 2/\tau_1 + k_{ex}^{A}$. When $<N_0> = 1.5$, A_1 and A_2 are 0.78 (52%) and 0.56 (37%), indicating that most of the dynamics can be fitted with biexponential decay function. The relative experimental amplitudes A_2 were examined to evaluate this model. Experimentally, A_2 was ranging from 15 to 30% for $<N_0> \sim 1$, and A_2 was from 25 to 36% for $<N_0> \sim 1.5$. In addition, population dynamics was approximately analyzed by a two-exponential decay function for $<N_0> = 2$ as shown later. These results suggest that the stochastic approach developed by Barzykin and Tachiya is considered to be a good model for biexciton Auger recombination dynamics.

Population dynamics in Figure 4.5a is fitted with triexponential function by fixing a middle component of 70 ps and the lifetime of biexciton Auger recombination was estimated to be 16 ps for 3.4 nm CdTe QDs. In large size QDs, dynamics is similar to small size QDs at low excitation intensities and the decay is nearly fitted with a single exponential function. The precise analysis gives an additional fast lifetime of 61 ps with a few % amplitude. With

increasing excitation intensity, Auger recombination appeares as faster decay component. Population dynamics is fitted with biexponential function and the lifetime of biexciton Auger recombination is 85 ps. The lifetime of biexciton Auger recombination increases with the increase of the QD size. In the case of relatively low Φ OA/TOP capped CdTe QDs (15-30%) with D = 2.6-3.1 nm, population dynamics is different from that of high Φ OA/TOP capped CdTe QDs. Population dynamics of OA/TOP capped CdTe QDs with D = 2.6 nm are illustrated in Figure 4.6 as a function of excitation intensity. In spite of the low excitation intensity, clear fast decay component is detected in Figure 4.6 inset as compared with the dynamics of high Φ QDs. Fast decay component is probably due to the trapping of deep surface defects, which cannot be detected in luminescence spectrum. With increasing excitation intensity, an additional fast decay component appears and dominates in the decay dynamics as clearly shown in Figure 4.6, $\langle N_0 \rangle$ = 1.4. The lifetime of fast decay component is very similar irrespective of the exciton population $\langle N_0 \rangle$ from 1.0-2.0, and has a value of 2.2 ± 0.1 ps. On the other hand, population dynamics of small size TGA capped CdTe QDs is different from that of OA/TOP capped CdTe QDs. Figure 4.7 shows population dynamics of QDs capped with TGA for D = 2.3 and 3.4 nm. In spite of relatively lower Φ, fast decays are negligibly small as compared to that of OA/TOP capped QDs, suggesting that fast decay component of a few ps cannot be detected even for low excitation intensity, $\langle N_0 \rangle$ = 0.06. This result indicates that TGA capped CdTe QDs are better passivated than OA/TOP capped CdTe QDs. Population dynamics at the low excitation intensity is nearly fitted with a single exponential decay function as similar to high Φ OA/TOP capped QDs. With increasing excitation intensity, the additional fast decay component of 1.9 ps appeared, which is attributed to the biexciton lifetime of Auger recombination (Figure 4.7a). The lifetime of biexciton Auger recombination becomes longer with increasing size, and 12.1 ± 0.7 ps for 3.4 nm TGA capped CdTe QDs. The biexciton lifetime is a little shorter than that of the same size

OA/TOP capped CdTe QDs, 16 ± 2 ps (Figure 4.5a).

The lifetime of biexciton Auger recombination (τ_{Auger}) is logarithmic plotted against QD diameter (D) in Figure 4.8. As mentioned in the introduction, theoretical calculation of the lifetime of Auger ionization is proportional to D^{α} ($5 < \alpha < 7$) for CdS NCs.[23] τ_{Auger} of TGA capped CdTe QDs is proportional to $D^{4.6}$ in diameter range from 2.3-3.5 nm. On the other hand, τ_{Auger} of OA/TOP capped CdTe QDs is propotional to $D^{7.0}$ in diameter range of D = 3.3-4.5 nm, where Φ is over 60% for all examined CdTe QDs. This relationship does not hold for small size OA/TOP capped CdTe QDs (D = 2.6-3.1 nm) with rather low Φ (15-30%), in which τ_{Auger} becomes as short as 2-3 ps irrespective of the diameter.

The size dependence of τ_{Auger} has been widely examined for CdSe QDs by Klimov et al.,[1,7,8,45] in which α is determined to be 3.0 for CdSe QDs capped with TOPO. A similar tendency has been reported for zinc-blende CdSe QDs by Pandey et al.,[28] where the diameter scaling is approximately D^3 for the radius of 2.5-3.5 nm, although the steeper scaling index of 4.5-5.0 is expected for all CdSe QDs including small size CdSe (radius down to ~1.8 nm). The result reported by Klimov et al. was different from the theoretical prediction. They concluded that in 3D-confined systems the Auger constant depends on the particle size. On the other hand, Efros et al. concluded the difference of Auger recombination from Auger ionization is connected with a finite density of the states where the Auger electron can be transferred.

Chepic et al. considered the QD surface contribution to Auger recombination by using Fermi's golden rule.[23] The rate of Auger recombination in NCs is expressed by[23,47]

$$\frac{1}{\tau_{Auger}} = \frac{2\pi}{\hbar} \sum_{k,l,m} \left| \left\langle \Psi^{f}{}_{k,l,m} \middle| v(\vec{r}_1, \vec{r}_2) \middle| \Psi^{i} \right\rangle \right|^2 \delta(E_i - E_f)$$

$$v(\vec{r}_1, \vec{r}_2) = \frac{e^2}{(\varepsilon |\vec{r}_1 - \vec{r}_2|)} \qquad (4.6)$$

where, E_i, E_f and Ψ^i, Ψ^f are the total energies and wavefunctions of the initial and final multi-electron states of the QDs, respectively. The sum goes over all states of the system (*k, l, m*) and v is the Coulomb potential, where ε is the dielectric constant. When we estimate the Auger rate it is important how to calculate the matrix elements, $M = \langle\Psi^i|v|\Psi^f\rangle$. As the integrated M can be written as a product of a rapidly oscillating function and a smooth function $f(\boldsymbol{r})$, it can be rewritten as below with the momentum that Auger electron has in the final state $k_f \approx \sqrt{2m_e E_g/\hbar}$:[23,48]

$$M = \left\langle f(\vec{r})\exp(i\vec{k}\vec{r})\right\rangle \approx f'|_a\,(ak_f)^{-2} + f''|_a\,(ak_f)^{-3} + f'''|_a\,(ak_f)^{-4} \qquad (4.7)$$

where the coefficients of $(ak_f)^{-2}$ and $(ak_f)^{-3}$ vanish because of the continuity of the wave function at the QD surface. The left term is then proportional to $f'''|_a$. In the case of QDs, Auger recombination takes place right at the abrupt heterostructure because of large uncertainty of the electron momentum so that electrons can get enough momentum at the interface. As a result, the scaling index in the power low dependence of Auger recombination changes from 5 to 7.[23,47] This result is consistent with the deviation of the scaling index between TGA capped CdTe QDs and OA/TOP capped CdTe QDs. More recently, Wang et al. calculated the Auger rate by using confined states derived from pseudopotential theory.[24] They concluded that QD surface contributes far more to the Auger rate than the inside of QD, which is in agreement with the previous calculations by Chepic et al.[23]

4.5 Conclusion

We synthesized CdTe QDs capped with OA/TOP and TGA to examine the size dependence of biexciton Auger recombination by femtosecond transient absorption spectroscopy. τ_{Auger} is proportional to D^{α}, and α theoretically depends on the QD interfacial conditions.τ_{Auger} of TGA capped CdTe QDs is experimentally proportional to $D^{4.6}$ in diameter ranged from 2.3 to 3.5 nm. On the other hand, τ_{Auger} of OA/TOP capped CdTe QDs is

propotional to $D^{7.0}$ in diameter range of D = 3.3-4.5 nm with higher Φ over 60%. This relationship did not hold for small size OA/TOP capped CdTe QDs (D = 2.6-3.1 nm) with rather low Φ (15-30%), in which τ_{Auger} became as short as 2-3 ps irrespective of the diameter. These results agree with theoretical expectation and suggest that Auger recombination of CdTe QDs strongly depends on the QD surface conditioins and capping reagents.

References

(1) Klimov, V. I.; Mikahailovsky, A. A.; McBranch, D. W.; Leatherdale, C. A., Bawendi, M. G. *Science* **2000**, 287, 1011.

(2) Nirmal, M.; Dubbousi, B. O.; Bawendi, M. G.; Macklin, J. J.; Trautman, J. K.; Harris, T. D.; Brus, L. E. *Nature* **1996**, 383, 802.

(3) Murray, C. B.; Norris, D. J.; Bawendi, M. G. *J. Am. Chem. Soc.* **1993**, 115, 8706.

(4) Brus, L. E. *Appl. Phys. A* **1991**, 53, 465.

(5) Alivisatos, A. P. *Science* **1996**, 271, 933.

(6) Pan, L.; Tamai, N; Kamada, K.; Deki, S. *Appl. Phys. Lett.* **2007**, 91, 51902.

(7) Schaller, R. D.; Klimov, V. I. *Phys. Rev. Lett.* **2004**, 92, 186601.

(8) Schaller, R. D.; Pietryga, J. M.; Klimov, V. I. *Nano Lett.* **2007**, 7, 3469.

(9) Ueda, A.; Matsuda, K.; Tayagaki, T.; Kanemitsu, K.; *Appl. Phys. Lett.* **2008**, 92, 233105.

(10) Larson, D.; Zipfel, W.; Williams, R.; Bruchez, M.; Clark, S.; Wise, F. W. Webb, W. W. *Science* **2003**, 300, 1434.

(11) Alivisatos, A. P. *Nat. Biotechnol.* **2004**, 22, 47.

(12) Coe, W. S.; Woo, W.-K.; Bawendi, M. G.; Bulovic, V. *Nature* **2002**, 420, 800.

(13) Colvin, V. L.; Schlamp, M. C.; Alivisatos, A. P. *Nature* **1994**, 370, 354.

(14) Dabbousi, B. O.; Bawendi. M. G.; Onitsuka, O.; Rubner, M. F. *Appl. Phys. Lett.* **1995**, 66, 1316.

(15) Tessler, N.; Medvedev, V.; Kazes, M.; Kan, S.; Banin, U. *Science* **2002**, 295, 1506.

(16) Klimov, V. I.; Mikhailovsky, A.; Xu, S.; Malko, A.; Hollingsworth, J.; Leatherdale, C. A.; Bawendi, M. G. *Science* **2000**, 290, 314.

(17) Malko, A. V.; Mikhailovsky, A. A.; Petruska, M. A.; Hollingsworth, J. A.; Htoon, H.; Bawendi, M. G.; Klimov, V. I. *Appl. Phys. Lett.* **2002**, 81, 1303.

(18) Eisler, H.-J.; Sunder, V. C.; Bawendi, M. G.; Walsh, M.; Smith, H. I.; Klimov, V. I. *Appl. Phys. Lett.* **2002**, 80, 4614.

(19) Kazes, M.; Lewis, D. Y.; Ebenstein, Y.; Mokari, T.; Banin, U. *Adv. Mater.* **2002**, 14, 317.

(20) Nozik, A. J. *Physica E* **2002**, 14, 115.

(21) Klimov, V. I. *Appl. Phys. Lett.* **2006**, 89, 123118.

(22) Mandal, A.; Nakayama, J; Tamai, N; Biju, V.; Ishikawa, M. *J. Phys. Chem. B* **2007**, 111, 12765.

(23) Chepic, D. I.; Efros, Al. L.; Ekimov, A. I.; Ivanov, M. G.; Kudriavtsev, I. A.; Yazava, T. V. *J. Lumin.* **1990**, 47, 113.

(24) Wang, L. W.; Califano, M.; Zunger, A.; Franceschetti, A. *Phys. Rev. Lett.* **2003**, 91, 056404.

(25) Efros, Al. L.; Efros, A. L. *Sov. Phys. Semicond.* **1982**, 16, 772

(26) Nanda, J.; Ivanov, S. A.; Htoon, H.; Bezel, I.; Piryatinski, A.; Tretiak, S. Klimov, V. I. *J. Appl. Phys.* **2006**, 99, 034309.

(27) Oron, D; Kazes, M; Banin, U *Phys. Rev. B* **2007**,75, 035330.

(28) Pandey, A; Guyot-Sionnest, P *J. Chem. Phys.* **2007**, 127, 111104.

(29) Kloper, V.; Osovsky, R.; Kolny-Olesiak, J.; Sashchiuk, A.; Lifshitz, E. *J. Phys. Chem. C* **2007**, 111, 10336.

(30) Osovsky, R.; Klooper, V.; Kolny-Olesiak, J.; Sashchiuk, A.; Lifshitz, E. *J. Phys. Chem. C* **2007**, 111, 10841.

(31) Gaponik, N.; Talapin, D. V.; Rogach, A. L.; Hoppe, K.; Shevchenko, E. V.; Kornowski, A.; Eychmuller, A.; Weller, H. *J. Phys. Chem. B* **2002**, 106, 7177.

(32) Wolcott, A.; Gerion, D.; Visconate M.; Sun, J.; Schwartzberg, A.; Chen, S.; Zhang, Z. *J. Phys. Chem. B* **2006**, 110, 5759.

(33) Tomasulo, M.;Yildiz, I.; Raymo, F.M. *J. Phys. Chem. B* **2006,** 110, 3853.

(34) Li, C.; Murase, N. *Chem. Lett.* **2005**, 34, 92.

(35) Arbeloa, F. L.; Ojeda, P. R.; Arbeloa, I. L. *J. Lumin.* **1989**, 44, 105.

(36) Reynold, G. A.; Drexhange, K. H. *Optics Commun.* **1975**, 13, 222.

(37) Yu, W. W.; Qu, L.; Guo, W.; Peng, X. *Chem. Mater.* **2003**, 15, 2854.

(38) Perez-Conde, J.; Bhattacharjee, A. K.; Chamarro, M.; Lavallard, P.; Petrikov, V. D.; Lipovskii, A. A. *Phys. Rev. B* **2001**, 64, 113303.

(39) Talapin, D. V. *PhD thesis*; The University of Hamburg, 2002.

(40) Rogach, A. L. *Mater. Sci. Eng. B* **2000**, 69, 435.

(41) Valeur, B. *Molecular Fluorescence*; Wiley-VCH: Weinheim, 2002.

(42) Norris, D. J.; Sacra, A.; Murray, C. B.; Bawendi, M. G. *Phys. Rev. Lett.* **1994**, 72, 2612.

(43) Klimov, V. I.; McBranch, D. W. *Phys. Rev. Lett.* **1998**, 80, 4028.

(44) Klimov, V. I.; McGuire, J. A.; Schaller, R. D. *Phys. Rev. B* **2008**, 77, 195324.

(45) Tachiya, M.; *Chem. Phys. Lett.* **1980**, 69, 605.

(46) Sano, H.; Tachiya, M. *J. Chem. Phys.* **1981**, 75, 2870.

(47) Efros, A. L.; Lockwood, D. J.; Tsybeskov, L. *Semiconductor Nanocrystals*; Plenum Pub.: New York, 2003.

(48) Migdal, A. B. *The qualitative methods of quantum theory*; Preseus Pub.: New York, 2000.

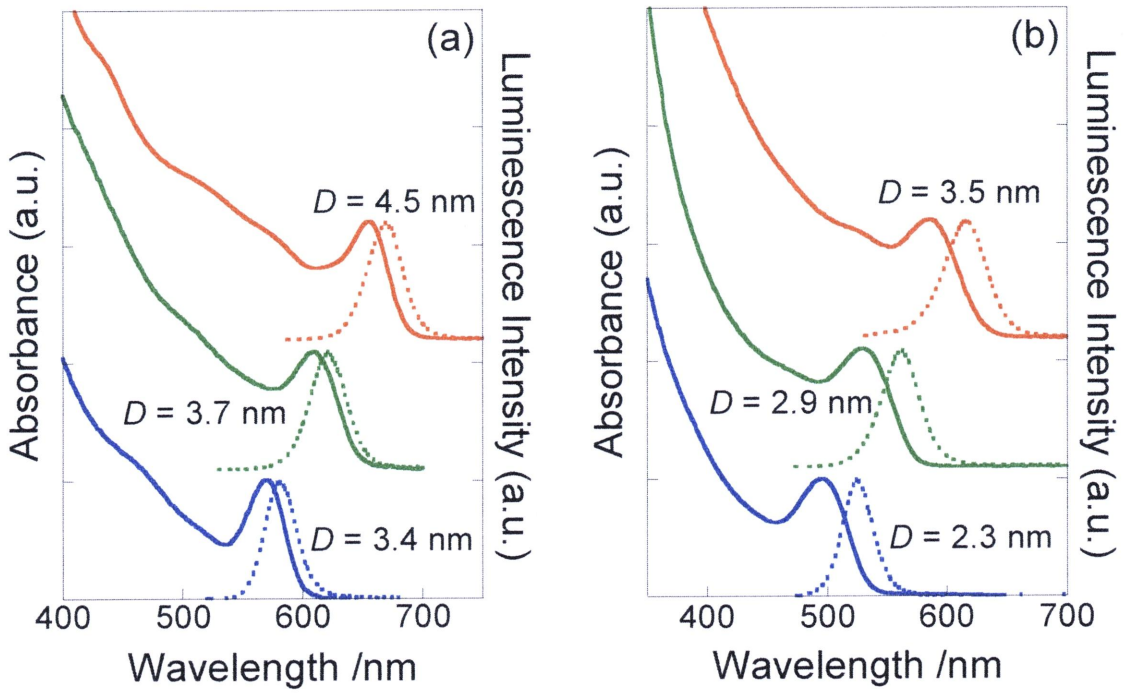

Figure 4.1 Absorption spectra (solid line) and emission spectra (dashed line) of different size CdTe QDs capped with OA (D = 3.4, 3.7 and 4.5 nm) (a) and TGA (D = 2.3, 2.9 and 3.5 nm) (b).

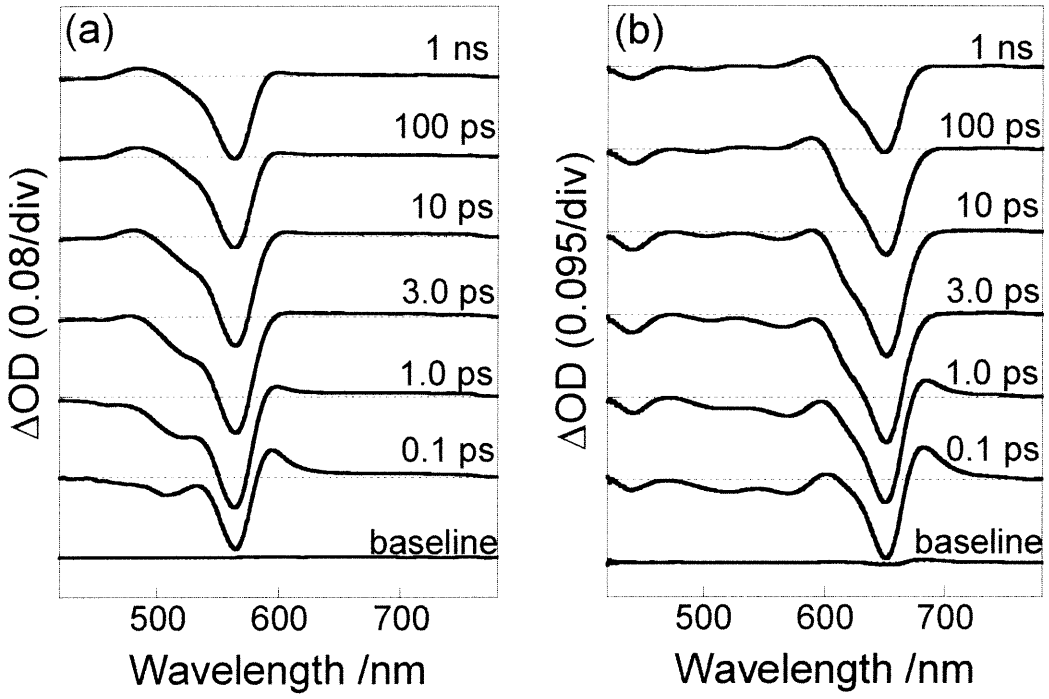

Figure 4.2 Transient absorption spectra of OA/TOP capped CdTe QDs with D = 3.4 nm ($<N_0>$ = 1.6) (a) and D = 4.5 nm ($<N_0>$ = 1.9) (b).

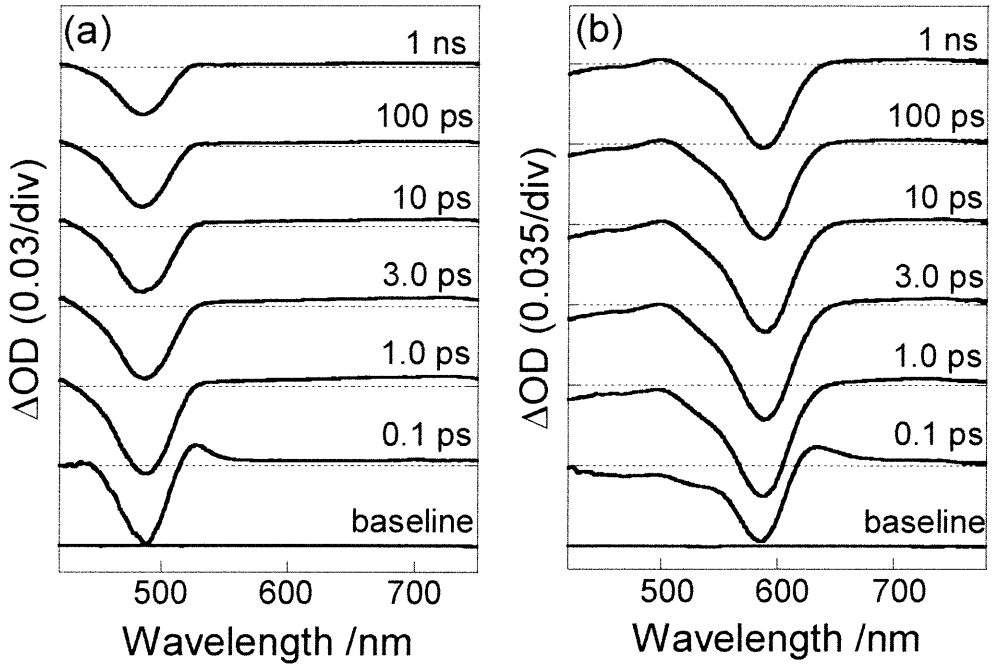

Figure 4.3 Transient absorption spectra of TGA capped CdTe QDs with D = 2.3 nm ($\langle N_0 \rangle$ = 1.5) (a) and D = 3.5 nm ($\langle N_0 \rangle$ = 1.7) (b).

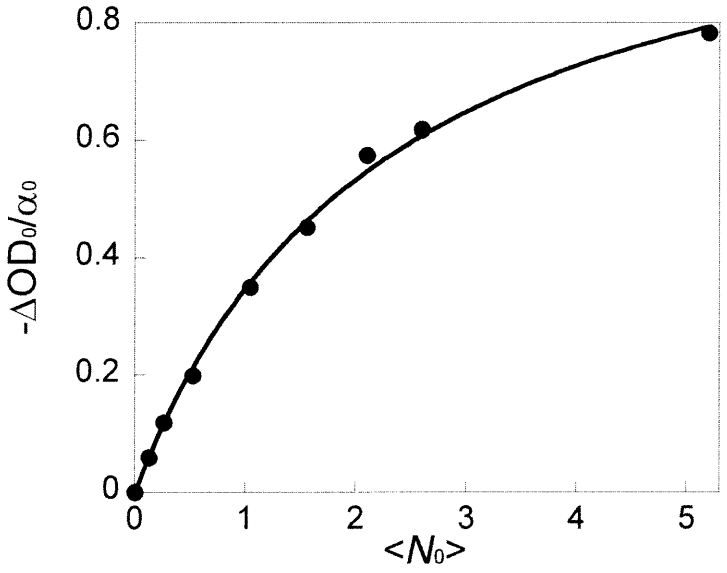

Figure 4.4 Excitation dependence of the normalized first exciton absorption bleaching for OA/TOP capped QDs with D = 3.4 nm. $\langle N_0 \rangle$ is the average number of excitons per QD.

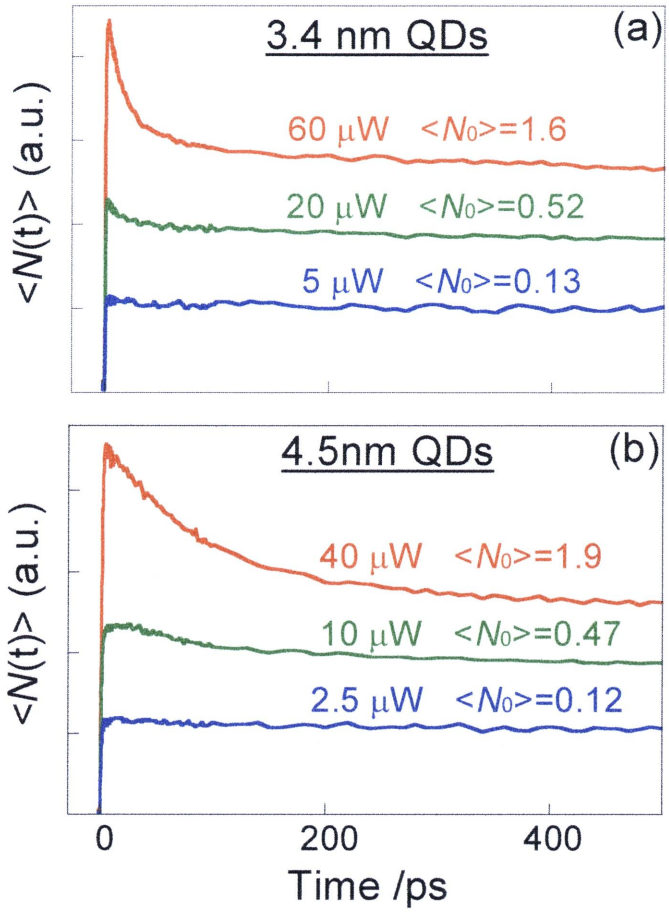

Figure 4.5 Population dynamics at the first exciton bleaching peak of OA/TOP capped CdTe QDs with D = 3.4 nm (a) and D = 4.5 nm (b). $\langle N(t) \rangle$ is the average population dynamics. Each dynamics is multiplied to arbitrary unit for comparison.

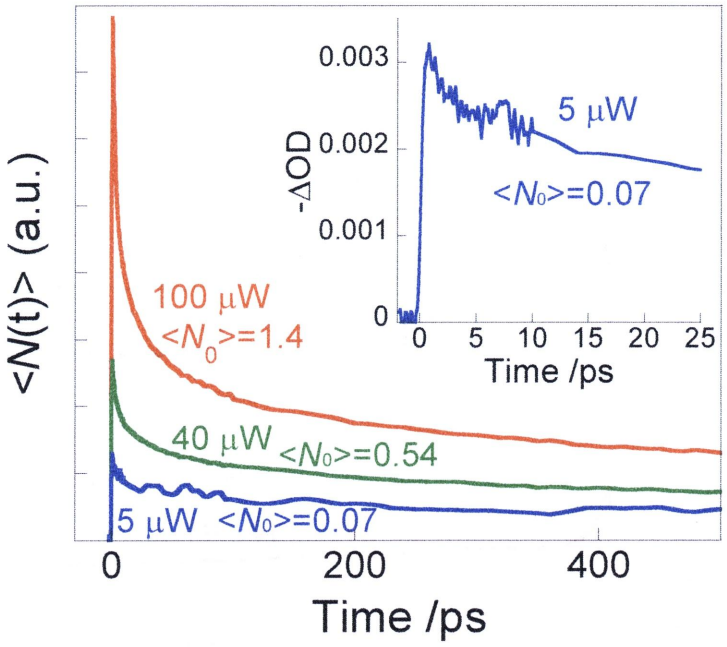

Figure 4.6 Population dynamics at the first exciton bleaching peak of low Φ OA/TOP capped CdTe QDs with D = 2.6 nm and the dynamics of low excitation intensity at short times (inset). Each dynamics is multiplied to arbitrary unit for comparison.

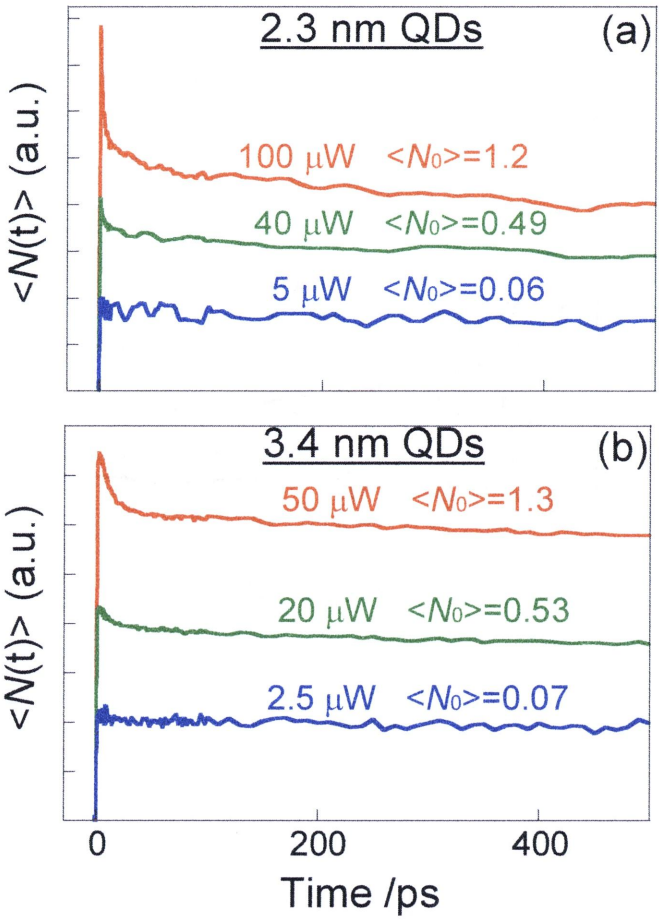

Figure 4.7. Population dynamics at the first exciton bleaching peak of TGA capped CdTe QDs with D = 2.3 nm (a) and D = 3.4 nm (b). Each dynamics is multiplied to arbitrary unit for comparison.

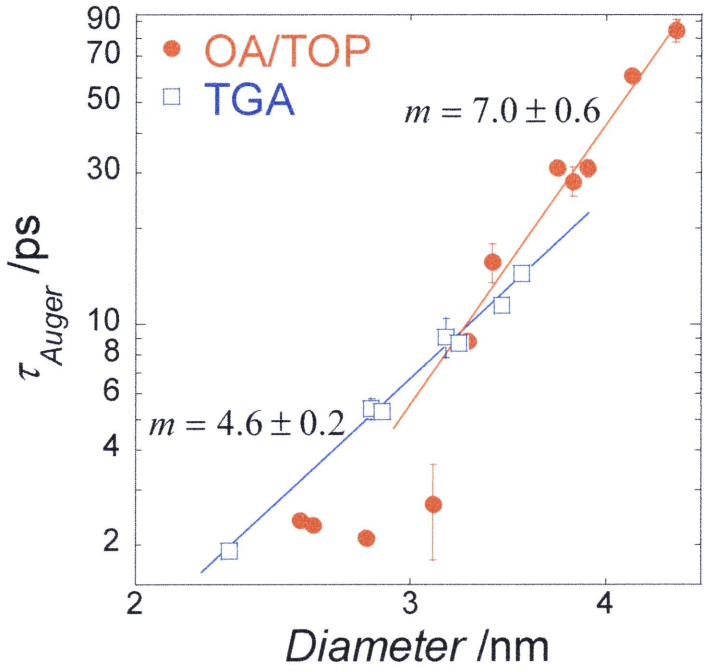

Figure 4.8. The diameter dependence on the lifetime of Auger recombination (τ_{Auger}) of CdTe QDs capped with OA/TOP (solid circles) and TGA (open squares). Lines are fit to the power low dependence $\tau_{Auger} \propto D^m$.

Chapter 5

Effect of surface defects on Auger recombination in CdS QDs

: Role of surface states

5.1 Abstract

The effect of surface states originating from surface defects and capping reagents on Auger recombination in CdS quantum dots (QDs) are investigated by femtosecond transient absorption spectroscopy. Because of the strong size dependent nature of Auger recombination and surface defects, the size dependence of Auger recombination is also conducted to reveal the effect of surface states. The lifetime of Auger recombination is very similar irrespective of surface states in all size regions and was proportional to D^6 (D: QD diameter). This result clearly shows that Auger recombination in CdS QDs does not depend on interfacial electronic structures originating from surface defects and capping reagents of one monolayer level.

5.2 Introduction

Semiconductor quantum dots (QDs) are promising materials for solar cells and laser amplifications because of strong Coulomb interactions and efficient carrier multiplication.[1-5] In colloidal QDs, by conjugating biomolecules and inorganic materials to the QD surface, various potential applications are obtained such as biological tagging and resonant energy-transfer detection.[6-8] On the other hand, the single exciton relaxation processes strongly depend on the capping reagents, surface defects and environmental conditions.[9-11] Defects on the QD surface such as cation or anion dangling bonds make broad electronic states near the band edge and they serve as hole or electron trappings.[12,13] The hot electron relaxation to the band edge is also affected by capping reagents of QDs due to the efficient energy transfer process to the vibrational states of capping reagents.[14] As similar to single exciton dynamics, QD surface states are expected to affect the multi-excitonic interaction such as Auger recombination. Auger recombination in semiconductor QDs have been extensively investigated from the view point of the effect of QD size, shape, inorganic shell, pressure, and so on.[1,15-23] Recently, alloyed QDs and giant multishell QDs achieved the

significant suppression of Auger recombination by changing their potential shapes.[24,25] While these complex structures have opened up a new methodology to suppress Auger recombination, the effect of intrinsic surface properties such as surface defects on Auger recombination has not been comprehensively revealed.[16,26-28] A numerical calculation by empirical pseudopotential theory predicted that Auger recombination mainly occurs at the QD surface, which is determined by the dielectric function at the interior and the surface of QDs.[29] A calculation by Fermis's golden rule also predicted that Auger recombination depends on the abrupt surface inducing a large uncertainty of the electron momentum.[30,31] The experimental investigation of the intrinsic surface effect on Auger recombination plays a important role in understanding the theoretically predicted surface effect. In addition, because of the strong size dependent nature of Auger recombination and surface defects, the size dependent analysis is important to reveal the effect of surface states on Auger recombination comprehensively.

In this chapter, we examined the effect of surface states originating from surface defects and capping reagents on Auger recombination in colloidal CdS QDs as a function of QD size by femtosecond transient absorption spectroscopy. Surface defects of CdS QDs were confirmed with luminescence spectroscopy. The size dependence of the lifetime of Auger recombination (Auger lifetime) was found to be very similar irrespective of surface states. This result clearly shows that Auger recombination in CdS QDs does not depend on interfacial electronic structures originating from surface defects and capping reagents. The size dependence of Auger recombination in CdS QDs was different from that of CdSe QDs ($\sim D^3$), and the possible reason of this deviation is also discussed.

5.3 Experimental

CdS QDs capped with different organic materials were prepared by high temperature colloidal methods in organic solvents reported in the literature and described in Chapter 2. Φ

of CdS QDs was determined at room temperature by comparing the integrated emission to that of coumarin 343 in ethanol (Φ = 63%). Emission quantum yields are Φ =2-11% for MA capped CdS QDs, Φ = 9-55% for OA capped CdS QDs, and Φ = 5-23% for GSH capped CdS QDs. UV-Vis absorption and emission spectra were recorded using U-4100 (Hitachi) and FluoroMax-2 (Jobinyvon-Spex) spectrophotometers, respectively. Transient absorption spectra were measured by femtosecond pump-probe experiments described previously.[25] CdS QDs were excited at 266 and 400 nm by an amplified mode-locked Ti:Sapphire laser with the excitation intensity varying from 1 to 200 μW. Absorption transients were probed by delayed pulses of a femtosecond white-light continuum generated by focusing a fundamental (800 nm) or second harmonic (400 nm) laser pulse into a D_2O cell. The temporal resolution was 100 fs and the temporal dispersion of the white-light continuum was collected for the transient absorption spectra. All measurements were performed at room temperature.

5.4 Results and discussion

Figure 5.1 shows absorption and emission spectra of CdS QDs synthesized by different procedures. In the absorption spectra, the peak associated with the optically allowed $1S_{3/2}$(h)-$1S$(e) transition is observed at the absorption edge in all samples. A sharp $1S_{3/2}$(h)-$1S$(e) peak and several peaks at higher energy are especially observed in MA and OA capped CdS QDs (Figure 5.1b and c), which are probably assigned to $1S_{1/2}$(h)-$1S$(e) and $1P_{3/2}$(h)-$1P$(e) transitions.[35,36] The absorption spectra of GSH capped CdS QDs are broad and the $1S_{1/2}$(h)-$1S$(e) and $1P_{3/2}$(h)-$1P$(e) peaks cannot be observed, possibly because of a larger size dispersion. In the emission spectra, a sharp excitonic emission peak is observed in MA and OA capped CdS QDs. On the other hand, only the broad emission at longer wavelength is observed in GSH capped CdS QDs, which is associated with the emission from surface defects. This result indicates that the dangling bonds at the QDs surface are not fully

passivated with GSH.

We measured transient absorption spectra of GSH, OA and MA capped CdS QDs as a function of the excitation intensity. Figure 5.2 illustrates the transient absorption spectra of OA, GSH and MA capped CdS QDs with average diameters of 2.7 nm. We don't discuss transient absorption spectra and dynamics of MA capped CdS QDs because their features are very similar to those of OA capped CdS QDs. The excitation intensity of 60 μW (3.0×10^{13} photon cm^{-2}) in Figure 5.2 corresponds to about three excitons per CdS QD on average. The initial average number of excitons per QD, $\langle N_0 \rangle$, was calculated by the equation $\langle N_0 \rangle = j_p \sigma_0$, where j_p is the pump photon fluence, and σ_0 is the QD absorption cross section.[37] In both spectra, a negative bleaching peak corresponding to the ground-state $1S_{3/2}$(h)-$1S$(e) absorption is observed. On the other hand, a positive peak is observed at a longer wavelength of the $1S_{3/2}$(h)-$1S$(e) bleaching in OA and MA capped CdS QDs. This signal has a longer decay component than experimental window (500 ps) at low excitation intensity (5 μW, $\langle N_0 \rangle$ = 0.19), and the additional rise component is observed with increasing the excitation intensity (Figure 5.3a). Klimov and McBranch reported that the positive transient signal of glass-doped CdS QDs is assigned to dc Stark effect of the ground state absorption caused by the Auger-process-induced charge separation.[38] However, a positive peak in our experiments exists even at low excitation intensity, and the signal amplitude is linearly proportional to the excitation intensity, which is similar to the trend of the $1S_{3/2}$(h)-$1S$(e) bleaching (Figure 5.3b). This linearity indicates that the positive signal is due to one photon process. In addition, the rise time (~6 ps) is slower than the Auger lifetime (2.3 ps for D = 2.7 nm). These results suggest that the positive peak is not due to the Auger process. Spectral features around the absorption bleaching are almost the same from few ps to up to hundreds of ps in both samples, although the biexciton spectra of CdSe and CdTe QDs was slightly shifted as compared with those of the single exciton.[23,39,40] This result suggests that the effect of multiple excitons on

the spectral feature of the $1S_{3/2}$(h)-$1S$(e) absorption is negligible. ΔOD at the $1S_{3/2}$(h)-$1S$(e) peak is converted to the instantaneous average number of excitons per QD, $\langle N(t)\rangle$, because absorption changes are not linear at higher excitation intensity i.e. for larger $\langle N_0\rangle$. The population dynamics were analyzed by the stochastic approach of multiple charge carrier dynamics in semiconductor nanosystems proposed by Barzykin and Tachiya.[41]

Figure 5.4 shows population dynamics of OA, GSH and MA capped CdS QDs excited at different excitation intensities. In OA capped CdS QDs of D = 3.4 nm, the dynamics at low excitation intensity of 20 μW ($\langle N_0\rangle$ = 0.23) are analyzed by a single exponential decay with a lifetime of ~ns scale, which correspond to the single exciton decay. With increasing the excitation intensity, an additional fast decay component associated with Auger recombination appears (120, 180 μW; $\langle N_0\rangle$ = 1.3, 1.9). These dynamics are well fitted with a bi-exponential decay function and the lifetime of Auger recombination (Auger lifetime) is 6.3 ps for D = 3.4 nm (Figure 5.4a). As the size of CdS QDs increases, the Auger lifetime becomes longer and is 39 ps for D = 4.7 nm (Figure 5.4b). This behavior is consistent with those of CdSe and CdTe QDs.[16,19] In the case of GSH capped CdS QDs, different trends are expected because of surface defects. However, the intensity-dependent population dynamics of GSH capped CdS QDs are very similar to that of OA and MA capped CdS QDs. These dynamics are well fitted with a bi-exponential decay function and the Auger lifetime corresponding to D = 3.1 and 4.9 nm is 3.5 (Figure 5.4c) and 57 ps (Figure 5.4d), respectively. The amplitudes of the component related to Auger recombination are small as compared with the theoretical predictions, which may be due to the fact that not all the photons are converted to band-edge excitons.

We plotted the Auger lifetime logarithmically against QD diameter in Figure 5.5. The size dependence of the Auger lifetime of CdS QDs capped with different reagents does not show significant discrepancies and scales with $\sim D^6$. This result clearly indicates that Auger

recombination in CdS QDs does not depend on surface defects and capping reagents in any size regions. We have shown previously that the size dependence of biexciton Auger recombination varied from $D^{4.6}$ for thioglycolic acid (TGA) capped CdTe QDs to $D^{7.0}$ for OA and trioctylphosphine capped CdTe QDs.[19] In that study, two possible reasons were considered for the different size dependences of the Auger lifetime. One was the capping reagents and the other was the formation of a thin CdS gradient at surface for TGA capped CdTe QDs. By considering the current result, the different size dependence of Auger recombination in CdTe QDs was most probably due to the formation of the thin CdS gradient. The Auger lifetime of CdS QDs clearly shows a D^6 dependence, although Robel et al. reported that the Auger lifetime is proportional to D^3 in various QDs (CdSe, PbSe, InAs and Ge).[42] Theoretically, the lifetime of Auger ionization was proportional to D^m (m = 5-7) depending on the band offset.[30] In Auger recombination, the Auger lifetime was proportional to D^m (m = 2-4) by considering a density of final states proportional to the volume where the Auger electron can be transferred.[43] From above discussion, the D^6 dependence may indicates that CdS QDs are ionized through Auger recombination: Auger ionization may occur in these systems. However, whether Auger electron is ionized could not be clarified in the bleaching analysis of transient absorption and other experiments such as transient absorption measurements in near IR region should be performed to analyze the ejected electron. Besides, detailed numerical calculations suggested that the size dependence of Auger recombination has a strong oscillatory character.[30,31] The scaling index of CdSe QDs examined by Pandey and Guyot-sionnest was steeper than that examined by Klimov et al. (m > 4) if smaller QDs were included.[27] It may become complex to compare the detailed size dependence of Auger recombination in different compounds because of various factors to modify the wavefunctions of QDs.

5.5 Conclusion

In conclusion, we examined the effect of surface states originating from surface defects and capping reagents on Auger recombination in various sized CdS QDs by femtosecond transient absorption spectroscopy. The size-dependent analysis clearly shows that Auger recombination in CdS QDs does not depend on these factors. The lifetime of Auger recombination is proportional to D^6, and this result is different from those of CdSe QDs. This deviation may indicate the presence of Auger ionization in CdS QDs. The analysis of the ejected electron by transient absorption in near IR region may give useful information on which process, Auger recombination or Auger ionization, plays an important role.

References

(1) Klimov, V. I. *Ann. Rev. Phys. Chem.* **58**, 635 (2007)

(2) Beard, M. C.; Midgett, A. G.; Hanna, M. C.; Luther, J. M.; Hughes, B. K.; Nozik, A. J. *Nano. Lett.* **2010**, *10*, 3019.

(3) Kobayashi, Y.; Udagawa, T.; Tamai, N. *Chem. Lett.* **2009**, *38*, 830.

(4) Stubbs, S. K.; Hardman, S. K. O.; Graham, D. M.; Spencer, B. F.; Flavell, W. R.; Glarvey, P.; Masala, O.; Pickett, N. L.; Binks, D. J. *Phys. Rev. B* **2010**, *81*, 081303.

(5) Ueda, A.; Matsuda, K.; Tayagaki, T.; Kanemitsu, Y. *Appl. Phys. Lett.* **2008**, *92*, 233105.

(6) Bruchez, M.; Moronne, M.; Gin, P.; Weiss, S.; Alivisatos, A. P. *Science* **1998**, *281*, 2013.

(7) Biju, V.; Muraleedharan, D.; Nakayama, K.; Shinohara, Y.; Itoh, T.; Baba, Y.; Ishikawa, M. *Langmuir*, **2007**, *23*, 10254.

(8) Willard, D. M.; Carillo, L. L.; Jung, J.; Van Orden, A. *Nano Lett.* **2001**, *1*, 469.

(9) Jones, M.; Lo, S. S.; Scholes, G. D. *J. Phys. Chem. C* **2009**, *113*, 18632.

(10) Chon, B.; Lim, S. J.; Kim, W.; Seo, J.; Kang, H.; Joo, T.; Hwang, J.; Shin, S. K. *Phys. Chem. Chem. Phys.* **2010**, *12*, 9312.

(11) Loginov, S.; Green, T.; Marguet, S.; El-Sayed, M. A. *J. Phys. Chem. A* **1998**, *102*, 5652.

(12) Spanhel, L.; Haase, M.; Weller, H.; Henglein, A. *J. Am. Chem. Soc.* **1987**, *109*, 5649.

(13) Bryant, G. W.; Jaskolski, W. *J. Phys. Chem. B* **2005**, *109*, 19650.

(14) Guyot-Sionnest, P.; Wehrenberg, B.; Yu, D. *J. Chem. Phys.* **2005**, *123*, 074709.

(15) Delerue, C.; Lannoo, M.; Martin, E.; Mihalcescu, I.; Vial, J. C.; Romestain, R., Muller, F.; Bsiesy, A. *Phys. Rev. Lett.* **1995**, *75*, 2228.

(16) Klimov, V. I.; Mikhailovsky, A. A.; McBranch, D. W.; Leatherdale, C. A.; Bawendi, M. G. *Science*, **2000**, *287*, 1011.

(17) Htoon, H.; Hollingsworth, J. A.; Dickerson, R.; Klimov, V. I. *Phys. Rev. Lett.* **2003**, *91*, 227401.

(18) Oron, D.; Kazes, M.; Banin, U. *Phys. Rev. B* **2007**, *75*, 035330.

(19) Kobayashi, Y.; Pan, L.; Tamai, N. *J. Phys. Chem. C* **2009**, *113*, 11783.

(20) Zavelani-Rossi, M.; Lupo, M. G.; Tassone, F.; Manna, L.; Lanzani, G. *Nano Lett.* **2010**, *10*, 3142.

(21) Ueda, A.; Tayagaki, T.; Kanemitsu, Y. *J. Phys. Soc. Jpn.* **2009**, *78*, 083706.

(22) Taguchi, S.; Ishizumi, A.; Kanemitsu, Y. *J. Phys. Soc. Jpn.* **2010**, *79*, 063710.

(23) Kobayashi Y.; Tamai, N. *J. Phys. Chem. C* **2010**, *114*, 17550.

(24) Wang, X. Y.; Ren, X. F.; Kahen, K.; Hahn, M. A.; Rajeswaran, M.; Maccagnano-Zacher, S.; Silcox, J.; Cragg, G. E.; Efros, A. L.; Krauss, T. D. *Nature*, **2009**, *459*, 686.

(25) Garicia-Santamaria, F.; Chen, Y. F.; Vela, J.; Schaller, R. D.; Hollingsworth, J. A.; Klimov, V. I. *Nano Lett.* **2009**, *9*, 3482.

(26) Roberti, T. W.; Cherepy, N. J.; Zhang, J. Z. *J. Chem. Phys.* **1998**, *108*, 2143.

(27) Pandey, A.; Guyot-sionnest, P. *J. Chem. Phys.* **2007**, *127*, 111104.

(28) Jiang, Z. J.; Kelley, D. F. *J. Phys. Chem. C* **2010**, *114*, 17519.

(29) Wang, L. W.; Califano, M.; Zunger, A.; Franceschetti, A. *Phys. Rev. Lett.* **2003**, 91, 056404.

(30) Chepic, D. I.; Efros, Al. L.; Ekimov, A. I.; Ivanov, M. G.; Kudriavtsev, I. A.; Yazava, T. V. *J. Lumin.* **1990**, 47, 113.

(31) Cragg, G. E.; Efros, A. L. *Nano Lett.* **2010**, *10*, 313.

(32) Zou, L.; Fang, Z.; Gu, Z.; Zhong, X. *J. Lumin.* **2009**, *129*, 536.

(33) Ouyang, J. Y.; Kuijiper, J.; Brot, S.; Kingston, D.; Wu, X.; Leek, D. M.; Hu, M. Z.; Ripmeester, J. A.; Yu, K. *J Phys. Chem. C*, **2009**, *113*, 7579.

(34) Yu, W. W.; Qu, L.; Guo, W.; Peng, X. *Chem. Mater.* **2003**, *15*, 2854.

(35) Yu, Z. H.; Li, J. B.; O'Connor, D. B.; Wang, L. W.; Barbara, P. F. *J. Phys. Chem. B* **2003**, *107*, 5670.

(36) Diaz, J. G.; Planelles, J.; Bryant, G. W.; Aizpurua, J. *J. Phys. Chem. B* **2004**, *108*, 17800.

(37) Klimov, V. I. *J. Phys. Chem. B* **2000**, *104*, 6112.

(38) Klimov, V. I.; MacBranch, D. W. *Phys. Rev. B* **1997**, *55*, 13173.

(39) Franceschetti, A.; Zhang, Y. *Phys. Rev. Lett.* **2008**, *100*, 136805.

(40) Sewall, S. L.; Cooney, R. R.; Anderson, K. E. H.; Dias, E. A.; Sagar, D. M.; Kambhampati, P. *J. Chem. Phys.* **2008**, *129*, 084701.

(41) Barzykin A. V.; Tachiya, M. *J. Phys.: Condens. Matter* **2007**, *19*, 065105.

(42) Robel, I.; Gresback, R.; Kortshagen, U.; Schaller, R. D.; Klimov, V. I. *Phys. Rev. Lett.* **2009**, *102*, 177404.

(43) Efros, A. L.; Lockwood, D. J.; Tsybekov, L. *Semiconductor Nanocrystals;* Plenum: New York, 2003.

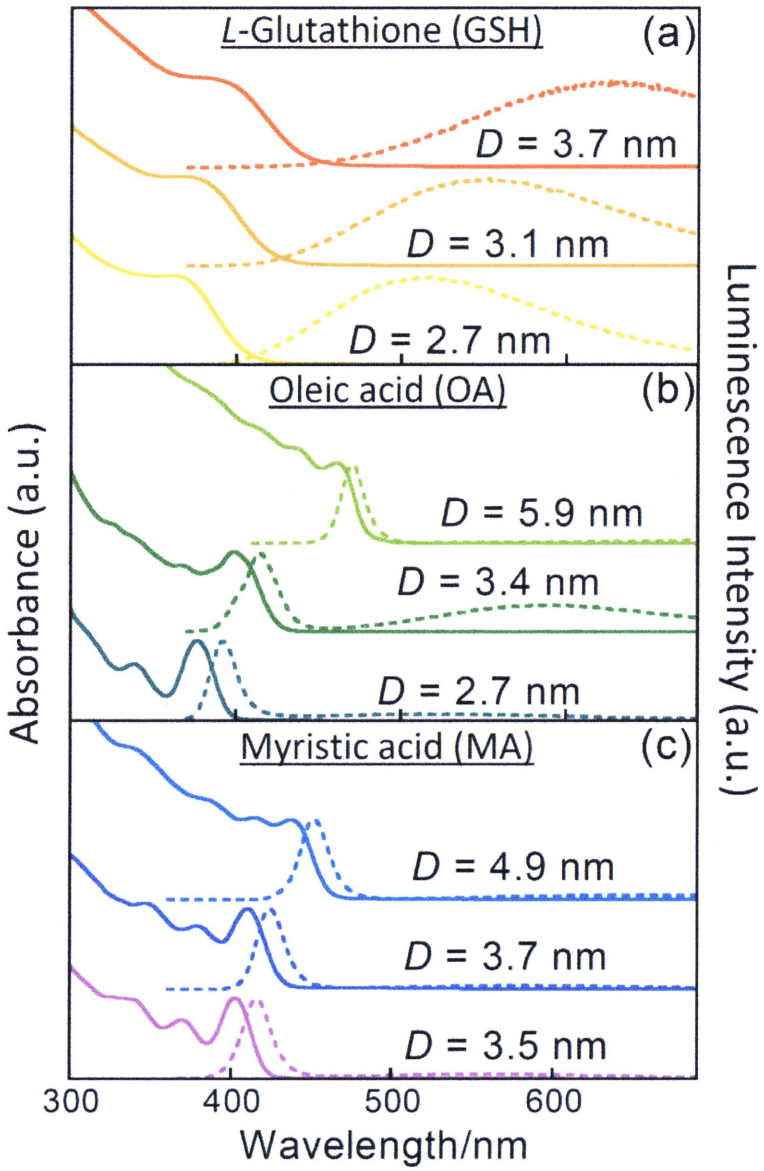

Figure 5.1 Absorption (solid lines) and emission spectra (dashed lines) of GSH (a), OA (b), and MA (c) capped CdS QDs.

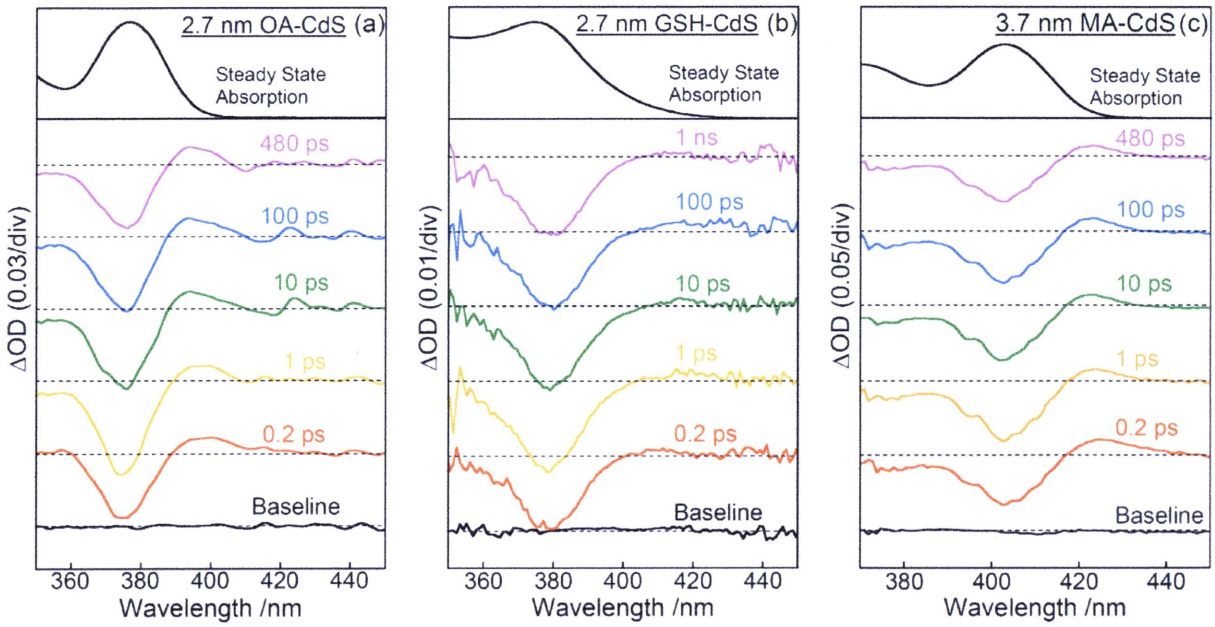

Figure 5.2 Transient absorption spectra of OA (a), GSH (b) and MA (c) capped CdS QDs whose diameters are 2.7, 2.7 and 3.7 nm, respectively. The pump intensity of Figure 5.2a and b are 60 μW, which corresponds to $\langle N_0 \rangle \sim 3$. $\langle N_0 \rangle$ is the average number of excitons per QD. Transient absorption spectra of MA capped CdS QDs are similar to those of OA capped CdS QDs in all size region.

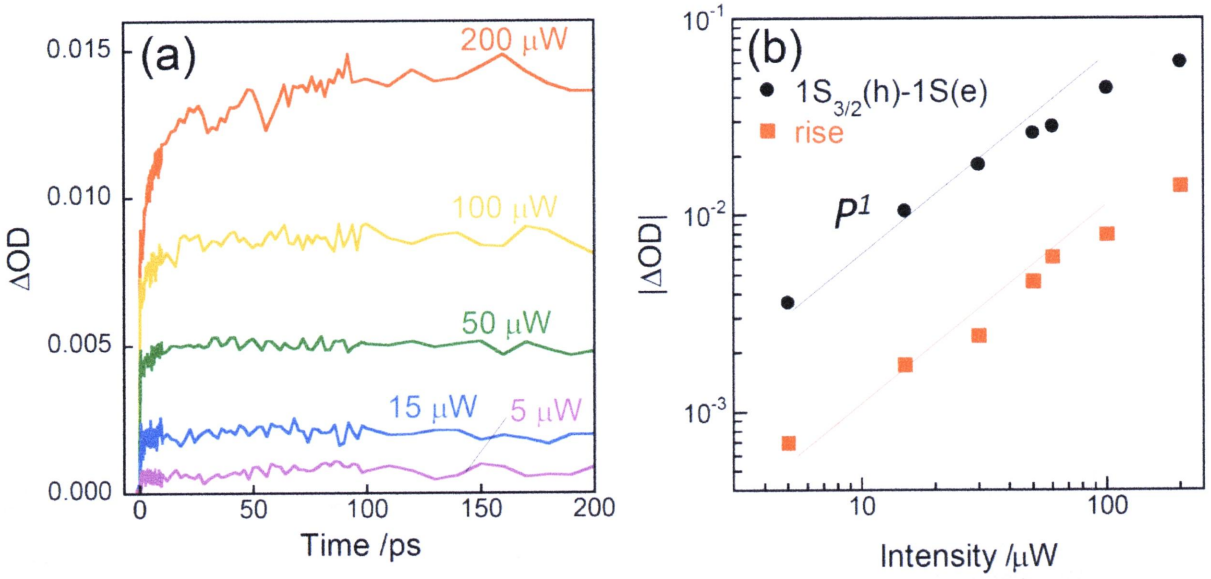

Figure 5.3 Transient absorption dynamics at the positive peak located at the longer wavelength of the 1*S* bleaching of OA capped CdS QDs (D = 2.7 nm) (a). The intensity dependence of the positive peak (b). P denotes the excitation intensity.

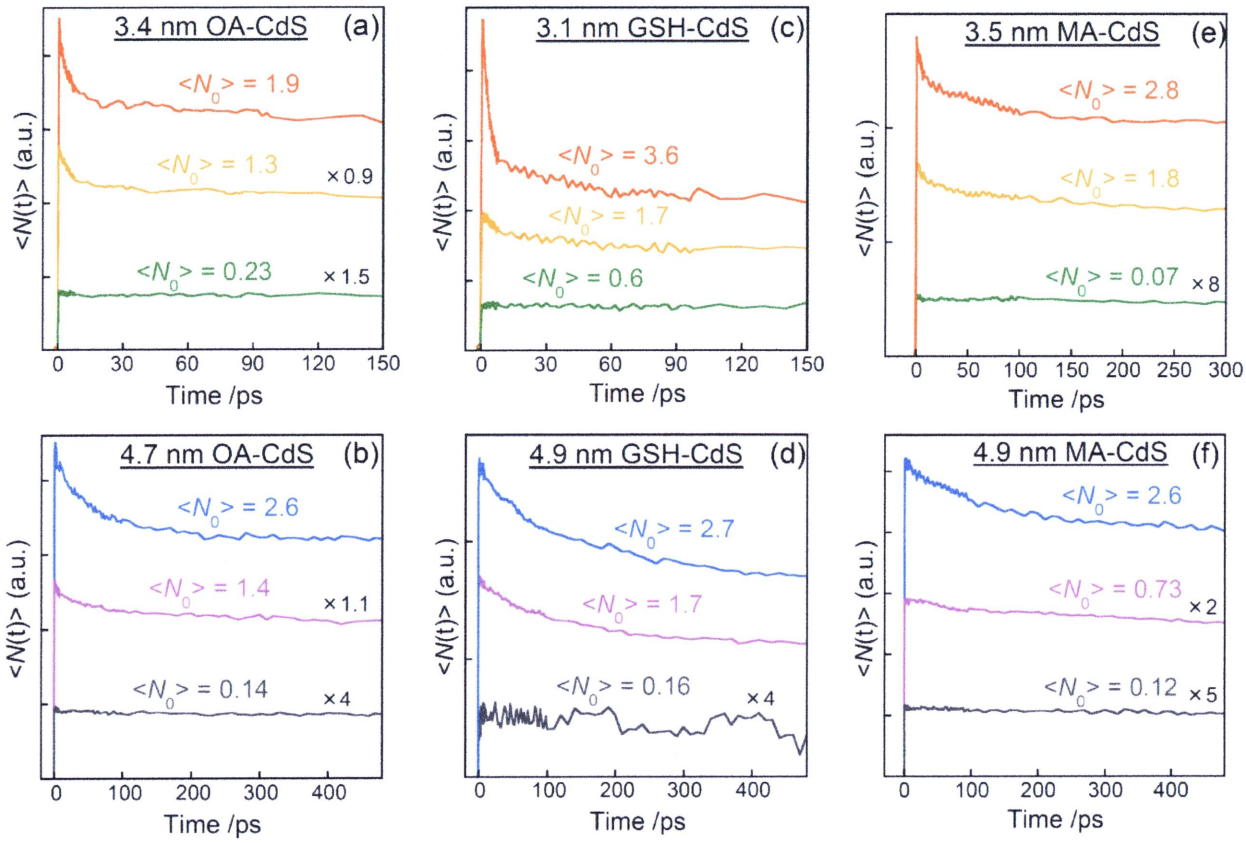

Figure 5.4 Population dynamics of OA (a, b), GSH (c, d) and MA capped CdS QDs (e, f). The QD diameter and $\langle N_0 \rangle$ are listed in the figures.

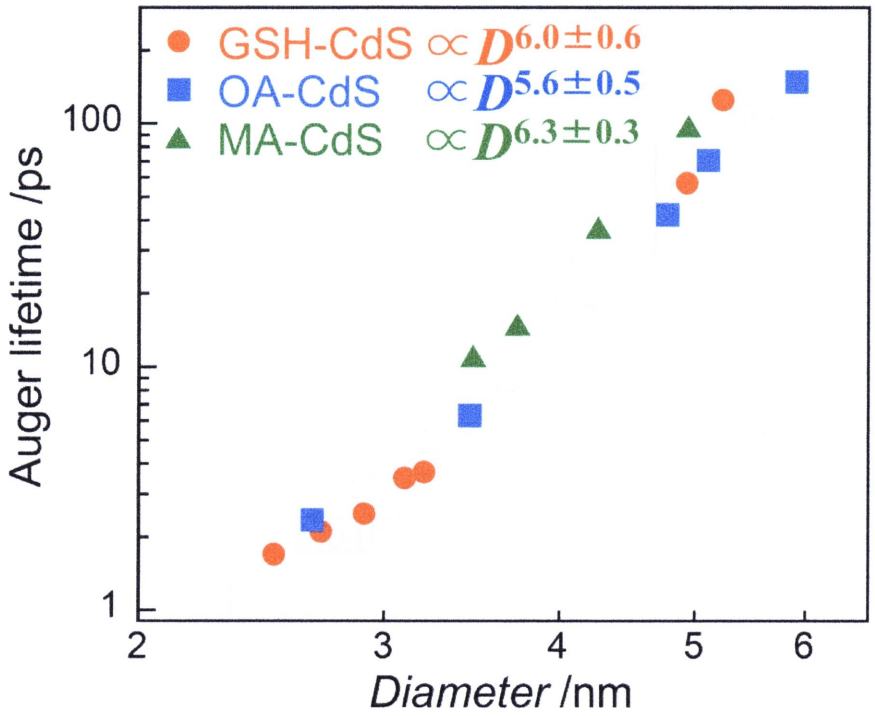

Figure 5.5 Size dependence of the Auger lifetime (τ_{AR}) of CdS QDs capped with GSH (red circles), OA (blue squares) and MA (green triangles). The grey band indicates a power law dependence $\propto D^6$, where D is the QD diameter.

Chapter 6

Multiexciton spectroscopy of CdTe QDs

6.1 Abstract

Size-dependent emission properties of multiexcitons such as the biexciton and the $1S1S1P$ $(1S_{3/2}(h)\text{-}1S(e))^2(1P_{3/2}(h)\text{-}1P(e))$ triexciton were examined in colloidal CdTe quantum dots (QDs) capped with oleic acid and trioctylphosphine (OA/TOP) by time-resolved luminescence spectroscopy. The biexciton and the $1S1S1P$ triexciton binding energy is estimated from the spectral shift of the multiexciton emission. The binding energy of CdTe QDs is larger than that of CdSe QDs, possibly due to the stronger confinement of the CdTe QDs. The size dependence of the biexciton luminescence dynamics is comparable to that of biexciton Auger recombination examined by transient absorption spectroscopy. It suggests that the biexciton dynamics is dominated by Auger recombination. On the other hand, the size dependence of the $1P$ dynamics is different from that of the biexciton dynamics. The $1P$ emission dynamics is dominated by the dynamics of the $1S1S1P$ triexciton, which might be the reason for the different size dependence of the biexciton and the $1P$ emission dynamics.

6.2 Introduction

Strong carrier-carrier interactions in semiconductor QDs have many important spectral and dynamical implications. They result in large, tens-of-meV spectral shift of the multiexciton emission bands with respect to single exciton transition energy. Multiexciton states in semiconductor QDs are of importance for the fundamental understanding of many-body interactions in these systems and for their applications in optical amplification,[1] lasing[2] and quantum-bit pair[3] for quantum information processing. Several reports on multiexcitons have been studied by time-resolved luminescence spectroscopy, especially for CdSe QDs.[4,5] Recently, quasi-continuous-wave optical pumping techniques and single QD microspectroscopy were also used for the study of multiexcitons in semiconductor QDs.[6-9]

These techniques can provide precise spectral information on multiexcitons, while time-resolved luminescence spectroscopy gives both dynamical and spectral information. Strong Coulomb interactions in semiconductor QDs also enhance nonradiative Auger recombination. Auger recombination becomes highly effective in the multiexciton states and therefore multiexciton emissions are dominated by multiexciton Auger recombination.

In this chapter, we examined the size-dependent multiexciton spectroscopy of colloidal CdTe QDs capped with OA/TOP by time-resolved luminescence spectroscopy. Size dependence of the emission from the biexciton and the $1P$ state in CdTe QDs were clearly detected.

6.3 Experimental

CdTe QDs capped with OA/TOP were prepared according to the procedure reported in the literature and described in Chapter 2.[10,11] QD diameters (D) were estimated from the first excitonic absorption peak as described in previous reports[12] and confirmed by a HRTEM (Tecnai G2 F20 200keV, FEI). The diameter of CdTe QDs in our experiments was 3.3-4.3 nm. Time-resolved luminescence spectra were measured using a streak camera (synchronous blanking unit M5678 and synchroscan sweep unit M5675, Hamamatsu). CdTe QDs were excited at 400 nm by the second harmonic of an amplified mode-locked Ti:Sapphire laser (Spitfire and Tsunami, Spectra-Physics). The pump pulse was focused into 1 mm diameter spot and the excitation intensity ranged from 5 to 500 μW with a repetition rate of 1 kHz. The excitation intensity was measured by a calibrated power meter (Orion/PD, Ophir). The temporal resolution of the Streak camera at room temperature was 6 ps.

6.4 Results and discussion

Typical absorption and emission spectra of OA/TOP capped CdTe QDs with different diameters are shown in Figure 6.1. A sharp first excitonic absorption peak and a single Gaussian emission were observed in all the absorption and emission spectra as previously reported.[13] Emission quantum yields were over 50% in all samples. We examined the excitation intensity dependence of the time-resolved luminescence spectra at room temperature. The average number of excitons per QD, $\langle N_0 \rangle$, was calculated by the pump photon fluence, j_p, and the QD absorption cross section, σ_0, as similar to the previous section.[13,14] Figure 6.2 shows time-resolved luminescence spectra (D = 3.9 nm) recorded at 6 ps after the excitation at different excitation intensities. At low excitation intensity (6 μW and $\langle N_0 \rangle$ = 0.1, Figure 6.2a), the time-resolved luminescence spectra were fitted with a single Gaussian function corresponding to the steady-state emission spectrum. This spectrum is attributed to the single excitonic emission from the 1S state. With increasing excitation intensity, the spectrum shifts to lower energy and another emission peak is observed at higher energy (500 μW and $\langle N_0 \rangle$ = 8.6, Figure 6.2b). At high pump intensity, biexciton states are formed in CdSe QDs leading to shifted spectra of the 1S emission.[4,5] Besides, when QDs are excited at much higher pump intensity and the 1S state is fully occupied, the emission from higher state (1P) is also observed at higher energy region. We attributed the intensity-dependent spectra to the emission from the biexciton state and the 1P state, and the emission spectra were well fitted with three Gaussian functions. The shift of the biexciton emission band with respect to the single exciton peak is due to the exciton-exciton interaction energy and provides a direct measurement of the biexciton binding energy.[15,4] The biexciton binding energies range from 33 meV (D = 4.3 nm) to 56 meV (D = 3.5 nm). It appears to increase with decreasing QD size, although the trend is not so clear (Figure 6.3a). The biexciton binding energies of CdSe QDs are 20-35 meV (D = 3.0-5.0 nm) and they are

smaller than that of CdTe QDs with sizes comparable to CdSe QDs.[4] This is probably due to the larger Bohr radius of CdTe as compared with that of CdSe, which leads to a stronger confinement of the electron and the hole in CdTe QDs. Achermann et al. reported an abrupt decrease in the biexciton shift in smaller size CdSe QDs due to the electron-electron and hole-hole repulsions,[4] while Bonati et al. did not observe this phenomenon.[17] The effect of carrier-carrier repulsions was not observed in our experiments of CdTe QDs in similar size ranges.

The energy difference between $1S$ and $1P$ emission is much greater than the biexciton shift. It is 152 meV for D = 4.3 nm, gradually increases with the decrease of the QD size and finally reaches 216 meV for D = 3.4 nm. This value is smaller than that of CdSe QDs with a similar diameter (~160 meV for CdTe QDs and ~190 meV for CdSe QD with D = 4.2 nm s).[4,5] The $1P$ emission is assigned to a triexciton of the type $(1S_{3/2}(h)\text{-}1S(e))^2(1P_{3/2}(h)\text{-}1P(e))$ ($1S1S1P$ triexciton) by Carge et al.[5] and Bonati et al.[17] The $1S1S1P$ triexciton binding energy can be estimated by taking the difference between the energy of the $1P$ emission and the absorption of $1P_{3/2}(h)\text{-}1P(e)$. The size dependence of the transition energy of $1P_{3/2}(h)\text{-}1P(e)$ in CdTe QDs has been experimentally[18] and theoretically[19] examined and we refer to the experimental analysis of Zhong et al.[18] The $1S1S1P$ triexciton binding energy is plotted as a function of the diameter of CdTe QDs in Figure 6.3b. It gradually increases with decreasing diameter and saturates below D = 3.6 nm (~160 meV). The triexciton binding energy of CdTe QDs is larger than that of CdSe QDs (70-120 meV for D = 3.0-4.0 nm), which is also due to the stronger confinement of CdTe QDs as the case of biexciton binding energy. On the other hand, the triexciton binding energy is much larger than the biexciton binding energy. This difference may be explained by the polarization nature of the $1S$ and $1P$ state. The $1P$ state has a much polarizable character than the $1S$ state and thus, multiexcitons are better stabilized in the $1P$

state, which might be the reason why the triexciton binding energy is larger than the biexciton binding energy.

Figure 6.4 displays emission decays at the peak of the $1S$ and $1P$ band. At low pump intensity (6 μW), the emission decay at the $1S$ peak was fitted with a single exponential decay function with a lifetime of several ns. As the pump intensity increases, an additional decay component of tens of ps appears. This component only develops at high pump intensity over $\langle N_0 \rangle \sim 1$, and thus it can be safely assigned to the biexciton decay component. The lifetimes of the biexciton and the $1P$ decay (D = 3.9 nm) are 34 and 16 ps, respectively. under low excitation intensity, excited electrons of the $1P$ state relax to the $1S$ state within hundreds of fs by transferring their energy to holes (Auger cooling).[20,21] Because of this ultrafast relaxation, the $1P$ emission cannot be observed at low pump intensities. The $1P$ emission can be observed only when the $1S$ state is occupied and when Auger cooling is effectively suppressed. The ratio of the biexciton lifetime to the $1P$ lifetime is 2.3 ± 0.2 for almost all samples except the largest diameter, D = 4.3 nm. From previous reports, the ratio of the biexciton lifetime to the triexciton lifetime (τ_2/τ_3) of CdSe QDs is assessed to be 2.25 by transient absorption spectroscopy. A theoretical calculation suggests that τ_2/τ_3 under the electronic configuration, in which two excitons occupy the $1S$ state and the third exciton occupies the $1P$ state, is 2.5 in stochastic Auger recombination model, although this calculation ignores efficient Auger cooling and therefore it is quite rough approximation.[22] This result suggests that the $1P$ decay at high power is likely due to the $1S1S1P$ triexciton Auger recombination.

The lifetimes of the biexciton and the $1P$ decay are plotted on a semi-logarithmic coordinate against the QD diameter in Figure 6.5. In our previous report, biexciton Auger recombination examined by transient absorption spectroscopy was proportional to D^m (m: scaling index, m = 6.3 ± 0.6) in the range of D = 3.5-4.4 nm (size dependence of wider range

was $m = 7.0 \pm 0.7$).[23] The size dependence of the biexciton decay examined by time-resolved luminescence spectroscopy is well consistent with the lifetime of Auger recombination examined by transient absorption spectroscopy. This strongly suggests that the biexciton state in CdTe QDs is dominated by Auger recombination as in previous reports on CdSe and PbSe QDs, and time-resolved luminescence spectroscopy is one of the effective tools to examine Auger recombination.[4,24] The lifetime of the $1P$ emission is shorter than that of the biexciton for all samples of CdTe QDs and the scaling index, m, was 4.1 ± 0.3. In the previous report on the $1S$ transient absorption dynamics of CdSe QDs, the size dependence of the $1S1S1P$ triexciton Auger recombination is similar to that of biexciton Auger recombination ($\propto D^3$, $m = 3$ for $D = 2.4$-8.0 nm).[25,22] The difference in the scaling index between the biexciton and the $1S1S1P$ triexciton in our experiments might come from the difference of the recombination process of the triexciton. $1S_{3/2}$(h)-$1S$(e) Auger recombination of $1S1S1P$ triexciton can be observed by transient absorption dynamics of the $1S$ state, while $1P_{3/2}$(h)-$1P$(e) Auger recombination of $1S1S1P$ triexciton can be observed by $1P$ emission dynamics. In the case of CdSe QDs the scaling index of the $1P$ state looks smaller ($m < 2$) in the size range of $D =$ 2.5-7.0 nm as compared to the value obtained by transient absorption measurements.[4] This relationship between the scaling exponents of the biexciton Auger recombination and of the $1P$ decay is comparable to that of CdTe QDs (m = 6-7 and $m = 4$ for biexciton Auger recombination and $1P$ decay).

6.5 Conclusion

In conclusion, we examined the size-dependent emission properties of multiexcitons were examined in colloidal CdTe QDs capped with OA/TOP by time-resolved luminescence spectroscopy. The binding energy of CdTe QDs is larger than that of CdSe QDs, possibly due to stronger confinement of CdTe QDs. The size dependence of the biexciton luminescence

dynamics is comparable to that of biexciton Auger recombination examined by transient absorption spectroscopy. It is strongly suggested that the biexciton dynamics is dominated by Auger recombination. On the other hand, the size dependence of the $1P$ dynamics is different from that of the tendency for the biexciton. The $1P$ emission dynamics is dominated by that of $1S1S1P$ triexciton, which might be the reason for the different size dependence of the biexciton and the $1P$ emission dynamics.

References

(1) Klimov, V. I.; Mikhailovsky, A. A.; Xu, S.; Malko, A.; Hollingsworth, J. A.; Leatherdale, C. A.; Eisler, H. –J.; Bawendi, M. G. *Science*, **2000**, *290*, 314.

(2) Mikhailovsky, A. A. ; Malko, A. V.; Hollingsworth, J. A.; Bawendi, M. G.; Klimov, V. I. *Appl. Phys. Lett.* **2002**, *80*, 2380.

(3) Chen, G.; Bonadeo, N. H.; Steel, D. G.; Gammon, D.; Katzer, D. S.; Park, D.; Sham, L. J. *Science* **2000**, *289*, 1906.

(4) Achermann, M.; Hollingsworth, J. A.; Klimov, V. I.; *Phys. Rev. B* **2003**, *68*, 245302.

(5) Caruge, J.; Chan, Y.; Sundar, V.; Eisler, H. J.; Bawendi, M. G. *Phys. Rev. B* **2004**, *70*, 085316.

(6) Ficher, B.; Caruge, J. M.; Zehnder, D. ; Bawendi, M. *Phys. Rev. Lett.* **2005**, *94*, 087403.

(7) Osovsky, R.; Cheskis, D.; Kloper, V.; Sashchiuk, A.; Kroner, M.; Lifshitz, E. *Phys. Rev. Lett.* **2009**, *102*, 197401.

(8) Oron, D.; Kazes, M.; Shweky, I.; Banin, U. *Phys. Rev. B* **2006**, *74*, 115333.

(9) Sitt, A.; Sala, F. D.; Menagen, G.; Banin, U. *Nano Lett.* **2009**, 9, 3470.

(10) Kloper, V.; Osovsky, R.; Kolny-Olesiak, J.; Sashchiuk, A.; Lifshitz, E. *J. Phys. Chem. C* **2007**, *111*, 10336.

(11) Osovsky, R.; Klooper, V.; Kolny-Olesiak, J.; Sashchiuk, A.; Lifshitz, E. *J. Phys. Chem. C* **2007**, *111*, 10841

(12) Yu, W. W.; Qu, L.; Guo, W.; Peng, X. *Chem. Mater.* **2003**, *15*, 2854.

(13) Klimov, V. I. *J. Phys. Chem. B* **2000**, *104*, 6112.

(14) Valeur, B. *Molecular Fluorescence*; Wiley-VCH: Weinheim, **2002**.

(15) Klimov, V. I. *Ann. Rev. Phys. Chem.* **2007**, *58*, 635.

(16) Esch, V.; Fluegel, B.; Khirtova, G.; Gibbs, H. M.; Jiajin, X.; Kang, K.; Koch, S. W.; Liu, L.C.; Risbud, S. H.; Peyghambarian, N. *Phys Rev. B* **1990**, *42*, 7450.

(17) Bonati, C.; Mohamed, M. B.; Tonti, D.; Zgrablic, G.; Haacke, S.; Mourik, F. V.; Chergui, M. *Phys. Rev. B* **2005**, *71*, 205317.

(18) Zhong, H.; Nagy, M.; Jones, M.; Scholes, G. D. *J. Phys. Chem. C* **2009**, *113*, 10465.

(19) Efros, Al. L.; Rosen, M. *Phys. Rev. B* **1998**, *58*, 7120.

(20) Efros, Al. L.; Kharchenko, V. A.; Rosen, M. *Solid State Commun.* **1995**, *93*, 281.

(21) Klimov, V. I.; McBranch, D. W. *Phys. Rev. Lett.* **1998**, *80*, 4028.

(22) Klimov, V. I.; McGuire, J. A.; Schaller, R. D.; Rupasov, V. I. *Phys. Rev. B* **2008**, *77*, 195324.

(23) Kobayashi, Y.; Pan, L.; Tamai, N. *J. Phys. Chem. C* **2009**, *113*, 11783.

(24) Ellingson, R. J.; Beard, M. C.; Johnson, J. C.; Yu, P.; Micic, O. I.; Nozik, A. J.; Shabaev, A.; Efros, A. L. *Nano Lett.* **2005**, *5*, 865.

(25) Klimov, V. I.; Mikhailovsky, A. A.; McBranch, D. W.; Leatherdale, C. A.; Bawendi, M. G. *Science*, **2000**, *287*, 1011.

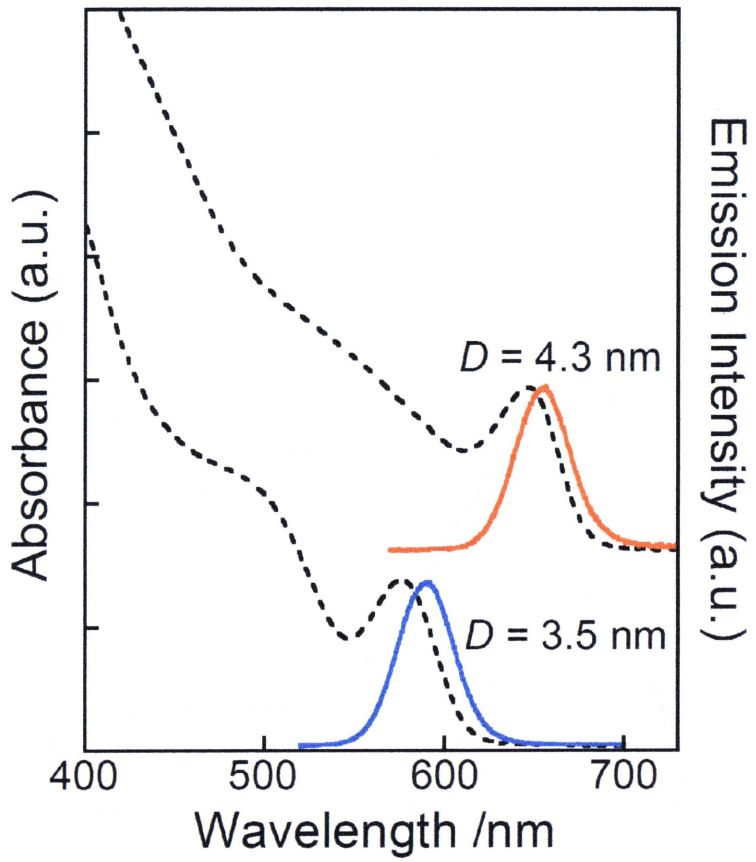

Figure 6.1 Absorption spectra (dashed lines) and emission spectra (solid lines) of different size CdTe QDs capped with OA/TOP (D = 3.5 and 4.3 nm)

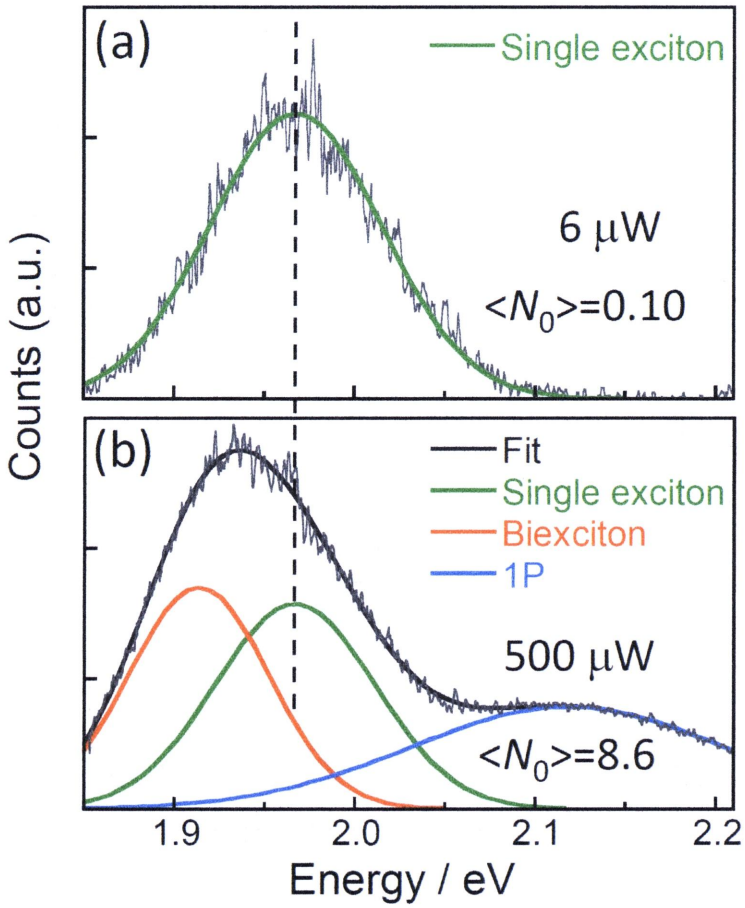

Figure 6.2 Time-resolved luminescence spectra of CdTe QDs with D = 3.9 nm recorded at 6 ps after the excitation. The pump intensities are 6 μW (<N_0> = 0.10) (a) and 500 μW (<N_0> = 8.6) (b). The spectra at 500 μW can be fitted with three Gaussian functions (the single exciton (green), the biexciton (red) and the 1P state (blue)).

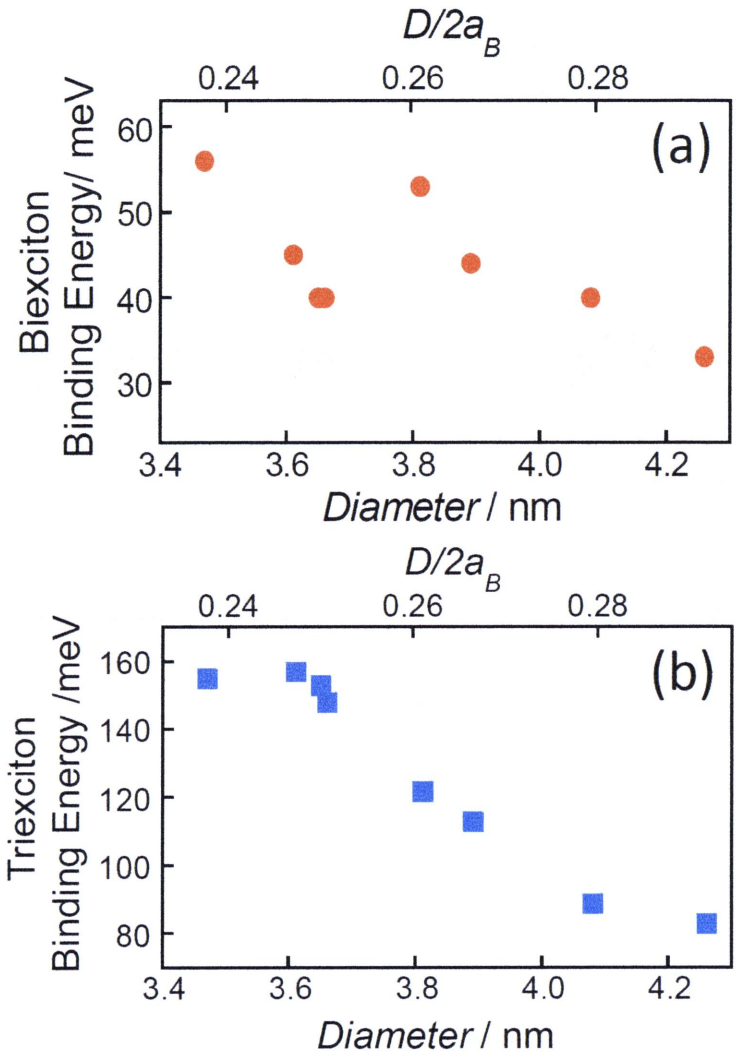

Figure 6.3 Biexciton (a) and triexciton (b) binding energy of CdTe QDs as a function of the diameter. a_B is the exciton Bohr radius of bulk CdTe (a_B = 7.3 nm)[16].

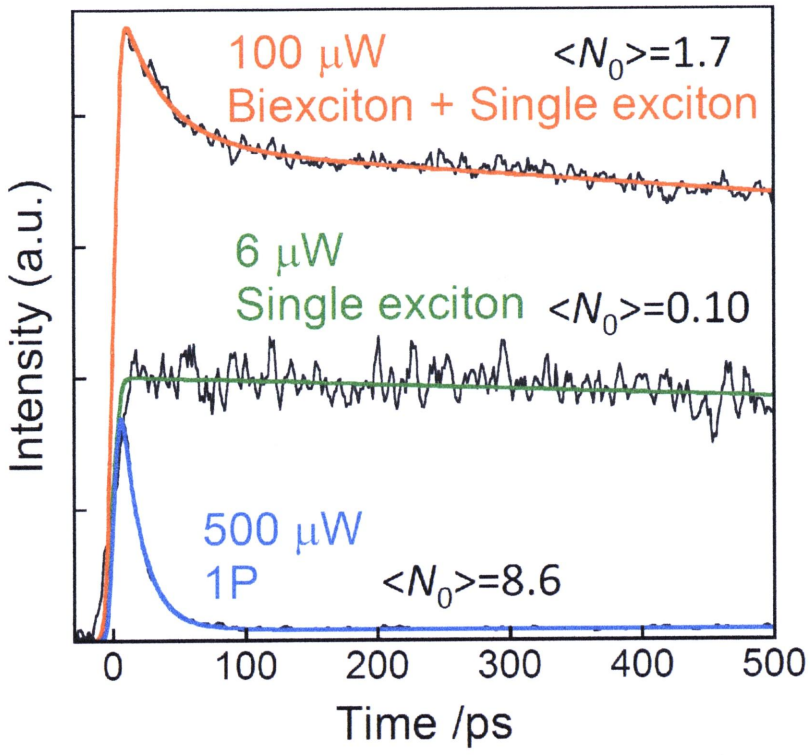

Figure 6.4 Emission decays of the single exciton (6 μW, $\langle N_0 \rangle$ = 0.10), the biexciton + the single exciton (100 μW, $\langle N_0 \rangle$ = 1.7) and the 1*P* state (500 μW, $\langle N_0 \rangle$ = 8.6).

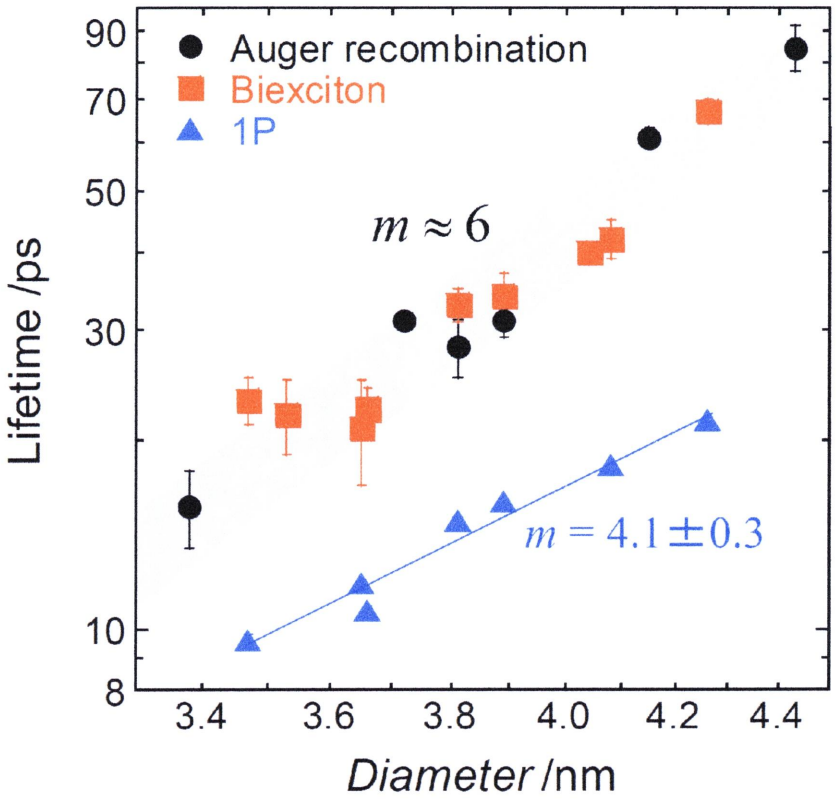

Figure 6.5 Size dependence of the biexciton lifetime of CdTe QDs. Lines correspond to power-law ($\propto D^m$) fits of the data ($m \cong 6$ for the biexciton, $m = 4.1$ for the $1P$ triexciton).

Chapter 7

Effect of temperature on Auger recombination in CdTe QDs

7.1 Abstract

The effect of temperature on biexciton Auger recombination was examined in the range of 10 to 350 K with CdTe QDs (D = 4.0 nm) capped with OA/TOP. It shows moderate temperature dependence of Auger recombination below 175 K. In a theoretical calculation, Auger recombination in semiconductor QDs is independent on temperature because the activation threshold of Auger recombination is eliminated by the relaxation of the translational momentum conservation. This temperature dependence suggests that a phonon participates in the final state of Auger recombination in CdTe QDs because of the reduced availability of states satisfying energy conservation.

7.2 Introduction

In bulk semiconductors, the Auger process has to require energy and translational momentum conservation because the energy of the electronic state forms band structures as a function of the translational momentum. For these reasons, Auger recombination in bulk semiconductors depends exponentially on the energy gap and temperature as given later in eq 7.1, which is called threshold Auger recombination.[1,2] In the case of indirect-gap semiconductors, Auger recombination is strongly suppressed because of few electronic structures satisfying these conservations. Auger recombination can be observed only when the translational momentum conservation relaxes with the participation of a phonon (phonon-assisted Auger recombination).[3] This effect can be examined by temperature-dependent measurements. According to a theoretical calculation, the temperature dependence of phonon-assisted Auger recombination in bulk semiconductors is more moderate than that of threshold Auger recombination.[4]

In the case of semiconductor QDs, the translational momentum conservation reduces because of the reduced effect of the periodical crystal structure, while the angular momentum

has to be conserved like atoms. Because of the reduction of translational momentum conservation and strong Coulomb interactions by quantum confinement effects, Auger recombination dramatically increases as compared with bulk materials.[5] The mechanism of Auger recombination in semiconductor QDs have been discussed by several researchers.[6-8] Theoretically, Zegrya and Samosvat demonstrated that two kinds of mechanisms of Auger recombination are conceivable in InGaAsP/GaAs QDs, Auger recombination with an activation threshold and nonthreshold Auger recombination.[9] Auger recombination with a threshold is associated with the spatial confinement of the wave functions of the charge carriers in the QD region, while nonthreshold Auger recombination is connected with the scattering of a crystal momentum by the QD interface. They concluded that nonthreshold Auger recombination is dominant and does not change with temperature in QDs whose radius is much smaller than the exciton Bohr radius, while Auger recombination with a threshold depends on temperature. Kharchenko and Rosen also concluded that the rate of Auger recombination in QDs strongly depends on the QD interface and that nonthreshold Auger recombination is dominant in QDs.[10]

Experimentally, we demonstrated that the rate of Auger recombination in CdTe QDs is affected by the interface structures modified by the capping reagents.[11] Garcia-Santamaria et. al. reported that giant multishell (thick CdS shell) CdSe QDs can greatly reduce Auger recombination rates because of the dramatic improvements of the QD interface potential.[34] Recently, Pietryga et. al. experimentally demonstrated that the energy threshold does not exist in Auger recombination in colloidal PbSe QDs by pressure dependence of Auger lifetime.[12]

Previous theoretical and experimental studies in semiconductor QDs show that the nonthreshold Auger recombination is the dominant process. However, because of the discrete electronic structures of QDs, the final state of Auger recombination should be restricted. To satisfy the energy requirements, phonons should play an important role in Auger

recombination. Auger recombination in direct-gap semiconductor also occurs with the participation of a phonon in order to satisfy the energy and momentum conservations,[14,15] while the effect of phonons on Auger recombination in semiconductor QDs has never been demonstrated.

In this chapter, we examined the effect of temperature on Auger recombination of colloidal CdTe QDs capped with OA/TOP by time-resolved luminescence spectroscopy. The lifetime of Auger recombination moderately depends on temperature below 175 K. It suggests that a phonon participates in the final state of Auger recombination because of the reduced availability of states satisfying energy conservation.

7.3 Experimental

CdTe QDs capped with OA/TOP were prepared according to the procedure reported in the literature and described in Chapter 2.[16,17] QD diameters were estimated from the first excitonic absorption peak as described in previous reports[18] and confirmed by a HRTEM (Tecnai G2 F20 200keV, FEI). The diameter of CdTe QDs in our experiments was 4.0 nm. Time-resolved luminescence spectra were measured using a Streak camera (synchronous blanking unit M5678 and synchroscan sweep unit M5675, Hamamatsu). CdTe QDs were excited at 400 nm by the second harmonic of an amplified mode-locked Ti:Sapphire laser (Spitfire and Tsunami, Spectra-Physics). The pump pulse was focused into 1 mm diameter spot and the excitation intensity ranged from 5 to 150 μW with a repetition rate of 1 kHz. The excitation intensity was measured by a calibrated power meter (Orion/PD, Ophir). Temperature dependent measurements were examined by a He flow cryogenic systems (Daikin Cryotec), whose temperature ranged from 10 to 350 K. The sample was sealed in a

0.1 mm thin quartz cell and placed within a conductive brass holder. The temporal resolution of the Streak camera at room temperature was 6 ps.

7.4 Results and discussion

Figure 7.1 shows time-resolved luminescence spectra of CdTe QDs excited at 100 μW ($<N_0> = 1.9$) and recorded at 20 and 600 ps after the excitation at 300 and 10 K. As compared with the spectrum at 300 K, the spectrum at 10 K is blue-shifted and the spectral width decreases, which is consistent with the previous reports on steady-state experiments.[19,20] Time-resolved spectra recorded at various delay times are very similar and the biexciton emission is not observed, although the biexciton emission can be observed at much higher excitation intensity (Figure 6.2b in Chapter 6). This result suggests that the quantum yield of the biexciton emission of CdTe QDs is low.

Emission decays of CdTe QDs excited at different excitation intensities at 300 and 10 K are shown in Figure 7.2. At 300 K, the emission decay of QDs excited at 5 μW ($<N_0> = 0.094$) is fitted with a single exponential decay whose lifetime is in the ~ns scale. With increasing excitation intensity, an additional fast decay component associated with Auger recombination appears (50, 100 μW; $<N_0> = 0.94, 1.9$). These dynamics are well fitted with a bi-exponential decay function and the lifetime of Auger recombination (Auger lifetime) is 40 ± 3 ps. At 10 K, the emission decay of CdTe QDs excited at different pump intensities is similar to that at 300 K. However, when the excitation intensity increases, the additional fast decay component becomes slower as clearly shown in Figure 7.2b. Dynamics are well fitted with a bi-exponential decay function and the Auger lifetime is 87 ± 7 ps. Pandey and Guyot-Sionnest also reported Auger recombination dynamics at 300 and 14 K in CdSe QDs and the Auger lifetime becomes slightly longer at 14 K as compared with that at 300 K.[21]

However, the origin of the difference has not been discussed. The Auger lifetime is plotted as a function of the temperature in Figure 7.3. In the temperature range from 350 to 175 K, the Auger lifetime is almost constant (~40 ps). Below 175 K, it starts to increase with decreasing temperature and finally reaches 87 ps at 10 K. As the rate of Auger recombination (k_{Auger}) is expressed by the reciprocal Auger lifetime, logarithmic k_{Auger} are plotted as a function of inverse temperature ($1/T$) in the inset Figure 7.3. In a classical Arrhenius type plot, $\ln k_{Auger}$ is proportional to $1/T$ and the activation energy can be estimated from the slope. However, the temperature dependence of the rate of Auger recombination does not follow a simple Arrhenius equation. k_{Auger} is well fitted with an empirical equation $k_{Auger} \propto \ln T$, although there is no theoretical basis.

There are three possible interpretations for the temperature dependence of Auger recombination in CdTe QDs, which are related to the effects of the activation threshold, of the exciton fine structure and of the phonons. First, we discuss the effect of the activation threshold on the temperature dependence. As mentioned in the introduction, two kinds of Auger recombination exist, Auger recombination with and without an activation threshold in QDs.[9] Nonthreshold Auger recombination does not depend on temperature, while Auger recombination with a threshold depends on temperature. The rate of Auger recombination in bulk semiconductors ($k_{Auger(bulk)}$) having an activation threshold exponentially depends upon T and E_g as

$$k_{Auger(bulk)} \propto \left(\frac{1}{T}\right)^{3/2} \exp(-\gamma E_g / k_B T) \tag{7.1}$$

where γ is the constant depending on the electronic structure and k_B is the Boltzmann constant.[1,2] The Auger lifetime obtained at 10 K in our experiments changes much moderately with temperature (at most twice times as compared with that at room temperature). This behavior is not consistent with the threshold Auger recombination model as reported for the

bulk. Besides, E_g shifts to higher energies in QDs with the decrease of temperature.[19,22] Our experimental results obtained in OA/TOP capped CdTe QDs are also consistent with this result and changes of about 60 meV with the decrease of temperature from 300 to 150 K (Figure 7.4). In bulk InGaAsSb, the rate of Auger recombination changes of 5 orders of magnitude per 1-eV variation of E_g.[23] If the activation threshold plays a dominant role in Auger recombination of CdTe QDs, the shift of E_g should change the Auger lifetime (about 10-times-longer lifetimes are expected for the E_g shift of 60 meV). However, the Auger lifetime in our experiments remains completely unchanged from 300 to 175 K. These results strongly suggest that Auger recombination in CdTe QDs has no activation threshold, which is consistent with the experimental results of Pietryga et al.[13] and with the theoretical calculation performed by Kharchenko et al.[32] Other mechanism causing temperature dependence should be considered.

In the second, the effect of exciton fine structures of the $1S$ state is conceivable. The $1S$ state of CdTe QDs split into two states (dark and bright states) because of the crystal structure, the symmetry and the electron-hole exchange interaction of QDs.[20,24] If the electron distribution at low temperature is different from that at room temperature due to the dark-bright splitting, the number of the initial state of Auger recombination decreases and thus, the rate of Auger recombination decreases. The dark-bright splitting energy of CdTe QDs (D = 4.0 nm) based on the effective mass approximation (EMA) model was ~5 meV, which corresponded to a thermal energy of ~50 K.[25] The effect of the dark state can be observed by the temperature dependence of long-lived emission decays. However, as shown in Figure 7.5, the emission decay of CdTe QDs (D = 4.0 nm) is almost the same as those for different temperatures below 100 K. Besides, the Auger lifetime in our experiments began to increase at 175 K. The effect of the exciton fine structure is observed only below ~50 K, which is inconsistent with the experimental results. These results suggest that the exciton fine

structure does not have an important role on the temperature dependence of Auger recombination.

The most likely possibility is the effect of phonons on Auger recombination. In spite of the strong enhancement of Auger recombination in semiconductor QDs, several researchers have predicted a relationship between Auger recombination and phonons.[5,26] For example, Wang et. al. reported that phonons can be involved in Auger recombination in order to mitigate the energy conservation in QDs having discrete energy levels.[25] Klimov et. al. also reported that Auger recombination in QDs can occur efficiently with the participation of a phonon because of the reduced availability of final states satisfying energy conservation (Figure 7.6).[5] From these discussions, the temperature dependence of Auger recombination may be due to the participation of phonons in the process. At present, a fully developed theoretical model including phonon effects on the temperature dependence of Auger recombination in QDs does not exist. Phonon-assisted Auger recombination in bulk semiconductors ($k_{Auger(bulk\text{-}phonon)}$) is written by[27,28]

$$k_{Auger(bulk-phonon)} \propto \frac{T}{E_{th}^{3/2}} \frac{1}{e^{E_{LO}/k_B T}-1}\left[\frac{e^{E_{LO}/k_B T}}{(E_{th}-E_{LO})^2}+\frac{1}{(E_{th}+E_{LO})^2}\right] \tag{7.2}$$

where E_{LO} is the bulk LO phonon energy and E_{th} is the threshold energy of Auger recombination. Although the tendency of this function is in good agreement with the temperature dependence of Auger recombination in CdTe QDs, the rate of phonon-assisted Auger recombination in the bulk semiconductors decreases more sharply with the decrease of temperature as compared with our experimental results (Figure 7.7). This deviation may originate from the nonthreshold effect in semiconductor QDs and from the difference of the role of phonons in bulk and QDs for Auger recombination. Kaze et al. reported that the optical gain of CdSe/ZnS QDs and quantum rods (QRs) film increases with decreasing temperature.[29] They concluded that this moderate increase of the optical gain is assigned to a

thermally activated nonradiative process due to the carrier trapping in defects and surface states.[30] We believe that the temperature dependent Auger recombination also contributes to the temperature dependence of the optical gain because the temperature dependence of the optical gain is comparable to that of Auger recombination.

7.5 Conclusion

In our time-resolved luminescence measurements at different temperatures, we observed the moderate temperature dependence of Auger recombination. Theoretically, Auger recombination in semiconductor QDs is believed to be independent on the temperature because the energy threshold of Auger recombination is eliminated by the relaxation of the momentum conservation. Our experimental results suggest that a phonon participates in Auger recombination in direct-gap semiconductor QDs at the final state of Auger recombination because of the reduced availability of states satisfying energy conservation.

References

(1) Beattie, A. R.; Landsberg, P. T. ; *Proc. R. Soc. A* **1959**, *249*, 16.

(2) Haug, A. *J. Phys. Chem. Solids* **1988**, *49*, 599.

(3) Lochmann, W. *Phys. Stat. Sol. (a)* **1978**, *45*, 423.

(4) Svantesson, K. G.; Nilsson, N. G. *J. Phys. C: Solid State Phys.* **1979**, *12*, 5111.

(5) Klimov, V. I.; Mikhailovsky, A. A.; McBranch, D. W.; Leatherdale, C. A.; Bawendi, M. G. *Science*, **2000**, *287*, 1011.

(6) Chepic, D. I.; Efros, Al. L.; Ekimov, A. I.; Ivanov, M. G.; Kudriavtsev, I. A.; Yazava, T. V. *J. Lumin.* **1990**, *47*, 113.

(7) Pan, J. L. *Phys. Rev. B* **1992**, *46*, 3977.

(8) Wang, X.; Ren, X.; Kahen, K.; Hahn, M. A.; Rajeswaran, M.; Maccagnano-Zacher, S.; Silcox, J.; Cragg, G. E.; Efros, A. L; Krauss, T. D. *Nature* **2009**, *459*, 686.

(9) Zegrya, G. G.; Samosvat, D. M. *J. Exp. Theor. Phys.* **2007**, *104*, 951.

(10) Kharchenko; V. A.; Rosen; M. *J. Lumin.* **1996**, *70*, 158.

(11) Kobayashi, Y.; Pan, L.; Tamai, N. *J. Phys. Chem. C* **2009**, *113*, 11783.

(12) Garcia-Santamaria, F. ; Chen, Y.; Vela, J. ; Schaller, R. D. ; Hollingworth, J. A. ; Klimov, V. I. *Nano Lett.* **2009**, *9*, 3482.

(13) Pietryga, J. M.; Zhuravlev, K. K.; Whitehead, M.; Klimov, V. I.; Schaller, R. D. *Phys. Rev. Lett.* **2008**, *101*, 217401.

(14) Takeshima, M. *Jpn. J. Appl. Phys.* **1983**, *22*, 491.

(15) Nee, T.; Cheng, C,; Lin, R. *Jpn. J. Appl. Phys.* **2004**, *43*, 890.

(16) Kloper, V.; Osovsky, R.; Kolny-Olesiak, J.; Sashchiuk, A.; Lifshitz, E. *J. Phys. Chem. C* **2007**, *111*, 10336.

(17) Osovsky, R.; Klooper, V.; Kolny-Olesiak, J.; Sashchiuk, A.; Lifshitz, E. *J. Phys. Chem. C* **2007**, *111*, 10841

(18) Yu, W. W.; Qu, L.; Guo, W.; Peng, X. *Chem. Mater.* **2003**, *15*, 2854.

(19) Morello, G.; Giorgi, M. D.; Kudera, S.; Manna, L.; Cingolani, R.; Anni, M. *J. Phys. Chem. C* **2007**. *111*, 5846.

(20) Nonoguchi, Y.; Nakashima, T.; Kawai, T. *J. Phys. Chem. C* **2008**. *112*, 19263.

(21) Pandey, A; Guyot-Sionnest, P *J. Chem. Phys.* **2007**, *127*, 111104.

(22) Varshni, Y. P. *Physica* **1967**, *34*, 149.

(23) Charache, G. W.; Baldasaro, P. F.; Danielson, D. M.; DePoy, D. M.; Freeman, M. J.; Wang, C. A., Choi, H. K.; Garbuzov, D. Z.; Martinelli, R. U.; Khalfin, V.; Saroop, S.; Borrego, J. M.; Gutmann, R. J.; *J. Appl. Phys.* **1999**, *85,* 2247.

(24) Efros, Al. L.; Rosen, M.; Kuno, M.; Nirmal, M.; Norris, D. J.; Bawendi, M. *Phys. Rev. B* **1996**, *54*, 14628.

(25) Schops, O.; Thomas, N. L.; Woggon, U.; Artemyev, M. V. *J. Phys. Chem. B* **2006**, *110*, 2074.

(26) Wang, L; Califano, M.; Zunger, A.; Franceschetti, A. *Phys. Rev. Lett.* **2003**, *91*, 56404.

(27) Polkovnikov, A. S.; Zegrya, G. G. *Phys. Rev. B* **1998**, *58*, 4039.

(28) Guichard, A. R.; Kekatpure, R. D.; Brongersma, M. L. *Phys. Rev. B* **2008**, *78*, 235422.

(29) Kaze, M.; Oron, D.; Shweky, I.; Banin, U. *J. Phys. Chem. C* **2007**, *111*, 7898.

(30) Valerini, D.; Creti, A.; Lomascolo, M.; Manna, L. ; Cingolani, R. ; Anni, M. *Phys. Rev. B* **2005**, *71*, 235409.

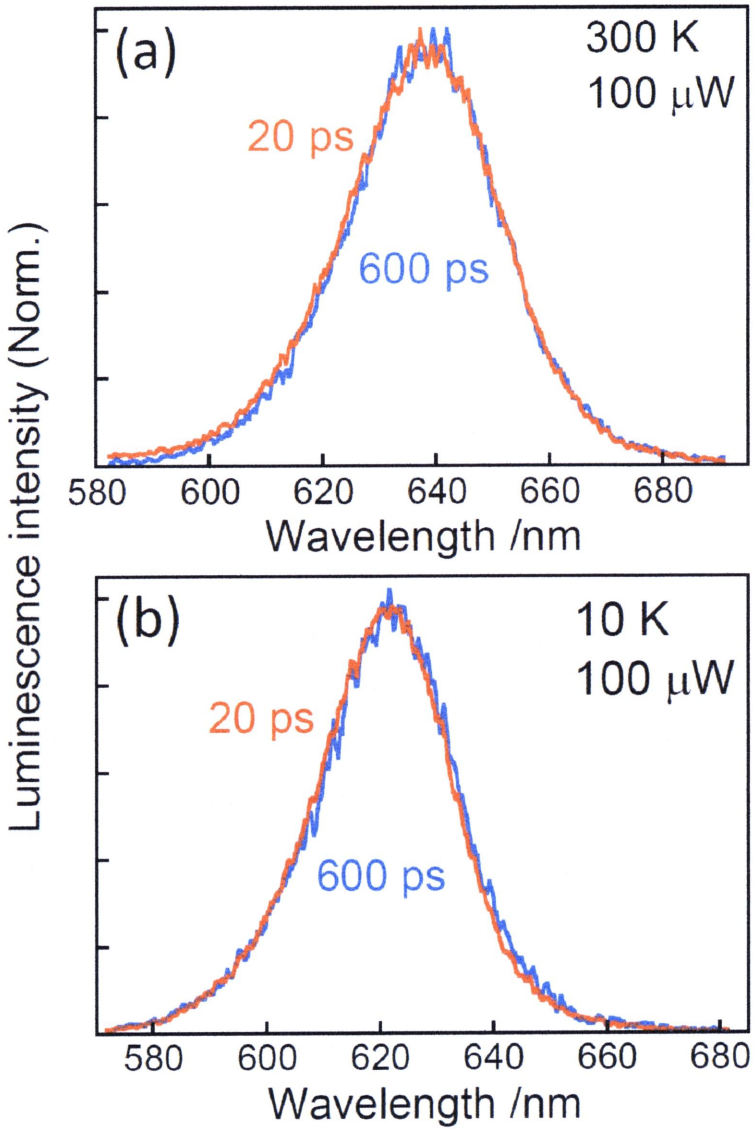

Figure 7.1 Normalized time-resolved luminescence spectra recorded at 20 and 600 ps after the excitation at 300 K (a) and 10 K (b).

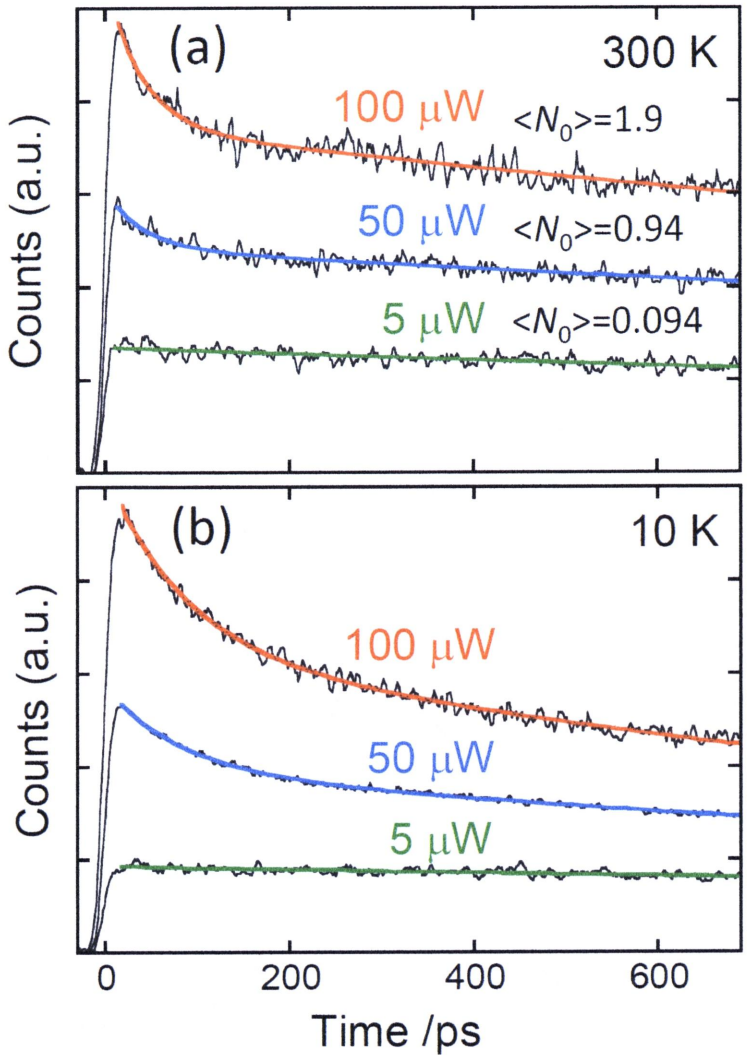

Figure 7.2 Emission decays excited at different pump intensities (5, 50 and 100 μW ; $\langle N_0 \rangle$ = 0.094, 0.94 and 1.9) at 300 K (a) and 10 K (b) of CdTe QDs (D = 4.0 nm). Intensity-dependent fast decay components can be assigned to Auger recombination.

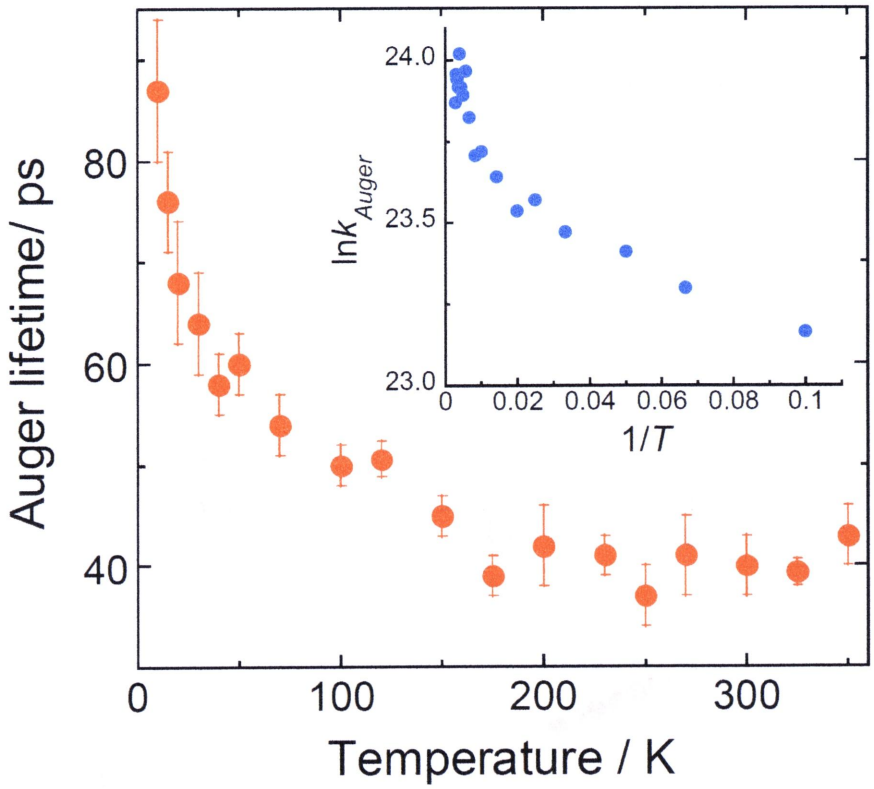

Figure 7.3 Temperature dependence of Auger lifetime of CdTe QDs (D = 4.0 nm) obtained from the fast decay component of the emission decay. A plot of the logarithmic k_{Auger} as a function of the inverse temperature (inset). It does not follow a classical Arrhenius type equation.

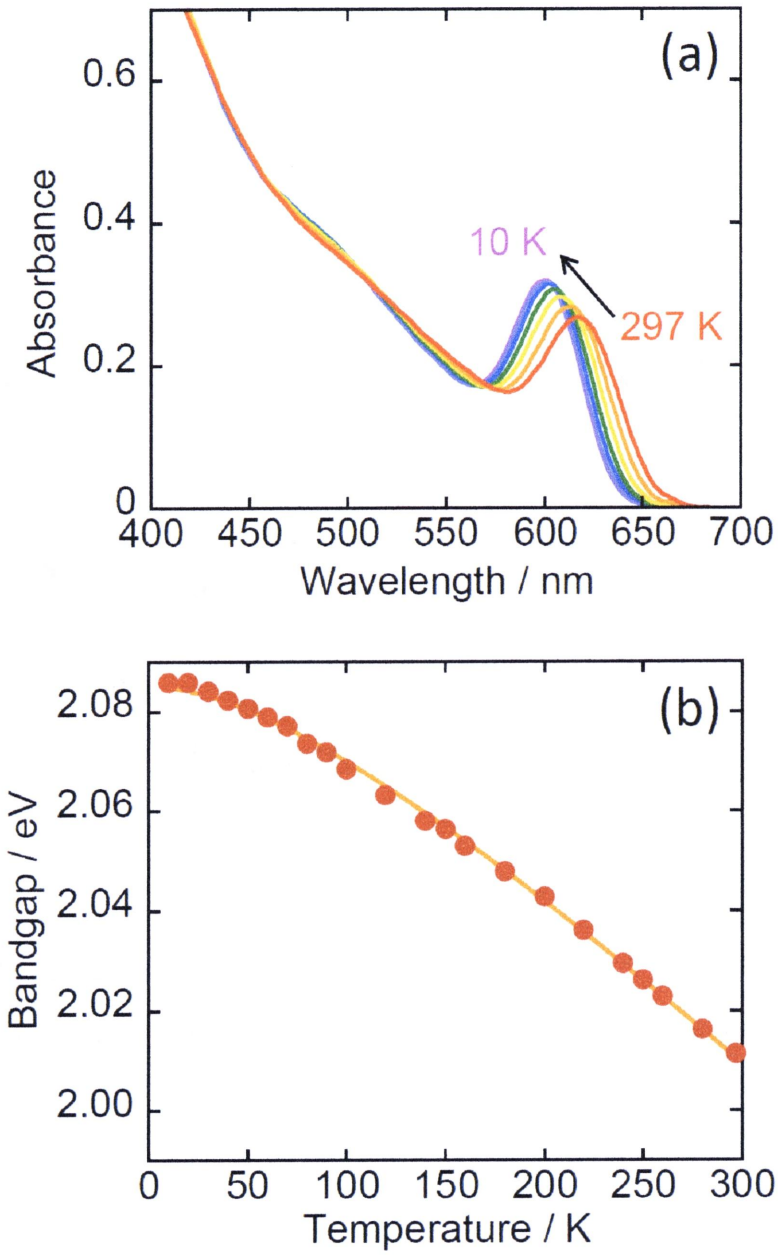

Figure 7.4 (a) Temperature dependence of steady-state absorption spectra of CdTe QDs capped with OA/TOP (D = 3.8 nm). (a) Temperature dependence of the bandgap of the same sample.

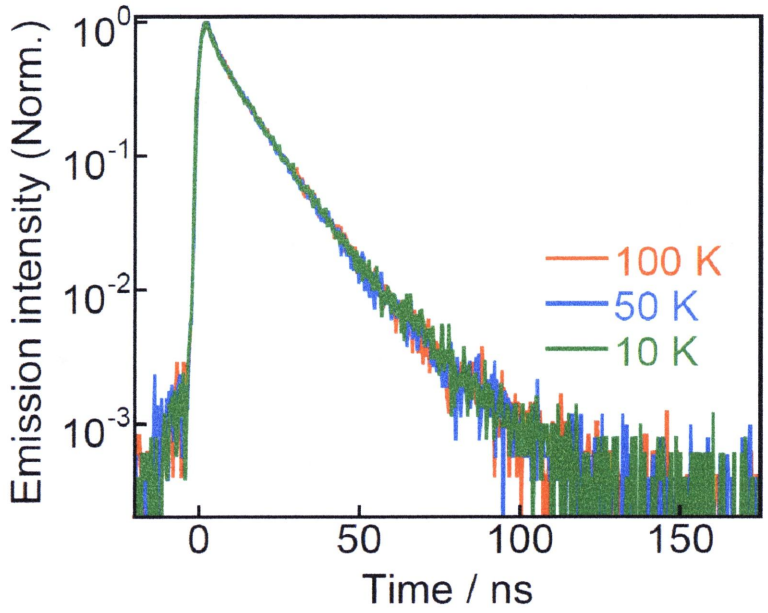

Figure 7.5 Emission decays of CdTe QDs capped with OA/TOP (D = 4.0 nm) at different temperature.

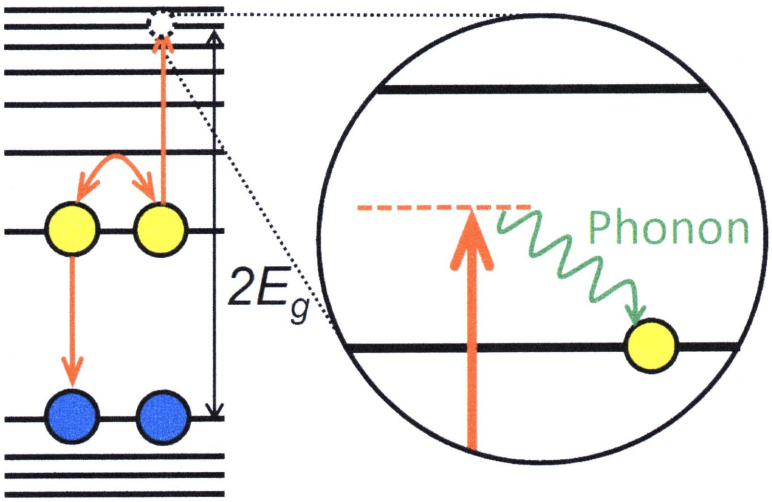

Figure 7.6 Schematic illustration of a participation of phonons in Auger recombination in semiconductor QDs.

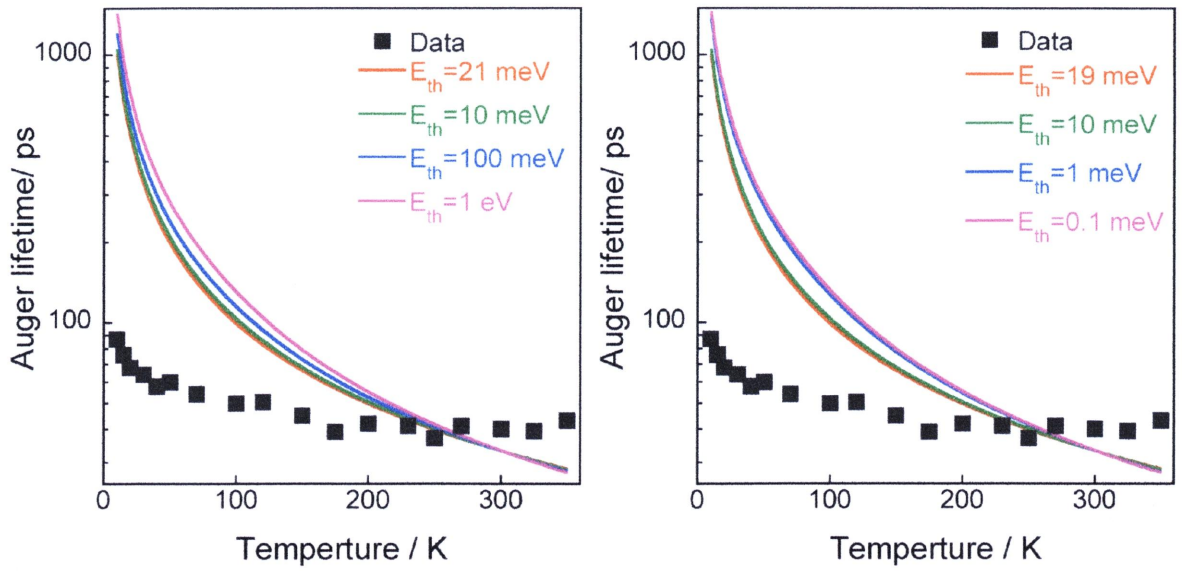

Figure 7.7 Fitting results of temperature-dependent Auger recombination with the equation of phonon assisted Auger recombination in bulk semiconductors (eq 7.2). E_{LO} is fixed to 20 meV (ref. 19).

Acknowledgement

Professor Tamai has always given me chances to meet excellent science world by many fruitful discussions and allowed me great freedom in my research life. I would like to express my great appreciation to Professor TAMAI for the encouragements, supporting and guidance of this work.

I would like to appreciate Professor Tachiya for his great indication to my paper and a fruitful discussion about exciton dynamics in quantum dots. I would like to deeply appreciate Professor Ishikawa in the National Institute of Advanced Industrial Science and Technology (AIST) for carefully checking my doctor thesis. I would also like to appreciate Professor Kawai, Professor Nakashima in Nara Institute of Science and Technology for valuable discussions.

I would like to appreciate Professor Masuo for stimulating discussions about the relationship between multiexciton dynamics and antibunching, and for giving me lots of advice for my career after graduation. Special thanks to Professor Kaneko for fruitful discussions about crystal growth of nanomaterials and for giving me lots of advice for my better life in lab. I would like to deeply thank Dr. Wang for her kind and sincere instructions of pump-probe experiments since I was an undergraduate student.

I would like to deeply appreciate Yoshida scholarship for their hearty and sincere supports. They gave me great opportunity for concentrating on my works and enjoyable research days. Even after finishing the scholarship Mr. Sakuma and Mr. Hiraki always gave me their hands in my private days. I really proud that I had belonged to Yoshida scholarship and I will sure to repay them for all the help they have given me.

I have spent really enjoyable and excited times in my research life thanks to guys who belong to Tamai lab. I want to thank Mr. Udagawa, Mr. Nishimura, Mr. Matsumoto and Dr.

Gabriel for not only helping my work but also deepening my knowledge with their exciting discussions. I am really proud that I had worked together.

I would like to thank colleagues of my age, Mr. Nishi, Miss. Hatano, Dr. Nonoguchi etc. They gave me many great opportunities to reaffirm connections and to spend really good times in my research and private life.

Special thanks to Mr. Yahanashi, Mr. Nakai, Mr. Kojima, Mr. Mori, Mr. Kitajima and Mr. Taniguchi for playing music and drinking. I hearty and deeply thank my parents, sister, brother, nieces and my cat. Their hearty and constant supports always encourage me.

Finally, I would like to express millions of thanks to Prof. Kameda in Yoyogi Seminar for teaching me great pleasure in learning and introducing me into excited science world.

List of publications

I. Original papers

(1) Yoichi Kobayashi, Lingyun Pan, and Naoto Tamai, **"Effects of Size and Capping Reagents on Biexciton Auger Recombination Dynamics of CdTe Quantum Dots"** *J. Phys. Chem. C* **2009**, *113*, 11783.

(2) Yoichi Kobayashi, Takeshi Udagawa, and Tamai, N. **"Carrier Multiplication in CdTe Quantum Dots by Single-photon Timing Spectroscopy"** *Chem. Lett.* **2009**, *38*, 830.

(3) Yoichi Kobayashi and Naoto Tamai, **"Size-Dependent Multiexciton Scpectroscopy and Moderate Temperature Dependence of Biexciton Auger Recombination in Colloidal CdTe Quantum Dots"** *J. Phys. Chem. C* **2010**, *114*, 17750.

(4) Gabriel Sagarzazu, Yoichi Kobayashi, Norio Murase, Ping Yang, and Naoto Tamai, **"Auger Recombination Dynamics in Hybirid Silica-coated CdTe Nanocrystals"** *Phys. Chem. Chem. Phys.* **2011**, in press (DOI: 10.1039/c0cp01957g).

(5) Yoichi Kobayashi, Takatoshi Nishimura, and Naoto Tamai, **"Effect of Surface Defects on Auger Recombination in CdS Quantum Dots"** *J. Phys. Chem. Lett.* **2011**, (Submitted).

II. Review and Book

(1) Lingyun Pan, Yoichi Kobayashi, and Naoto Tamai **"Nonlinear Optical Properties and Single Particle Spectroscopy of CdTe Quantum Dots"** *Molecular Nano Dynamics* Edited by H. Fukumura et al. Wiley-VCH, Weinheim, (2009), Section9, pp.155-169.

(2) 小林洋一、藩　凌云、玉井尚登 「CdTe量子ドットの非線形光学特性と単一微粒子分光」光化学，Vol.39，(2008)，pp.85-92